DEVELOPMENT AND EVALUATION OF ATTENUATED *TRYPANOSOMA CRUZI* LINES AS POTENTIAL CANINE VACCINES

by

ASHLEY NEARY HARTLEY

(Under the Direction of Rick L. Tarleton)

ABSTRACT

The protozoan parasite *Trypanosoma cruzi* infects humans, wildlife, and domestic animals. In endemic areas of Central and South America, it is estimated that ten million individuals are chronically infected with twenty-five million more at risk of infection. Current methods of parasite control, diagnostics, and treatment are inadequate in preventing new infections; no vaccines are available for human or veterinary use. In endemic regions, dogs are important sources of infection for the insect vector, and therefore, dogs are a critical control point for *T. cruzi* transmission. A transmission-blocking vaccine for dogs would greatly reduce the prevalence of *T. cruzi* infection in the canine and human population. Our goal was to develop a safe, well-defined attenuated *T. cruzi* strain for vaccination of dogs. With transcriptome and proteome analysis of the four life stages revealing metabolic pathways important to the parasite during mammalian infection, we hypothesized that these genes products serve critical roles in infectivity, development, maturation, and/or replication of *T. cruzi*. We believed selective gene disruption would result in parasite lines defective in these processes and therefore unable to maintain an infection, while still providing a stimulus for the development of a

protective immune response. Gene knockout lines of *T. cruzi* made utilizing a Multisite Gateway-based approach were evaluated for growth deficiencies while *in vivo* testing in a mouse model was used to determine vaccine efficacy. As a single line would ultimately be selected for further testing in dogs, the target of proposed future vaccine efforts in the field, we further aimed to identify methods and reagents to characterize the canine immune response. We tested anti-human and anti-bovine T cell-specific cell surface markers for cross-reactivity to delineate canine T cell subsets and evaluate T cell-specific effector function. We used a serodiagnostic assay, T cell phenotypic markers, and intracellular cytokine staining to correlate *T. cruzi*-specific antibody responses with T cell responses in naturally infected dogs. We believe development of a live, attenuated vaccine through selective gene disruption and establishment of canine-specific immunological methods for testing vaccine efficacy will provide significant evidence supporting the future use of canine vaccination to control *T. cruzi* transmission.

INDEX WORDS: *Trypanosoma cruzi*, Chagas disease, fatty acid metabolism, $CD8^+$ T cell, canine, dog, parasitic disease, flow cytometry

DEVELOPMENT AND EVALUATION OF ATTENUATED *TRYPANOSOMA CRUZI* LINES AS POTENTIAL CANINE VACCINES

by

ASHLEY NEARY HARTLEY

B.S. University of Georgia, 2005

A Dissertation Submitted to the Graduate Faculty of The University of Georgia in Partial Fulfillment of the Requirements for the Degree

DOCTOR OF PHILOSOPHY

ATHENS, GEORGIA

2013

DEVELOPMENT AND EVALUATION OF ATTENUATED *TRYPANOSOMA CRUZI* LINES AS POTENTIAL CANINE VACCINES

by

ASHLEY NEARY HARTLEY

Major Professor: Rick L. Tarleton

Committee: Mary K. Hondalus
Margie D. Lee
Boris Striepen

Electronic Version Approved:

Maureen Grasso
Dean of the Graduate School
The University of Georgia
May 2013

DEDICATION

This dissertation is dedicated to my parents, Richard and Elaine Neary, my sister and brother-in-law Erin and Steven Floyd, and my husband Daniel for their encouragement, understanding, and unconditional love during this process and throughout my life.

ACKNOWLEDGEMENTS

I would like to express my deepest gratitude to my major professor, Dr. Rick Tarleton, for opening his laboratory and giving me the opportunity to do science in such an enriching training environment. Thank you, Coach, for your patience, support, encouragement, and advice during these past five years; I admire and respect your determination and enthusiasm for science. I would also like to thank my committee members, Dr. Margie Lee, Dr. Mary Hondalus, and Dr. Boris Striepen for critical feedback, scientific discussions, and mentorship. A special thanks to Dr. Daniel Colley and Dr. Kim Klonowski for sharing their knowledge and life experiences in science. I am indebted to Dr. Susan Sanchez for the opportunity to first experience and develop a passion for research in her lab. To my lab mates, Dr. Juan Bustamante and Dr. Angel Padilla, thank you both for encouraging me to work at my very best. Charles Rosenberg, thanks for answering my questions and serving as a sounding board. A special thanks to other members of the Tarleton Lab, past and present, for your critical eye, guidance, and friendship; in particular, thank you Gretchen Cooley, Dr. Todd Minning, Dan Xu, and Courtney Boehlke for providing much need support and guidance during my time in the lab. Last but not least, I would like to thank my husband, Daniel, for supporting me throughout this journey; you have been my rock.

TABLE OF CONTENTS

Page

LIST OF TABLES

Page

LIST OF FIGURES

Page

CHAPTER 1

INTRODUCTION AND LITERATURE REVIEW

1.1 *Trypanosoma cruzi* and Chagas disease

1.1.1 Introduction

The hemoflagellate protozoan parasite *Trypanosoma cruzi* infects humans, wildlife, and domestic animals throughout the Americas. Worldwide, it is estimated that ten million individuals are chronically infected with *T. cruzi*, with twenty-five million more are at risk of infection (1). *T. cruzi* infection burdens countries of Central and South America, contributing 14,000 deaths annually and 700,000 daily adjusted life years (2). Current methods of parasite control, diagnostics, and treatment are inadequate in completely preventing new infections; no vaccines are available for human or veterinary use.

1.1.2 Chagas disease

Named after the Brazilian physician Carlos Chagas who first described the disease in 1909, Chagas disease is the result of *T. cruzi* infection and is characterized by two phases, acute and chronic. During the acute phase, individuals may be asymptomatic or experience very mild symptoms. Symptoms range from fever and general malaise to lymphadenopathy, skin lesions (chagoma), unilateral bipalpebral edema (Romana's sign), diarrhea, and heart failure (3). Following the acute phase, the disease often enters remission where individuals slowly begin to develop cardiac and/or gastrointestinal manifestations decades after infection. In the cardiac form, individuals may suffer from

fatigue, chest pain, stroke or even sudden cardiac death. Gastrointestinal disease is less commonly seen and may involve the esophagus, small intestine, and colon (4). Since individuals typically experience none or very mild symptoms, Chagas disease frequently remains undiagnosed for decades. Health care providers may only link symptoms with Chagas disease upon combining a history of living in endemic region with positive results to multiple serodiagnostic tests.

As domestic animals are also susceptible to *T. cruzi* infection, chagasic symptoms are not exclusive to humans. For example, infected dogs are prone to suffer from acute myocarditis resulting in sudden collapse, with death possible, especially in young dogs. Animals that do not die may develop right-sided heart failure characterized by ascites, hepatomegaly, and splenomegaly and further experience anorexia, diarrhea, and neurological signs (5). Dogs who survive acute myocarditis often enter an indeterminate phase were parasitemias become subpatent, individuals are asymptomatic, and electrocardiographs are normal (6). Some infected dogs will progress to the chronic phase, typified by cardiac dilation, ECG abnormalities, and sudden death. Histopathological analysis of heart tissue from naturally and experimentally infected dogs reveals diffuse and multifocal necrotic myocarditis with extensive lymphocyte infiltration and occasional parasite nests (7). Thus, both humans and their canine counterparts are susceptible to *T. cruzi* infection, suffer similar clinical manifestations, and may ultimately succumb to complications associated with Chagas disease.

1.1.3 Diagnosis and Treatment

With low levels of detectable parasites in infected hosts and non-specific or absent symptoms during *T. cruzi* infection, a diagnosis of human Chagas disease is often

reached following a combination of multiple positive serological tests, history of living in an endemic region, and clinical symptoms. The three most widely used serological tests included indirect immunoflourescence assay, indirect hemagluttin assay, and ELISA, which all identify circulating antibodies reactive to crude parasite lysate. As a positive serological diagnosis is dependent on a positive result from two of three tests, public health concerns arise for addressing single serological positive individuals. In domestic animals, similar serological tests are utilized (8) with seroprevalence varying widely by region and positive results confounded by suspected crossreactivity with other endemic trypanosomatids. The source of parasite lysate, from insect versus more relevant mammalian parasite life stages, and concerns for cross-reactivity with other parasitic infections highlights the need to develop more relevant and sensitive serological tests for both humans and their domestic animal counterparts.

The World Health Organization currently recommends the drugs benznidazole and nifurtimox for treatment of individuals with positive serology (9), yet curing efficacy in humans has been difficult to determine and prove unequivocally. A 40-day benznidazole-treated murine model of *T. cruzi* infection has confirmed parasitological cure and further correlated certain T cell surface markers expression with the absence of parasites (10). Despite these findings, significant adverse drug reactions in healthy individuals and contraindications in pregnant mothers and organ failure-suffering patients have limited full chemotherapeutic potential for treating Chagas disease. As the current drugs for treating human *T. cruzi* infection are imperfect, a significant need exists for generating new anti-*T. cruzi* compounds and developing strategies for preventing initial infection.

1.1.4 Host immunity to T. cruzi

Control of acute and chronic *T. cruzi* infection depends on a combination of both humoral and cell mediated immunity. In studies, B-cell deficient rats are more susceptible to acute *T. cruzi* infection compared to healthy rats as determined by increased parasitemias and mortality following anti-μ treatment during infection (11). Similar results found in *T. cruzi*-infected muMT mice, transgenic animals deficient in immunoglobulin production, confirmed the requirement for antibodies in *T. cruzi* infection control (12). Additionally, with the transfer of immune sera aiding in parasite clearance by the spleen and liver (13), the role of antibodies for *in vivo* immune control of blood parasitemias and clearance was further established.

Infection of anti-T cell antibody-treated and mice genetically deficient in various T cell subsets have highlighted the significant role T cells serve in immune control of *T. cruzi* and subsequent disease development (14, 15). In particular, single and double MHC I- and II-deficient mice experience higher parasite loads and mortality as compared to their wild-type counterparts (16). The significant role of T cells in recognition and control of *T. cruzi* is also emphasized by the presence of T cells in nonlymphoid parasitized tissues (17) and the ability of T cells to secrete effector cytokines, like IFNγ and TNFα, that can subsequently activate macrophages to produce trypanocidal nitric oxide (18). As evidenced by decreased antibody levels in infected MHC I- and II-deficient mice (16), T cells may further provide B cell help during the antibody response as antigen-specific antigen presenting cells and/or lymphokine-producing cells. With B cell-deficient mice surviving longer as compared to $CD4^+$ and $CD8^+$ T cells during *T.*

cruzi infection (12), the protection afforded by antibodies appears secondary to those cellular immune responses of T cells.

The identification of $CD8^+$ T cell epitopes focused on specific *T. cruzi* peptides provides a valuable tool for characterizing and monitoring the *T. cruzi*-specific $CD8^+$ T cell response in the murine model of *T. cruzi* infection. During acute infection with the virulent Brazil strain, the TSKB20/K^{b+} $CD8^+$ T cell epitope identifies cells comprising 20-30% of the entire $CD8^+$ T cell repertoire specific for *T. cruzi* (19). Parasite-specific $CD8^+$ T cells can be further phenotyped as effector $CD8^+$ T cells by expression of the activation markers $CD44^{hi}$ and CD11a and low expression of the lymph node homing molecule CD62L (20). In a drug-induced cure model of *T. cruzi* infection, $CD127^{hi}$, CCR7, and $CD62L^{hi}$ expression on *T. cruzi* specific $CD8^+$ T cells with the maintenance of IFNγ production is indicative of the development of a central memory phenotype (10). In this model, the *T. cruzi* specific $CD8^+$ T cells have decreased expression of killer cell lectin-like receptor G1 (KLRG1), a molecule induced by repetitive antigen stimulation, correlating with decreased parasite load. Together, these $CD8^+$ T cell specific markers provide a technique to monitor and qualitatively assess parasite persistence and clearance in a mouse model of *T. cruzi* infection.

1.2 Parasitology

1.2.1 *Taxonomy*

T. cruzi is a single cell parasite belonging to the Order Kinetoplastida, whose members also include the pathogenic organisms *Trypanosoma brucei* and *Leishmania* species. Trypanosomatids are almost exclusively parasitic, cycling through insect vectors and vertebrate, invertebrate, and plants hosts. The kinetoplast, a disc containing

mitochondrial DNA found near the base of the single flagellum, is a characteristic distinguishing these parasites from other eukaryotic organisms.

1.2.2 Life Cycle

The life cycle of *T. cruzi* is complex, involving obligate life stages in an insect vector and a mammalian host. The blood-feeding insect vector becomes infected after biting and ingesting trypomastigotes from the circulation of an infected host. These trypomastigotes transform into replicative epimastigotes in the insect hindgut and further mature into metacyclic trypomastigotes. During a subsequent blood meal, the insect vector defecates, releasing the metacyclic trypomastigotes in feces near the bite site. Through contamination of the bite wound or introduction to mucosa, these metacyclic trypomastigotes can then infect host cells. After entering the cell's cytoplasm, *T. cruzi* then matures and replicates as amastigotes. These amastigotes convert into trypomastigotes, egress from the host cell, and then either infect another cell or enter the bloodstream. These circulating trypomastigotes are the infectious form for the insect vector, which can acquire these parasites during a blood meal thereby propagating the life cycle.

1.2.3 Vectors

The insect vectors responsible for transmission between wild animals and humans predominately belong to the *Triatoma*, *Rhodnius*, and *Panstrongylus* genera. All three genera are distributed throughout the Americas, from Argentina and Chile to Mexico, though wild Triatominae capable of transmitting *T. cruzi* are present from southern Patagonia to the northern United States of America (9). Some Triatominae species have become highly adapted to domestic environments, living in domicillary structure crevices

and emerging at night to feed on humans and domestic animals. These important vectors include *T. infestans* in the southern cone regions (Argentina, Brazil, Bolivia, Chile, Paraguay, Peru, and Uruguay), *T. brasiliensis* (Brazil), and *Rhodnius prolixus* and *T. dimidiata* (Amazon basin) (21). The numerous vector species and their expansive geographical distribution emphasize the broad population at risk for *T. cruzi* transmission.

1.2.4 Transmission

T. cruzi transmission may occur via various routes including cutaneous, oral, transplantable, and congenital routes. Cutaneous transmission typically occurs when the insect vector deposits infective feces during a blood meal. Subsequent scratching of the bite site by the host facilitates parasite tissue penetration and ultimate infection. In humans, consumption of contaminated foods like sugar cane or açai juice compromises many of the documented cases of oral transmission (22). Contamination of food may occur through incidental inclusion of infected insect vectors during food processing or ingestion of crushed insect vectors. Ingestion of infected insect vectors is hypothesized as a transmission mechanism in dogs (6), while experimentally confirmed as a route plausible in wild reservoirs (23). *T. cruzi* infection by organ transplantation, via blood transfusions (24) or solid organ transplants (25), is documented and expands the population at risk to individuals outside endemic regions.

With reports of human congenital transmission surpassing the number of vector-mediated acute cases by a factor of ten in Argentina (26), transmission from mother-to-child has warranted further investigation in understanding less conventional *T. cruzi* transmission routes and the subsequent impact. In particular, *T. cruzi*-infected mothers

have higher maternal parasitemias and reduced peripheral blood mononuclear cell interferon gamma production indicating congenital transmission results in higher parasites loads and peripheral immmunodeficient responses in mothers (27). Following birth and despite the presence of parasites in milk, the risk of *T. cruzi* transmission appears low during breastfeeding in humans (28) or in experimentally-infected mouse models (29). In canines, documentation of bitch-to-pup transmission are limited, but putative cases have been observed in endemic regions (30). In a laboratory-based study, four puppies born and weaned from *T. cruzi*-infected parents displayed seroreactivity to *T. cruzi* lysate, cardiac inflammatory infiltrates, gastric abnormalities, but had no observable parasites (31). These puppies ultimately died at three months of age, emphasizing the potential lethal outcome for young, chagasic canines. Overall, the various infection routes highlight the complexity of *T. cruzi* transmission dynamics for humans and their domestic animal counterparts and stress the need to prevent infection in these hosts.

1.2.5 Parasite Control and Prevention

Current methods of parasite control are inadequate in preventing new infections, and no vaccines are available for human or veterinary use. Efforts targeting vectors through insecticidal spraying have been most effective in reducing domestic infestations and seroprevalance in sustained, supervised, community-based programs. (30). However, these efforts frequently become cumbersome to maintain over several years and in resource-limited settings. The resulting insect vector persistence and continued domestic transmission to dogs has therefore potentiated parasite resurgence following ineffective control and surveillance strategies.

As control programs are costly to maintain, require community trust and participation, and demand continued surveillance for success, alternative transmission control strategies have been investigated. Intervention strategies aimed at dogs have included continuous wearing of deltamethrin-treated collars, subsequently resulting in reductions in vector prevalence and fecundity (32). Culling of seropositive dogs has been suggested, but are arguably desirable and not proven to be consistently effective for other vector-mediated tropical diseases (33). As new infections continue to be identified, other strategies for parasite control and prevention are needed, particularly those targeting strategic transmission control points.

1.2.6 Role of Dogs in Transmission of T. cruzi

Though many mammals suffer from *T. cruzi* infection, dogs play a significant role in *T. cruzi* ecology and epidemiology. Studies show that the insect vector is several times more likely to feed on dogs than humans. For example, in engorged bugs, the ratio of blood meals from dogs to humans is 2.3 to 2.6 times the ratio of number of dogs to humans in the same area (34). In rural northwestern Argentina, dogs are epidemiologically important sources of infection for bugs and households, with dogs contributing 13.9 times more infection to the insect vector (35). As dogs live in close proximity to their human counterparts, dogs are a critical control point for *T. cruzi* transmission and a canine-targeted transmission-blocking vaccine would greatly reduce the prevalence of *T. cruzi* infection in the canine and human population. In previous studies, vaccination of dogs with field isolated attenuated parasite strains failed to prevent *T. cruzi* infection, but did substantially reduce transmissibility to insects (36). A more recent study involving vaccination of dogs with fixed epimastigotes of *T. rangeli*, a non-

pathogenic trypanosome also infecting people in the Americas, resulted in decreased parasitemias and reduced vectorial transmission (37). These previous studies support the concept that vaccination of dogs is a viable transmission control strategy for *T. cruzi* infection and warrants additional investigation into its development and application.

1.3 Project Objective

The goal of this project was to develop a safe, well-defined attenuated *T. cruzi* strain for vaccination of dogs. I predict that such a vaccine would reduce parasitemia and infection rates in dogs, insects, and ultimately, humans. One approach for creating live attenuated parasites involves disruption or deletion of genes whose products are predicted to be critical for parasite replication in mammals.

Transcriptome and proteome analysis of the four life stages of *T. cruzi* has revealed metabolic pathways that appear to be relatively more important to the parasite (38). I am particularly interested in gene products that are relatively increased in the amastigote stage as this is the only replicating stage in mammals and is a key target of host immune responses. I hypothesize that these gene products serve critical roles in infectivity, development, maturation and/or replication of *T. cruzi*, and the selective disruption of these genes would likely result in parasite lines with defects in one or more of these characteristics. I plan to make gene knockouts in the epimastigote stage, where the gene transcripts are not relatively high. These epimastigotes will be converted in culture to infective metacyclic trypomastigotes. I expect that upon infection, these parasites would be impaired in their ability to mature and replicate as amastigotes, and thus unable to maintain the infection. However, these dead and dying parasites would provide a potential stimulus for the development of protective immune responses.

Previous work in the Tarleton lab has provided evidence that gene knockouts in *T. cruzi* can be made using constructs produced utilizing a Multisite Gateway-based approach (39). Homologous recombination allows drug resistance markers to completely disrupt genes of interest while allowing selection of such parasites. Targeted genes for disruption will include putative fatty acid transporter and inosine-5'-monophosphate dehydrogenase proteins, both encoded by genes whose transcripts are increased in the amastigote life stage. Resulting mutant parasites will be evaluated via PCR and Southern blot for correct gene disruption. Complementation studies will validate the functional necessity of these genes and their products in null transgenic parasites. Mutant lines will be evaluated for growth deficiencies in the insect and mammalian life stages. *In vivo* testing in a mouse model will be used to determine infectivity, parasite load, and induction of immune responses. Mutant parasite infection followed by challenge with wild-type parasites will verify if these mutant parasites provide protection, the ideal of any vaccine candidate. As pilot work involving attenuated parasite vaccination *per os* stimulates *T. cruzi*-specific $CD8^+$ T cells and protects mice from wild-type *T. cruzi* footpad challenge (40), I contend the development and testing of knockout transgenic parasite lines is a viable strategy for developing live, attenuated *T. cruzi* parasite lines.

T. cruzi is an important public health issue in the Americas. I recognize that dogs play a significant role in the ecology and epidemiology of *T. cruzi* infection, and I propose that the vaccination of dogs is a viable transmission control strategy. The development of a live attenuated vaccine through selective gene disruption and establishment of canine-specific immunological methods for testing vaccine efficacy will

provide significant evidence supporting the future evaluation of canine vaccination to control *T. cruzi* transmission.

1.4 References

1. World Health Organization. 2010. Chagas disease (American trypanosomiasis).

2. Stuart, K., R. Brun, S. Croft, A. Fairlamb, R. E. Gurtler, J. McKerrow, S. Reed, and R. Tarleton. 2008. Kinetoplastids: related protozoan pathogens, different diseases. *J Clin Invest* 118:1301-1310.

3. Lescure, F. X., G. Le Loup, H. Freilij, M. Develoux, L. Paris, L. Brutus, and G. Pialoux. 2010. Chagas disease: changes in knowledge and management. *Lancet Infect Dis* 10:556-570.

4. Bern, C. 2011. Antitrypanosomal Therapy for Chronic Chagas' Disease. *New Engl J Med* 364:2527-2534.

5. Barr, S. C. 2006. American Trypanosomiasis. In *Infectious Diseases of the Dog and Cat*, 3 ed. C. E. Greene, ed. Saunders Elsevier, St. Louis. 676-681.

6. Barr, S. C. 2009. Canine Chagas' Disease (American Trypanosomiasis) in North America. *Veterinary Clinics of North America: Small Animal Practice* 39:1055-1064.

7. Barbabosa-Pliego, A., H. M. Diaz-Albiter, L. Ochoa-Garcia, E. Aparicio-Burgos, S. M. Lopez-Heydeck, V. Velasquez-Ordonez, R. C. Fajardo-Munoz, S. Diaz-Gonzalez, R. M. De Oca-Jimenez, M. Barbosa-Mireles, C. Guzman-Bracho, J. G. Estrada-Franco, N. J. Garg, and J. C. Vazquez-Chagoyan. 2009. Trypanosoma cruzi Circulating in the Southern Region of the State of Mexico (Zumpahuacan) Are Pathogenic: A Dog Model. *Am J Trop Med Hyg* 81:390-395.

8. Lauricella, M. A., M. B. Castanera, R. E. Gurtler, and E. L. Segura. 1998. Immunodiagnosis of Trypanosoma cruzi (Chagas' disease) infection in naturally infected dogs. *Mem I Oswaldo Cruz* 93:501-507.

9. WHO Expert Committee. 2002. Control of Chagas Disease. In *WHO Technical Report Series*. World Health Organization, Geneva.

10. Bustamante, J. M., L. M. Bixby, and R. L. Tarleton. 2008. Drug-induced cure drives conversion to a stable and protective CD8+ T central memory response in chronic Chagas disease. *Nature Medicine* 14:542-550.

11. Rodriguez, A. M., F. Santoro, D. Afchain, H. Bazin, and A. Capron. 1981. Trypanosoma cruzi infection in B-cell-deficient rats. *Infect Immun* 31:524-529.

12. Kumar, S., and R. L. Tarleton. 1998. The relative contribution of antibody production and CD8+ T cell function to immune control of Trypanosoma cruzi. *Parasite Immunol* 20:207-216.

13. Scott, M. T., and L. Moyes. 1982. 75Se-methionine labelled Trypanosoma cruzi blood trypomastigotes: opsonization by chronic infection serum facilitates killing in spleen and liver. *Clin Exp Immunol* 48:754-757.

14. Tarleton, R. L. 1990. Depletion of CD8+ T cells increases susceptibility and reverses vaccine-induced immunity in mice infected with Trypanosoma cruzi. *J Immunol* 144:717-724.

15. Tarleton, R. L., B. H. Koller, A. Latour, and M. Postan. 1992. Susceptibility of beta 2-microglobulin-deficient mice to Trypanosoma cruzi infection. *Nature* 356:338-340.

16. Tarleton, R. L., M. J. Grusby, M. Postan, and L. H. Glimcher. 1996. Trypanosoma cruzi infection in MHC-deficient mice: further evidence for the role of both class I- and class II-restricted T cells in immune resistance and disease. *Int Immunol* 8:13-22.

17. Vogt, J., C. D. A. Soto, M. P. Mincz, and G. A. Mirkin. 2008. Impaired Trypanosoma cruzi-specific IFN-gamma secretion by T cells bearing the BV9 T-cell receptor is associated with local IL-10 production in non-lymphoid tissues of chronically infected mice. *Microbes and Infection* 10:781-790.

18. Munozfernandez, M. A., M. A. Fernandez, and M. Fresno. 1992. Activation of Human Macrophages for the Killing of Intracellular Trypanosoma-Cruzi by Tnf-Alpha and Ifn-Gamma through a Nitric Oxide-Dependent Mechanism. *Immunology Letters* 33:35-40.

19. Martin, D. L., D. B. Weatherly, S. A. Laucella, M. A. Cabinian, M. T. Crim, S. Sullivan, M. Heiges, S. H. Craven, C. S. Rosenberg, M. H. Collins, A. Sette, M. Postan, and R. L. Tarleton. 2006. CD8+ T-Cell responses to Trypanosoma cruzi are highly focused on strain-variant trans-sialidase epitopes. *PLoS Pathog* 2:e77.

20. Martin, D., and R. Tarleton. 2004. Generation, specificity, and function of CD8+ T cells in Trypanosoma cruzi infection. *Immunol Rev* 201:304-317.

21. Schofield, C. J. 2001. Field testing and evaluation of insecticides for indoor residual spraying against domestic vectors of Chagas disease. World Health Organization, Geneva.

22. Bastos, C. J., R. Aras, G. Mota, F. Reis, J. P. Dias, R. S. de Jesus, M. S. Freire, E. G. de Araujo, J. Prazeres, and M. F. Grassi. 2010. Clinical outcomes of thirteen patients with acute chagas disease acquired through oral transmission from two urban outbreaks in northeastern Brazil. *Plos Neglect Trop D* 4:e711.

23. Roellig, D. M., A. E. Ellis, and M. J. Yabsley. 2009. Oral transmission of Trypanosoma cruzi with opposing evidence for the theory of carnivory. *The Journal of parasitology* 95:360-364.

24. Busch, M. P., S. H. Kleinman, and G. J. Nemo. 2003. Current and emerging infectious risks of blood transfusions. *Jama-J Am Med Assoc* 289:959-962.

25. Center for Disease Control and Prevention. 2006. Chagas disease after organ transplantation --- Los Angeles, California, 2006. In *MMWR Morbidity and Mortality Weekly Report*. 55(29): 798-800.

26. Gurtler, R. E., E. L. Segura, and J. E. Cohen. 2003. Congenital transmission of Trypanosoma cruzi infection in Argentina. *Emerg Infect Dis* 9:29-32.

27. Hermann, E., C. Truyens, C. Alonso-Vega, P. Rodriguez, A. Berthe, F. Torrico, and Y. Carlier. 2004. Congenital transmission of Trypanosoma cruzi is associated with maternal enhanced parasitemia and decreased production of interferon-gamma in response to parasite antigens. *The Journal of infectious diseases* 189:1274-1281.

28. Bittencourt, A. L., M. Sadigursky, A. A. Da Silva, C. A. Menezes, M. M. Marianetti, S. C. Guerra, and I. Sherlock. 1988. Evaluation of Chagas' disease transmission through breast-feeding. *Mem I Oswaldo Cruz* 83:37-39.

29. Martins, L. P., R. E. Castanho, A. B. Nogueira, O. T. Silva, and A. S. Gusmao. 2011. Incidence of Trypanosoma cruzi transmission through breastfeeding during acute experimental Chagas disease. *Braz J Infect Dis* 15:116-118.

30. Gurtler, R. E., U. Kitron, M. C. Cecere, E. L. Segura, and J. E. Cohen. 2007. Sustainable vector control and management of Chagas disease in the Gran Chaco, Argentina. *Proceedings of the National Academy of Sciences* 104:16194-16199.

31. Rodriguez-Morales, O., M. A. Ballinas-Verdugo, R. Alejandre-Aguilar, P. A. Reyes, and M. Arce-Fonseca. 2011. Trypanosoma cruzi Connatal Transmission in Dogs with Chagas Disease: Experimental Case Report. *Vector Borne Zoonotic Dis* 11:1365-1370.

32. Reithinger, R., L. Ceballos, R. Stariolo, C. R. Davies, and R. E. Gurtler. 2006. Extinction of experimental Triatoma infestans populations following continuous exposure to dogs wearing deltamethrin-treated collars. *Am J Trop Med Hyg* 74:766-771.

33. Nunes, C., V. Lima, H. Paula, S. Perri, A. Andrade, F. Dias, and M. Burattini. 2008. Dog culling and replacement in an area endemic for visceral leishmaniasis in Brazil. *Veterinary Parasitology* 153:19-23.

34. Cohen, J. E., and R. E. Gurtler. 2001. Modeling household transmission of American trypanosomiasis. *Science* 293:694-698.

35. Gurtler, R. E., M. C. Cecere, M. A. Lauricella, M. V. Cardinal, U. Kitron, and J. E. Cohen. 2007. Domestic dogs and cats as sources of Trypanosoma cruzi infection in rural northwestern Argentina. *Parasitology* 134:69-82.

36. Basombrio, M. A., M. A. Segura, M. C. Mora, and L. Gomez. 1993. Field trial of vaccination against American trypanosomiasis (Chagas' disease) in dogs. *Am J Trop Med Hyg* 49:143-151.

37. Basso, B., I. Castro, V. Introini, P. Gil, C. Truyens, and E. Moretti. 2007. Vaccination with Trypanosoma rangeli reduces the infectiousness of dogs experimentally infected with Trypanosoma cruzi. *Vaccine* 25:3855-3858.

38. Atwood, J. A., D. B. Weatherly, T. A. Minning, B. Bundy, C. Cavola, F. R. Opperdoes, R. Orlando, and R. L. Tarleton. 2005. The Trypanosoma cruzi proteome. *Science* 309:473-476.

39. Xu, D., C. P. Brandan, M. A. Basombrio, and R. L. Tarleton. 2009. Evaluation of high efficiency gene knockout strategies for Trypanosoma cruzi. *BMC Microbiol* 9:90.

40. Tarleton, R. L., M. H. Collins, J. M. Craft, and J. M. Bustamante. 2011. Oral Exposure to Trypanosoma cruzi Elicits a Systemic CD8(+) T Cell Response and Protection against Heterotopic Challenge. *Infection and Immunity* 79:3397-3406.

CHAPTER 2

DISRUPTION OF FATTY ACID TRANSPORTER PROTEIN INHIBITS INTRACELLULAR GROWTH AND REDUCES PERSISTENCE OF *TRYPANOSOMA CRUZI*[1]

[1] Hartley, A.N., J.M. Bustamante, A.M.C. Canavaci, and R.L. Tarleton. To be submitted to *PLOS Neglected Tropical Diseases*.

2.1 Abstract

Trypanosoma cruzi, the etiological agent of Chagas disease, infects individuals and wild and domestic animal reservoirs throughout the Americas. No vaccines are currently available for human or veterinary use. Using advances in targeted gene disruption for generating defined, genetically modified *T. cruzi* lines, we attempted to delete the genes encoding a putative fatty acid transporter FATP thought to be involved in fatty acid uptake. Although we were unable to generate null mutants, suggesting the *fatp* gene was essential, both epimatigotes and amastigotes were impaired in replication and in the ability to take up exogenous fatty acids *in vitro*. FATP-deficient parasites were also less pathogenic in vivo, stimulated strong *T. cruzi*-specific T cell responses, and were completely eradicated in some hosts. These data are consistent with the hypothesis that gene disruption of the uptake pathway in *T. cruzi* results in attenuated parasites impaired in persistence, yet able to prime a strong, *T. cruzi*-specific immune response.

2.2 Introduction

Eight to eleven million people are infected with *Trypanosoma cruzi*, with 14,000 individuals succumbing to the infection annually (1). Wild, domestic, and synatrophic mammals, including infected humans and their canine counterparts, are natural reservoirs for *T. cruzi* (2). Current methods for parasite control including insecticidal spraying, blood donor screening, and benznidazole drug treatment have been effective in lowering parasite burdens but have failed to completely eliminate parasite transmission in endemic regions. Identification of seropositive humans, dogs, and wildlife reservoirs (3) in the United States and individuals in Europe highlights the global expansiveness of T. cruzi and the need for diagnostic testing and investigation of transmission-blocking strategies.

No vaccine is currently available for human or veterinary use, but experimental canine vaccination protocols have illustrated decreased parasite transmission is possible with naturally attenuated *T. cruzi* parasite strains (4, 5). With unknown molecular basis for attenuation and reversion to virulence an ever-present concern for these naturally, attenuated strains, targeted gene disruption has emerged as an attractive method for generating defined, genetically modified *T. cruzi* parasites (6, 7). Targeting genes in metabolic pathways required for *T. cruzi* energy and growth appears ideal for creating parasite lines not only unable to persist indefinitely in mammalian hosts but also able to stimulate *T. cruzi*-specific immune responses, both model attributes of an ideal candidate vaccine.

As *T. cruzi* cycles from the insect vector gut to the cytoplasm of mammalian cells, it encounters strikingly different environments from which to derive energy. The *T. cruzi* proteome reveals a dramatic shift from carbohydrate- to lipid-related metabolism during the transition from trypomastigotes to intracellular amastigotes, suggesting fatty acids are a preferred energy source (8). *Combs et. al*. observed that *T. cruzi*-infected mice have significantly less adipose tissue during acute infection, higher parasite numbers in adipose tissue, and close proximity of parasites to lipid droplets in adipocytes (9). These data not only suggest *T. cruzi* may take advantage of free fatty acid uptake from lipid droplets but also identifies adipose tissue as a reservoir for *T. cruzi* infection. We hypothesize that fatty acids are an important energy source for intracellular *T. cruzi* amastigotes.

Cell acquisition of free fatty acids across biological membranes occurs through diffusion and protein-mediated mechanisms. *In vivo*, this process likely occurs due to the

latter as free fatty acids are typically found bound to such proteins as albumin at physiological conditions (10). Fatty acid transporter proteins (FATP) have been identified to function to not only facilitate but regulate fatty acid uptake during mammalian homeostasis (reviewed in (11)). FATPs are integral membrane-associated fatty-acid binding proteins, appear conserved evolutionarily, and create a family of six well-characterized FATPs proteins in mammals (10, 12). Various models have hypothesized how FATPs facilitate entry of fatty acids into cells, i.e. as sole transport proteins, in combination with other Acyl-CoA synthetases, or as dual FATP/Acyl-CoA synthetases (10). As we hypothesized that fatty acids are an important energy source for *T. cruzi* amastigotes and FATPs are critical for acquisition and translocation of fatty acids into a cell, we believed targeting disruption of a *T. cruzi* FATP would result in impaired parasite growth and persistence.

The *T. cruzi* genome annotates a single FATP-like gene (*fatp*) (13) which is highly expressed in amastigotes (14). To investigate the role of *Tc*FATP, a gene knockout strategy (6) was employed to disrupt *fatp*, resulting in double knockout parasites. Multiple attempts to make null *fatp* parasites failed, suggesting this gene was essential for *T. cruzi* survival. Transgenic *fatp* parasites exhibited decreased growth and fatty acid uptake as amastigotes. Decreased parasitemias and persistence in immunocompromised and immunocompetent hosts established that this parasite line was severely impaired, thus confirming the dependence of *T. cruzi* amastigotes on fatty acids *in vivo*.

2.3 Materials and Methods

2.3.1. *FATP sequence retrieval*

Nucleotide sequences for the single annotated *T. cruzi* fatty acid transporter protein-like (*fatp*) gene, designated as Tc00.1047053506799.10 and Tc00.1047053511907.110 alleles, were retrieved from the annotated CL-Brener *T. cruzi* genome (13).

2.3.2. *Construction of drug resistant cassettes for knockout*

Dual drug resistance cassettes flanked by the 5' and 3' untranslated regions (UTRs) were constructed utilizing Multisite Gateway Three-Fragment Vector Construction Kit (Invitrogen, Carlsbad, CA, USA) as previously described for *T. cruzi* (6). Briefly, 1102bp of 5'UTR and 890bp of 3' UTR flanking *fatp* were amplified using the following primers with UTR-specific sequences underlined: FATP_5F, GGGGACAACTTTGTATAGAAAAGTTGCTGCCTTTCGCCCAGATAG, FATP_5R, GGGGACTGCTTTTTTGTACAAACTTGCTCTTCCCTCCTGCAGTTTA, FATP_3F, GGGGACAGCTTTCTTGTACAAAGTGGGAGTGTTCTGCTTACATGTGC, and FATP_3R, GGGGACAACTTTGTATAATAAAGTTGCCTCACAACGTACCCCTCAC. Recombination of 5' and 3'UTRs into pDONRP4-P1R and pDONRP2R-P3, respectively, occurred during the BP reaction with BP Clonase. A pDONR221 plasmid containing either IF8-Hygromycin^R or IF8-Neomycin^R (6) served as a third plasmid during combination of the constructed UTR pDONRs with the final destination plasmid pDESTR4-R3 in an LR reaction. The final pDESTR4R3-5'UTR-IF8_drug^R-3'UTR plasmids was confirmed by sequencing and restriction enzyme digested to release 5'UTR-drug^R-3'UTR transfection cassettes.

2.3.3. *Parasites, transfection, and selection of transgenic strains*

CL strain *T. cruzi* epimastigotes were cultured at 27°C in supplemented liver digest-neutralized tryptose (LDNT) medium as previously described (15). For transfection, $1x10^7$ early log-phase epimastigotes were washed in 1xPBS, resuspended in 100μL Human T cell Nucleofactor™ Solution (Amaxa Inc, Cologne, Germany), mixed with 8-10μg transfection cassette or plasmid DNA, and electroporated using U-033 program and Amaxa Nucleofactor device (Amaxa Inc). Following LDNT culture overnight, electroporated parasites were supplemented with 600μg/mL Hygromycin B or 200μg/mL G418 for transfectants bearing the hygromycin resistance gene- or neomycin phosphotransferase gene-containing cassettes, respectively. Parasites were considered selected upon death of no DNA control transfectants. Previously constructed pTREX-TdTomato plasmids (16) bearing either the neomycin phophostransferase gene or blasticidin-resistance gene were transfected and selected with 250μg/mL G418 or 20μg/mL blasticidin. Subsequent transfection of single-drug resistant parasites with the alternative drug cassette or double-drug resistant parasites with pTREX-TdTomato plasmids were completed to create *fatp* dKO and *fatp* dKO-TdTom+ parasites lines.

2.3.4. Tc*FATP antibody production*

The C-terminal region of *fatp* was PCR amplified using PrimeSTAR HS DNA Polymerase (Takara Bio Inc, Japan) using the following primers with gene-specific regions underlined:

FATP_3F:GGGGACAAGTTTGTACAAAAAAGCAGGCTTCATGCCCTTTGCTTTCGGTAATGG and FATP_3R:

GGGGACCACTTTGTACAAGAAAGCTGGGTCCTATTACCACCCGCAATGCTGA.

The *fatp* gene amplicon was transferred to a pDONR plasmid and final his-tag bearing pEXP1-DEST plasmid via BP and LR reactions of the Multisite Gateway system. Following pEXP1-*fatp3*-DEST transformation into BL21(DE3)pLysS cells and overnight expression in autoinduction media (17), protein was extracted by sonication in 8M urea, 20mM HEPES, 100mM NaCl, pH8.0 (Buffer Z) containing 15mM imidazole. Lysate was incubated overnight with TALON^{TM} Metal Affinity Resin (BD Biosciences Clonetech, Palo Alto, CA, USA). Following elution with Buffer Z containing 250mM imidazole, proteins were processed with PD-10 desalting columns (GE Healthcare, Piscataway, NJ, USA) to remove imidazole, evaluated for correct size by SDS-PAGE, and stored at -20C until use. For mouse vaccination, 300ug *Tc*FATP3 protein was incubated with 750ul Dynabeads TALON^{TM} magnetic beads (Invitrogen) following manufacture instructions, washed to remove excess unbound protein, and resuspended in 1xPBS. BALB/C mice were injected with 100ul bead/protein preparation subcutaneously and boosted two and four weeks later. Sera testing against *Tc*FATP3- versus GFP-bound Qiagen Liquichip beads (Qiagen Inc, Valencia, CA, USA) in a bioplex assay, adapted from (18), confirmed anti-*Tc*FATP antibody specificity.

2.3.5. *Alamar blue growth assay*

Log-phase epimastigotes (1 x 10^6 parasites/well) were plated in 96 well Costar black plates (Corning Incorporated, Corning, NY, USA) in LDNT medium and incubated at 27°C. Following four hour incubation with Alamar Blue® reagent (AbD Serotec, Raleigh, NC, USA), triplicate wells were read in a Synergy H4 plate reader (Biotek, Winooski, VT, USA) with absorbance read at 670/685nm. Doubling times were

calculated by nonlinear regression curves for exponential growth using Prism 4.0 software (GraphPad Software, San Diego, CA, USA).

2.3.6. *Epimastigote transformation and metacyclic trypomastigote preparation*

Axenic induction of epimastigotes to metacyclic trypomastigotes were performed as previously described (14). Briefly, harvested log phase epimastigotes were inoculated at a starting density of $3x10^6$/ml in complete Grace's insect medium (Sigma no G8142, Sigma, St. Louis, MO, USA) supplemented with 10% fetal calf serum (HyClone Laboratories, ThermoScientific, Logan, UT, USA), pH 6.6 and incubated at 27°C for 12-13 days. Metacyclic trypomastigotes were harvested, washed in 1xPBS, and incubated in TAU media for 2 hr at 27°C (19). Following addition of TAU3AAG medium at a 1:7 TAU:TAU3AAG ratio, parasites were incubated horizontally overnight in cell culture flasks (Corning Incorporated) at 27°C. Nonadherent metacyclics were applied to a DEAE cellulose (Sigma no. D0909, Sigma) column and eluted with phosphate-buffered saline containing 5.4% glucose (PSG buffer), pH 8.0, as previously described (20).

2.3.7. In vitro *parasite infection and immuofluorescence assay*

For *in vitro* metacyclic trypomastigote infection, Vero cells (ATCC no. CCL-81) exposed to 2000 rad of gamma radiation (21) were cultured overnight at 37°C with RPMI supplemented with 10% FCS (14) in 96 well Greiner black bottom plates (cat no. 655090, Greiner Bio-One, Germany) or cell culture well plates (Corning Incorporated) with or without poly L-lysine-coated coverslips (cat no. #354085, BD Biosciences, Bedford, MA, USA). Metacyclic trypomastigotes were incubated at a 50 multiplicity of infection overnight, washed 3x to remove extracellular parasites, and assayed 4-5 days post infection. Microscopic images were taken with DeltaVision (Applied Precisions,

Issaquah, WA, USA) for slides and BD Pathway 435 (BD, Franklin Lakes, NJ, USA) for 96 well plate formats.

2.3.8. *BODIPY-C12 uptake assay*

T. cruzi epimastigotes were harvested, washed 2x in 1xPBS, and resuspended in 1xPBS at $1x10^8$ cells/mL. Parasites were incubated in 10uM BODIPY-C_{12} (Invitrogen) for 0-240 seconds and quenched in 0.3mM trypan blue. Cells were fixed in 3% paraformaldehyde in PBS for 20 minutes, permeabilized, and stained in 2μg/mL DAPI (Invitrogen). Parasites were resuspended in 1xPBS, spotted onto microscope slides, and visualized with a DeltaVision microscope (Applied Precisions). For the 96 well format, 50ul of epimastigotes resuspended in PBS at $6x10^7$/mL were aliquoted in triplicate into Greiner black bottom plates and incubated with 50ul of 5uM BODIPY-C_{12}:15uM free fatty acid BSA (Calbiochem cat no. 126575, EMD Biochemicals, Darmstadt, Germany) for 0-60 minutes. Following quenching with 50ul 1mM trypan blue, plate well fluorescence was read with Synergy H4 plate reader (Biotek, Winooski, VT, USA) with 485±20nm excitation and 528±20nm emission settings. For intracellular amastigote analysis, metacyclic trypomastigote-infected Vero cell cultures grown on poly L-lysine coated coverslips were washed 2x with PBS, incubated with 10uM BODIPY-C_{12} at 37°C for 0-60 minutes, washed 1x PBS, and fixed in 2% paraformaldehyde (in PBS) for 20mins at RT. Cells were permeablized in 0.25% Triton X100 (in PBS) for 10min, stained with 2ug/ml DAPI, and washed prior to mounting on slides. Images were acquired on a DeltaVision microscope and processed using SoftWorx software (both Applied Precisions).

2.3.9. In vivo *infection, parasitemias, and fluorescent imaging*

C57BL/6, BALB/c, and B6.IFNγ$^{-/-}$ (B6.129S7-*IFNg*^{tm1Ts}/J) mice were obtained from Jackson Laboratory and bred and maintained in the University of Georgia animal facility in microisolator cages under specific pathogen-free conditions. Metacyclic trypomastigote infections involved intraperitoneal or subcutaneous injections with $5x10^3$, $1x10^4$, or $2.5x10^5$ axenically derived metacyclic trypomastigotes. For challenge infections, mice were intraperitoneally injected with $1x10^4$ tissue culture trypomastigotes of *T. cruzi* Brazil strain harvested following Vero cell passage. For parasitemias, a minimum of 100-40x fields of 22mmx22mm coverslips of 5ul blood were examined for parasites. For fluorescent imaging following TdTom+ parasite footpad injection, mice were anaesthetized with 1.5% isofluorane and imaged daily using the Maestro2 *In Vivo* Imaging System (CRi, Woburn, MA, USA) as previously described (16). Footpad fluorescence was quantified with Maestro software v2.8.0A. All mouse protocols were approved by the University of Georgia Institutional Animal Care and Use Commmitee.

2.3.10. *T cell phenotyping*

Peripheral blood obtained by retro-orbital venipuncture and collected in sodium citrate solution was washed in PAB buffer (2% BSA, 0.02% azide in PBS (PAB)) prior to antibody staining. Blood was incubated in PAB with tetramer-phycoerythrin (PE) and a combination of the following antibodies: FITC-labeled antibody to CD44, APC- or APC-eflour780-labeled antibody to CD127, allophycocyanin-Cy7-labeled antibody to CD4, eflour-450-labeled CD8, PerCpCy5.5- or APC-labeled antibody to CD62L, and PE-Cy7-labeled antibody to KLRG1 (all eBioscience, San Diego, CA, USA). The *T. cruzi*-specific major histocompatibility complex (MHC) class I tetramer TSKB20/K^b

(ANYKFTLV on $H2K^b$) used in this study was synthesized at the Tetramer Core Facility (Emory University, Atlanta, GA, USA). Following antibody staining, red blood cells were lysed in hypotonic ammonium chloride solution, washed twice in PAB, and fixed in 2% formaldehyde. A minimum of 50,000 lymphocyte-gated cells was acquired on a CyAn ADP flow cytometer (DakoCytomation, Beckman Coulter Inc, Brea, CA).

2.3.11. *Immunosuppression to determine parasite persistence*

Immunosuppression by intraperitoneal cyclophosphamide (200mg/kg/d) administration was completed every 2-3 days for five total doses, as previously described (22). Following cyclophosphamide treatment, blood was collected for parasitemia, hemoculture, and hemotransfer. Parasitemias, as previously described here, and mortality of B6.IFN$\gamma^{-/-}$ mice receiving 200ul blood from negative parasitemic immunosuppressed C57BL/6 mice were determined. Hemocultures of 150ul blood in 10mL LDNT medium in T25 culture flasks (Corning) were examined at 15 and 30 days post inoculation. Mouse hind leg muscle, heart muscle, and adipose tissue were collected for DNA extraction as previously described (23). Real-time PCR analysis was performed on extracted DNA as described (23), utilizing iQ SYBR Green Supermix (Bio-Rad, Hercules, CA, USA) and specific primers for *T. cruzi* and mouse TNF-α genomic DNA (23). PCR reactions were performed with the iQ5 Multi-Color Real-Time PCR Detection System utilizing the iQ5 Standard Edition Optical System software, version 2 (both Bio-Rad). For each sample, division of *T. cruzi* satellite DNA quantity by mouse TNF-α DNA was used to determine *T. cruzi* parasite equivalents.

2.4. Results

Previous investigations of the whole organism proteome of all *T. cruzi* life cycle stages revealed an over-representation in amastigotes of enzymes involved in the beta oxidation of fatty acids conditions (8). The *T. cruzi* genome showed a single annotated fatty acid transporter protein-like gene (*fatp*) and previously published transcriptome data (14) revealed highest *fatp* expression in amastigotes, with a 2.2-fold increase relative to a reference RNA sample comprised of all four life-cycle stages (Figure 2.1A).

To help evaluate the necessity of *fatp*, the Multisite Gateway approach previously described for *T. cruzi* (6) was used to selectively disrupt both alleles of the *fatp* gene. Plasmids were constructed containing a drug resistance gene (hygromycin or neomycin) between the 5' and 3' untranslated regions (UTR) flanking *fatp*. Log-phase epimastigotes of *T. cruzi* were transfected with 5'UTR-drug resistance gene-3'UTR cassette and placed under drug selection 24 hours later. Parasites were selected within 3-4 weeks post-transfection suggesting homologous recombination utilizing the gene specific UTRs resulted in *fatp* replacement with a drug resistance marker gene. Isolated genomic DNA from *fatp* knockout (KO) epimastigotes was evaluated for correct replacement of one or both *fatp* alleles using southern blot and loci-specific primers for polymerase chain reaction (PCR). Following two successive rounds of targeting, southern blot analysis of gDNA from dual drug resistant transgenic *fatp* double knockout (dKO) epimastigotes utilizing an upstream 5'UTR sequence probe indicated insertion of both hygromycin and neomycin resistance genes at the *fatp* locus (Figure 2.1B-C). To confirm loss of *fatp*, PCR using internal *fatp*-specific primers was done and the results indicated retention of a *fatp* gene in *fatp* dKO epimastigotes (Figure 2.1D). Despite

repeated attempts using consecutive or simultaneous transfection and selection of drug resistant lines, the dual drug resistant parasites obtained always retained a *fatp* copy. To determine if these non-null double mutants had reduced expression of *fatp*, quantitative real-time PCR was performed. cDNA made from stage-specific harvested RNA revealed less *fatp* expression in *fatp* dKO amastigotes as compared to wild-type amastigotes (Figure 2.1E). Immunofluorescence using anti-TcFATP antibodies revealed cell surface amastigote expression of the transporter in both wildtype and *fatp* dKO parasite strains indicating *fatp* DKO parasites maintained a detectable level of FATP protein expression (Figure 2.1F). Reduced *fatp* transcripts in dual drug resistant amastigotes suggested these parasites may be deficient in fatty acid uptake despite maintaining *fatp*.

To determine the consequence of reduced FATP expression in *T. cruzi*, we examined *in vitro* parasite replication. *Fatp* dKO epimastigotes showed similar growth kinetics and doubling times to wild-type epimastigotes, consistent with the relatively low expression *fatp* in this insect resident stage of the life cycle (Figure 2.2A). In contrast, replication of intracellular amastigotes, assessed using lines expressing a transgene encoding the tdTomato (tdTom+) fluorescent protein, exhibited little to no replication in host cells (Figure 2.2B). Although FATP-deficient parasites infected host cells, significantly fewer cells remained infected at three days (Figure 2.2C-D) and cells infected with *fatp* dKO-TdTomato+ parasites produced significantly fewer parasites as compared to cells infected with wild-type-parasites (Figure 2.2E-F).

We next assessed exogenous fatty acid uptake in wild-type and *fatp* dKO parasites using BODIPY-C_{12}, a fluorescent fatty acid analog. BODIPY-C_{12} uptake was detectable in wild-type epimastigotes within ten seconds, while *fatp* dKO parasites were delayed for

up to 180 seconds (Figure 2.3A-B). BODIPY-C_{12} uptake into infected host cells also revealed delayed uptake in *fatp* dKO parasites as compared to wild-type amastigotes (Figure 2.3C-D). Overall, these data suggest that *fatp* dKO parasites are impaired in infectivity and/or replication and appear functionally impaired in fatty acid uptake.

The virulence of FATP-deficient parasites *in vivo* was evaluated initially in highly susceptible interferon-γ (IFN-γ)-knockout mouse model, where a single parasite results in lethal infection (Bustamante et al., unpublished). Throughout the infection, parasitemia levels in mice infected with *fatp* dKO parasites were 50- to 100-fold lower than in mice infected with WT parasites (Figure 2.4A). Although ultimately succumbing to the infection, *fatp* dKO-infected mice survived approximately three weeks longer than wild-type-infected mice (Figure 2.4B). Parasite replication at the infection site, an indication of *in vivo* intracellular expansion, was also significantly decreased in the case of FATP-deficient parasites relative to wild-type parasites (Figure 2.4C-D). Thus, *T. cruzi* deficient in the expression of FATP are inherently less virulent than wild-type parasites, irrespective of the immune competence of the host mice.

Infection of WT C57BL/6 mice with *fatp* dKO metacyclic trypomastigotes elicited a strong *T. cruzi*-specific $CD8^+$ T cell response, as determined using the MHC I-peptide tetramer of the immunodominant TSKB20/K^b epitope (Figure 2.5A). At 495dpi, *fatp* dKO-infected mice retained measureable, although reduced relative to wild-type mice, numbers of $CD8^+$TSKB20/K^{b+} T cells. Also in marked distinction to *T. cruzi*-specific T cells in wild-type mice at this point in infection, the majority of $CD8^+$TSKB20/K^{b+} T cells in mice infected with FATP-deficient parasites expressed high levels of the central memory cell surface marker CD127 (Figure 2.5B). As these

$CD8^{+}TSKB20/K^{b+}CD127^{hi}$ T cells were previously observed in mice cured of *T. cruzi* infection by treatment with benznidazole (22), we determined if parasites were cleared in these animals by immunosuppressing the mice using cyclophosphamide. Unlike wild-type-infected mice, *fatp* dKO-infected mice experienced no parasite recrudescence in blood following immunosuppression as determined by parasitemia and hemoculture. Furthermore, histological sections of skeletal muscle tissue of cyclophosphamide-suppressed mice previously infected with *fatp* dKO parasites revealed no evidence of parasite infection, in contrast to mice infected with wild-type parasites (Figure 2.5C). These data indicate that *fatp* dKO parasites establish a low-level infection in wild-type mice, generating long-lived *T. cruzi*-specific immune responses, but are ultimately cleared from these mice.

2.5. Discussion

Highly abundant and essential components, fatty acids are the building blocks of surface and compartmentalizing membranes, lipid-rich energy stores, and post-translational protein modifications. A fatty acid transport protein (FATP) were first identified as an integral membrane protein in murine adipocytes (24), and disruption of *FAT1*, a gene encoding a putative fatty acid transport protein, in *Saccharomyces cerevisiae* caused a decrease in cell growth and uptake of fatty acids, emphasizing the metabolic impact of FATP disruption (25). As intracellular amastigotes of *T. cruzi* exhibit a significant increase in the production of proteins involved in fatty acid beta oxidation (8), and preferentially persist in muscle cells and adipocytes (9), both cell types that import, store and utilize fatty acid as a primary energy source, (26), we hypothesized

that the uptake of fatty acid by *T. cruzi* would be crucial to the survival and replication of this intracellular parasite.

Reverse genetic approaches have long been used for validating particular gene functions. In *T. cruzi*, where gene silencing RNA interference has failed (27), high efficiency gene knockout strategies utilizing homologous recombination provide targeted gene deletion (6). In several instances, despite correct placement of cassettes, target gene persistence has made null parasite generation difficult (7) and thereby possibly identifying essential genes required for *T. cruzi*. In the present study, repeated attempts to make null *fatp* parasites failed, suggesting this gene's products were critical to *T. cruzi* survival. Alternatives for target gene deletion including the tetracycline inducible T7 promoter system (27) were considered but not pursued due to inherent leakiness of the systems. Small molecule control of targeted gene protein expression through destabilizing domains (DD) (28) was examined but concerns for insufficient proteasomal degradation and limited accessibility of the rescue ligand Shield-1 for membrane-bound FATP restricted DD applicability, despite recent advances described for *T. cruzi* (29). Adaptation and optimization of the *Trypanosoma brucei*-described CRE recombinase-based positive-negative selection system (30) for *T. cruzi* could facilitate future gene essentiality studies by completely eliminating *fatp*.

In the present study, *in vitro* growth assays showed similar doubling profiles between *fatp* dKO and wild-type insect-stage epimastigotes while *fatp* dKO mammalian-stage amastigotes infection resulted in significantly decreased percentage of infected cells and parasites burden within cells (Figure 2.2). Both *fatp* dKO epimastigotes and amastigotes experienced delays in BODIPY-C12 uptake studies as compared to wild-type

parasites (Figure 2.3). Though we did not predict epimastigotes to show a delay in fatty acid uptake phenotype but considering normal growth kinetics were observed, these data indicate *T. cruzi* epimastigotes are capable of fatty acid uptake but are likely not be the major energy source for insect stage growth. Fatty acid dependence of *fatp* dKO amastigotes for growth is consistent with different source requirements for each parasite stage, including histidine for insect-stage epimastigotes and fatty acids for mammalian-stage amastigotes, as corroborated by the relative abundance of fatty acid-related metabolism proteins in amastigotes (8).

With *fatp* dKO parasites attenuated in *in vitro* growth and functional assays, we evaluated infection, replication, and persistence in longer assaying periods (of greater than 9 days) by using the highly susceptible IFN$\gamma^{-/-}$ KO mouse model. Metacyclic trypomastigotes inoculation revealed *fatp* dKO parasites were able to infect but failed to produce as high parasitemias or as significant infection site pathology as wild-type infections (Figure 2.4). *Fatp* dKO infection did cause mortality in this model but were significantly delayed as compared to wild-type parasite infected counterparts. These data indicate *fatp* dKO parasites are able to infect and proliferate in a severely immune-deprived environment but do so at a significantly slower rate and magnitude as compared to wild-type parasites.

Thus far, our results indicate parasites deficient in the fatty acid transporter protein are severely impaired in the presence of little immune pressure. We next assessed the ability of *fatp* dKO parasites to persist in an immune competent host and to stimulate a *T. cruzi*-specific immune response. Monitoring the development and maintenance of *T. cruzi* specific $CD8^+$ T cells recognizing the dominant TSKB20 *trans*-sialidase gene-

encoding epitope (31) revealed *fatp* dKO parasites were primed and were maintained to chronic infection stage (Figure 2.5). The $CD8^{+}TSKB20/K^{b+}$ T cells present in *fatp* dKO-infected mice expressed high levels of the IL-7 alpha receptor CD127, which have been seen in drug-cured models of *T. cruzi* infection (22). No parasite recrudescence in blood, as indicated by negative hemocultures or parasitemias, and no parasite nests or inflammation in *fatp* dKO infections following cyclophosphamide treatment indicated *fatp* dKO parasites were cleared in infected animals (Figure 2.5C). *Fatp* dKO parasites were therefore unable to persist in mice to the chronic stage yet stimulate a *T. cruzi*-specific immune response.

In addition to exploring the dependence of intracellular amastigotes on fatty acids uptake for growth and persistence, we are interested in the use of genetically attenuated strains of *T. cruzi* as a possible vaccine strain. Ideally, an attenuated parasitic vaccine would infect a host "long" enough to stimulate a *T. cruzi*-specific immune response but then be hindered from persisting in a host, either through inherent or immune-driven methods. To our knowledge, genetically modified fatty acid transporter protein parasites are one of few described *T. cruzi* strains that appear to fit this characterization. Further work to assess the protective immune responses generated following *fatp* dKO parasite infection would need to be determined.

Though *fatp* dKO parasites are cleared in animals during the chronic stage of infection, coupling *fatp* dKO parasite vaccination with fatty acid reducing drugs, including many used in human cardiovascular studies, may help expedite parasite clearance while still priming a *T. cruzi*-specific immune response. The development of TdTomato fluorescent protein-expressing *fatp* dKO parasites may assist in screening such

compounds. At a minimum, further characterization of fatty acid metabolism in *T. cruzi* is critical for determining what next therapeutic and prophylactic modalities to pursue.

Overall, these studies describe a reverse genetics approach for identifying the essentiality and function of *fatp* and its protein product in *T. cruzi*. With attempts to disrupt *fatp* resulting in gene copy maintenance and resulting transgenic parasites impaired in fatty acid uptake, this work emphasizes the need to further characterize fatty acid metabolism in *T. cruzi*. Gene disruption resulting in attenuation and clearance of *fatp* dKO parasites in a mouse model of infection provides significant evidence for further evaluation of this parasite line as a transmission blocking vaccine candidate.

Figure 2.1. Targeted gene disruption of the amastigote-stage expressed *T. cruzi fatp* produces dual drug resistant parasites maintaining *fatp*. A, Level of *fatp* transcript expression as a log2 ratio over a cDNA reference sample in each life stage, as previously determined by Minning et al. (2009) *BMC Genomics*. B, Schematic representation of allelic BstYI restriction enzyme digestion of *fatp* loci with *fatp* maintenance or drug resistance gene replacement. Numbers indicate predicted fragments with a 5'UTR upstream probe. C, Southern blot of genomic DNA isolated from wild-type, single drug resistant (Neo sKO), and dual drug resistant (H+N dKO) epimastigotes and probed. D, PCR results of *fatp*-specific primers (intF, intR) with DNA from drug-resistant construction plasmids (hyg and neo plasmids) and from wild-type and transgenic *fatp* epimastigotes. E, Log2 ratio of *TcFATP* transcripts from *fatp* dKO over wildtype parasite cDNA samples from each life stage. F, Immunofluorescence analysis of *Tc*FATP expression on intracellular wild-type and *fatp* dKO amastigotes in Vero cells. Bar = 5μm.

Figure 2.1

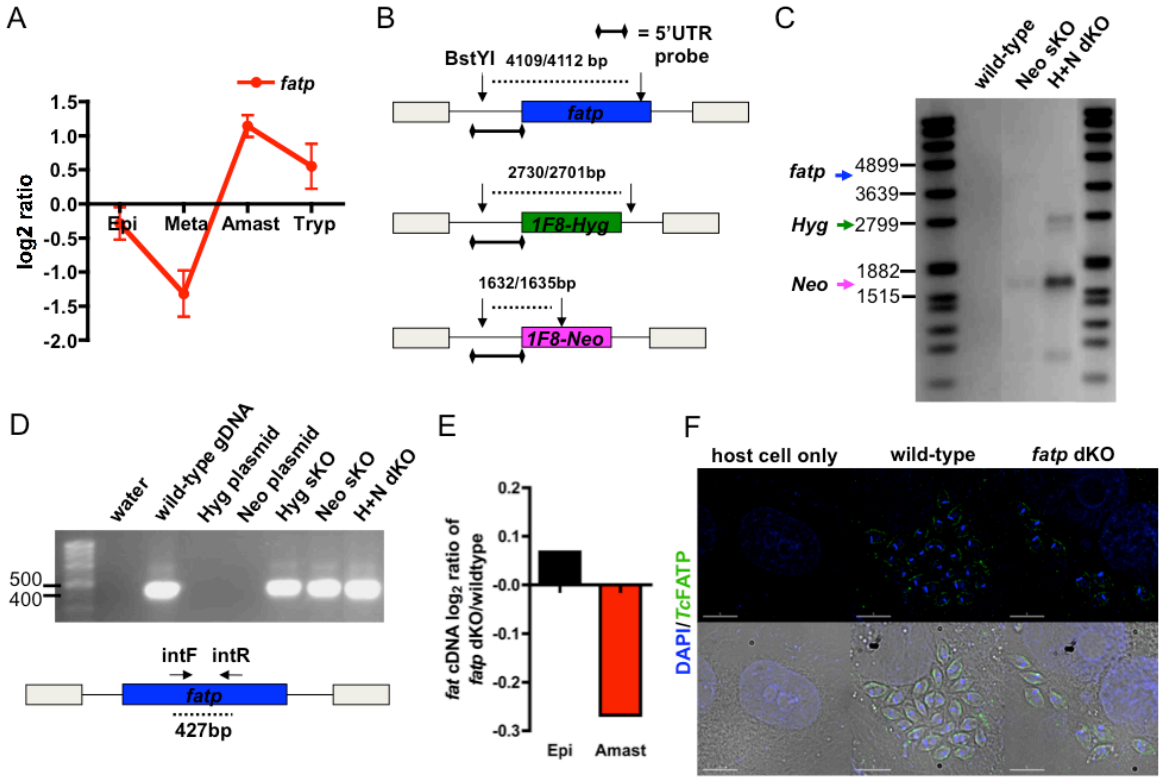
A
fatp
log2 ratio
1.5
1.0
0.5
0.0
-0.5
-1.0
-1.5
-2.0
Epi
Meta
Amast
Tryp
B
= 5'UTR probe
BstYI 4109/4112 bp
fatp
2730/2701bp
1F8-Hyg
1632/1635bp
1F8-Neo
C
wild-type
Neo sKO
H+N dKO
fatp
Hyg
Neo
4899
3639
2799
1882
1515
D
water
wild-type gDNA
Hyg plasmid
Neo plasmid
Hyg sKO
Neo sKO
H+N dKO
500
400
intF
intR
fatp
427bp
E
fat cDNA log2 ratio of fatp dKO/wildtype
0.2
0.1
-0.0
-0.1
-0.2
-0.3
Epi
Amast
F
host cell only
wild-type
fatp dKO
DAPI/TcFATP

Figure 2.2. *T. cruzi fatp* dKO epimastigotes grow at similar rates to wild-type parasites but exhibit decreased intracellular growth. A, Growth of wild-type and *fatp* dKO epimastigotes as determined by absorbance (670/685nm) of triplicate wells following 4hr alamar blue incubation. Numbers in legend indicate doubling time in days. B, Mean relative fluorescent units (RFU) from triplicate wells of Vero cells following 24 hour infection with wild-type-tdTom+ or *fatp* dKO-tdTom+ metacyclic trypomastigotes. C-D, Vero cells three days post infection with wild-type-tdTom+ or *fatp* dKO-TdTom+ stained with DAPI were imaged (C) and enumerated (D) for infected cells. E-F, DIC images and quantification of parasites per infected cells six days post infection with wild-type-tdTom+ and *fatp* dKO-tdTom+ metacyclic trypomastigotes.

Figure 2.2

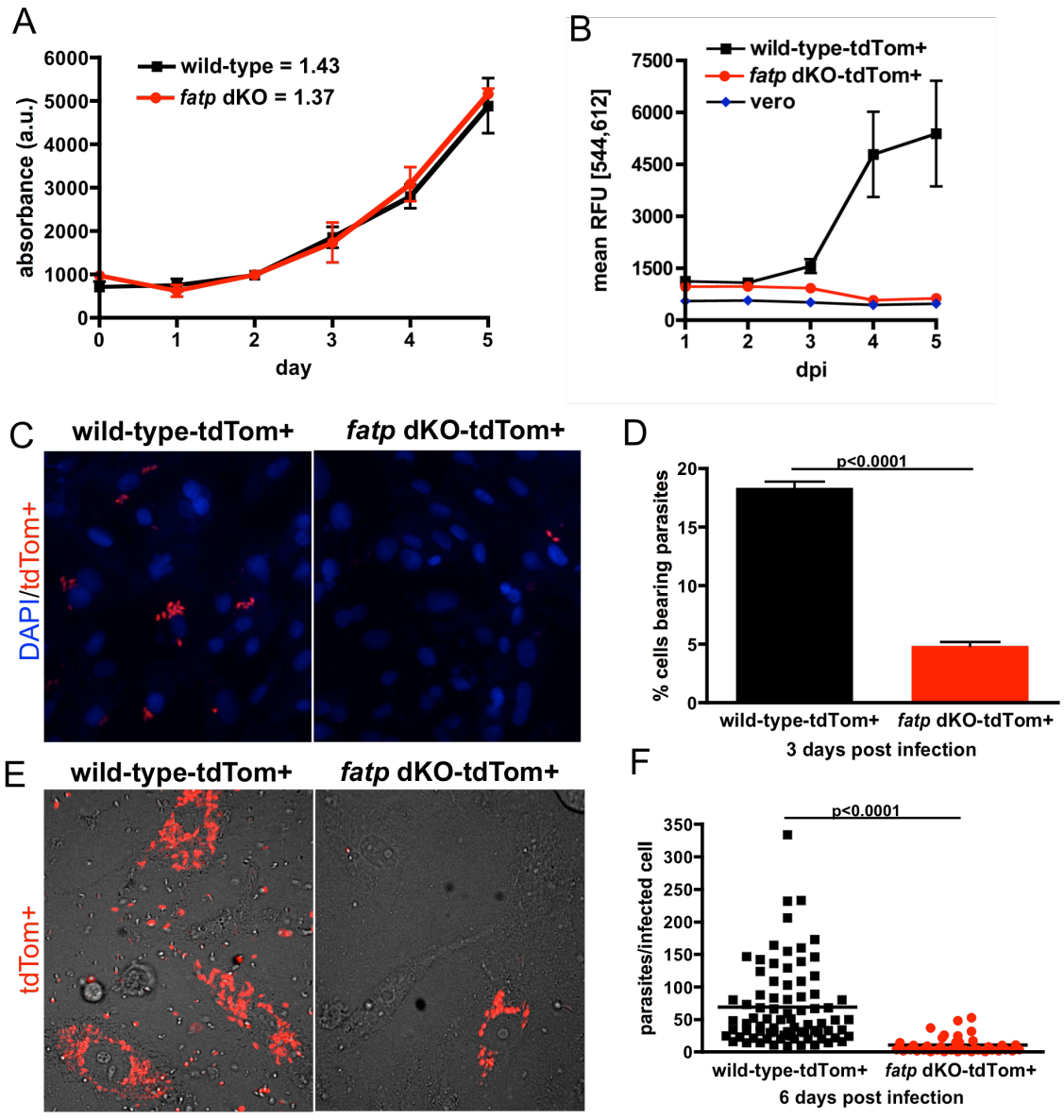
A
wild-type = 1.43
fatp dKO = 1.37
absorbance (a.u.)
day
B
wild-type-tdTom+
fatp dKO-tdTom+
vero
mean RFU [544,612]
dpi
C
wild-type-tdTom+
fatp dKO-tdTom+
DAPI/tdTom+
D
p<0.0001
% cells bearing parasites
wild-type-tdTom+
fatp dKO-tdTom+
3 days post infection
E
wild-type-tdTom+
fatp dKO-tdTom+
tdTom+
F
p<0.0001
parasites/infected cell
wild-type-tdTom+
fatp dKO-tdTom+
6 days post infection

Figure 2.3. Bodipy-C_{12} fatty acid analog uptake is impaired in *fatp* dKO parasites. Wild-type and *fatp* dKO epimastigotes were incubated with 10uM BODIPY-C_{12} for the indicated times, quenched with trypan blue, and imaged. B, Mean whole well fluoroescence intensity of wildtype and *fatp* dkO epimastigotes incubated with 10uM BODIPY-C_{12} and quenched with trypan blue. C, Images of wild-type- and *fatp* dKO-infected vero cells incubated with 10uM BODIPY-C_{12} for the indicated times, stained with DAPI, and imaged. D, Average mean fluorescence intensity of individual intracellular wild-type and *fatp* dKO amastigotes from (C).

Figure 2.3

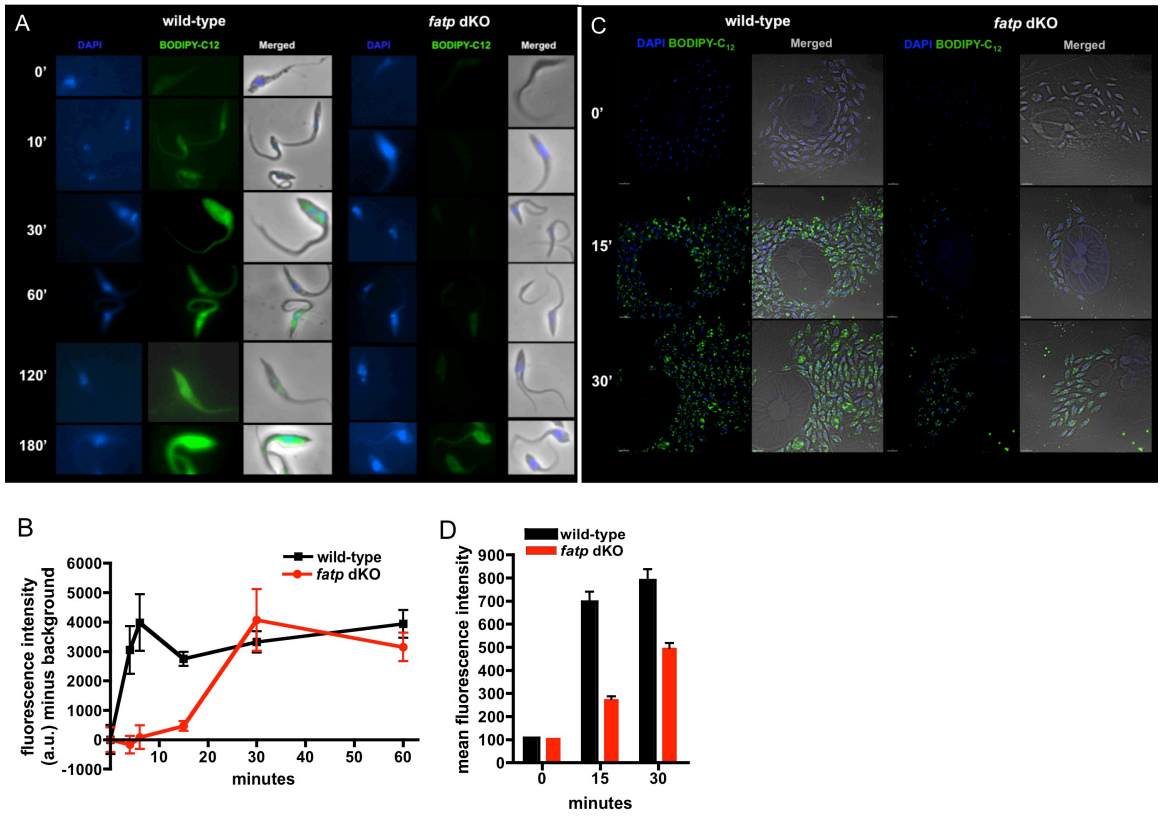
A
wild-type
fatp dKO
DAPI
BODIPY-C12
Merged
0'
10'
30'
60'
120'
180'
C
wild-type
fatp dKO
DAPI BODIPY-C12
Merged
0'
15'
30'
B
wild-type
fatp dKO
fluorescence intensity (a.u.) minus background
minutes
D
wild-type
fatp dKO
mean fluorescence intensity
minutes

Figure 2.4. Highly susceptible IFNγ$^{-/-}$ KO mice ultimately succumb to *fatp* dKO infection but experience decreased parasitemias and parasite persistence at the site of infection. Parasitemias (A) and survival (B) of IFNγ$^{-/-}$ mice infected with 5x10^{3} wild-type or *fatp* dKO metacyclic trypomastigotes. Data are cumulative from duplicate experiments. C, Representative *in vivo* foot pad imaging of IFNγ$^{-/-}$ mice one and ten days post-infection with 2.5x10^{5} wild-type-tdTom+ or *fatp* dKO-tdTom+ metacyclic trypomastigotes. D, Quantification of foot pad fluorescence from mice in (C) at indicated days post-infection.

Figure 2.4

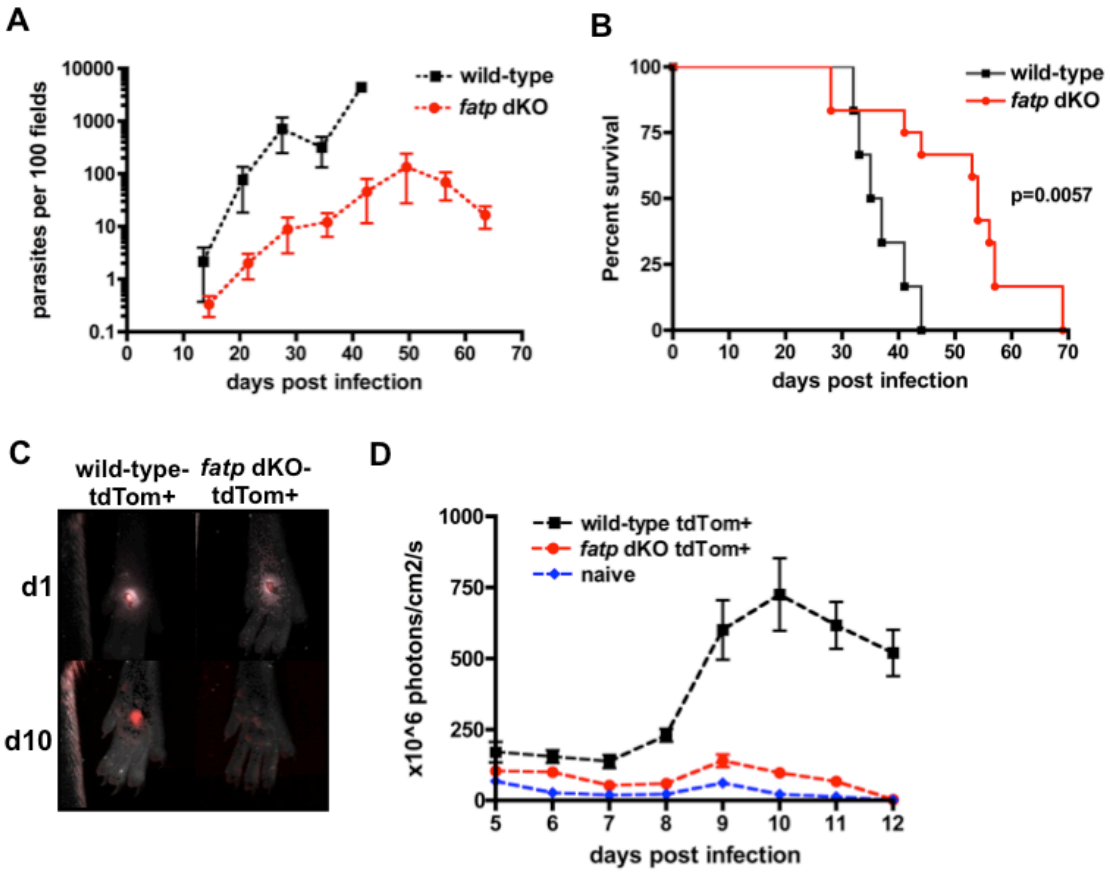
A
parasites per 100 fields
10000
1000
100
10
1
0.1
0
10
20
30
40
50
60
70
days post infection
wild-type
fatp dKO
B
Percent survival
100
75
50
25
0
days post infection
wild-type
fatp dKO
p=0.0057
C
wild-type-tdTom+
fatp dKO-tdTom+
d1
d10
D
x10^6 photons/cm2/s
1000
750
500
250
0
5
6
7
8
9
10
11
12
days post infection
wild-type tdTom+
fatp dKO tdTom+
naive

Figure 2.5 C57BL/6 mice infected with *fatp* dKO metacyclic trypomastigotes develop a dominant *T. cruzi*-specific T cell response with a central memory phenotype and no detectable parasite recrudescence following immunosuppression. A, A MHC-peptide tetramer of the immunodominant TSKB20/K^b detects *T.cruzi*-specific $CD8^+$ T cells in the blood 495 days post-infection. Numbers indicate percentage of TSKB20/K^b $tetramer^+$ among the total $CD8^+$ population. B, Expression of the central memory marker, $CD127^{hi}$ on $CD8^+$ T cells from naïve or $CD8^+$TSKB20/K^{b+} T cells from wild-type- or *fatp* dKO-infected animals. C, Histological sections from naïve, wild-type-infected, or *fatp* dKO-infected mice 27 days post immunosuppression. Arrowheads identifying amastigote nests. Scale bar, 200μm.

Figure 2.5

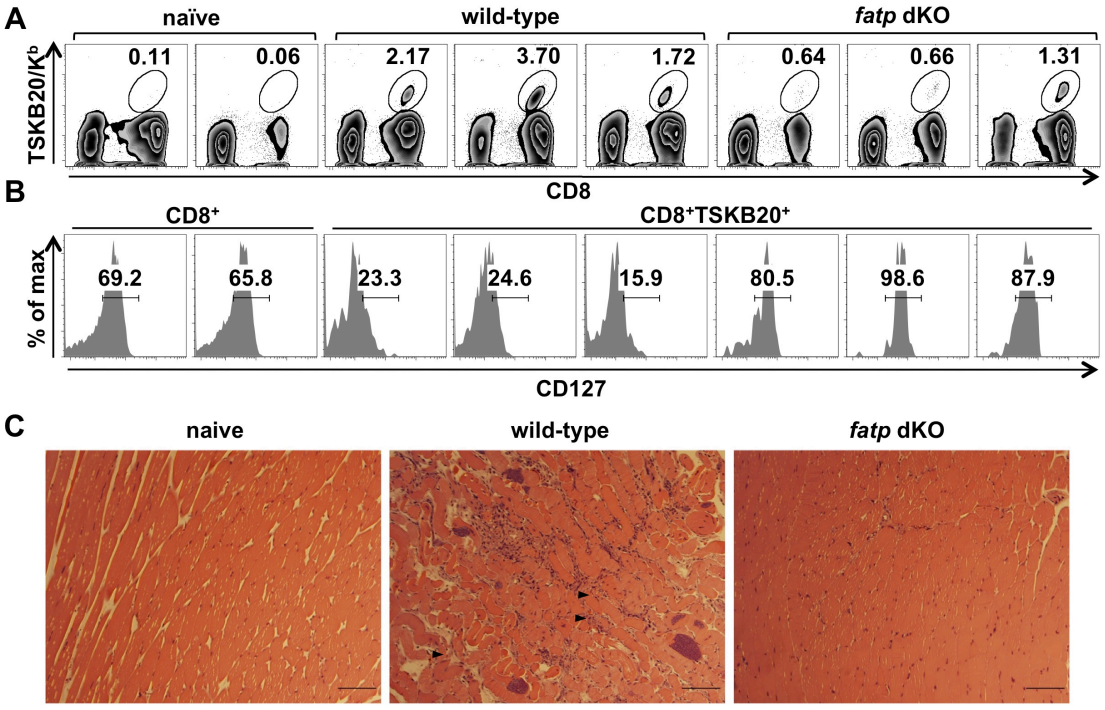
A
naïve
wild-type
fatp dKO
TSKB20/Kb
0.11
0.06
2.17
3.70
1.72
0.64
0.66
1.31
CD8
B
CD8+
CD8+TSKB20+
% of max
69.2
65.8
23.3
24.6
15.9
80.5
98.6
87.9
CD127
C
naive
wild-type
fatp dKO

2.6. References

1. Stuart, K., R. Brun, S. Croft, A. Fairlamb, R. E. Gurtler, J. McKerrow, S. Reed, and R. Tarleton. 2008. Kinetoplastids: related protozoan pathogens, different diseases. *J Clin Invest* 118:1301-1310.

2. WHO Expert Committee. 2002. Control of Chagas Disease. In *WHO Technical Report Series*. World Health Organization, Geneva.

3. Brown, E. L., D. M. Roellig, M. E. Gompper, R. J. Monello, K. M. Wenning, M. W. Gabriel, and M. J. Yabsley. 2010. Seroprevalence of Trypanosoma cruzi among eleven potential reservoir species from six states across the southern United States. *Vector Borne Zoonotic Dis* 10:757-763.

4. Basombrio, M. A., H. Arredes, D. A. Uncos, R. Rossi, and E. Alvarez. 1987. Field Trial of Vaccination against American Trypanosomiasis (Chagas-Disease) in Domestic Guinea-Pigs. *Am J Trop Med Hyg* 37:57-62.

5. Basombrio, M. A., M. A. Segura, M. C. Mora, and L. Gomez. 1993. Field trial of vaccination against American trypanosomiasis (Chagas' disease) in dogs. *Am J Trop Med Hyg* 49:143-151.

6. Xu, D., C. P. Brandan, M. A. Basombrio, and R. L. Tarleton. 2009. Evaluation of high efficiency gene knockout strategies for Trypanosoma cruzi. *BMC microbiology* 9:90.

7. Perez Brandan, C., A. M. Padilla, D. Xu, R. L. Tarleton, and M. A. Basombrio. 2011. Knockout of the dhfr-ts gene in Trypanosoma cruzi generates attenuated parasites able to confer protection against a virulent challenge. *Plos Neglect Trop D* 5:e1418.

8. Atwood, J. A., D. B. Weatherly, T. A. Minning, B. Bundy, C. Cavola, F. R. Opperdoes, R. Orlando, and R. L. Tarleton. 2005. The Trypanosoma cruzi proteome. *Science* 309:473-476.

9. Combs, T. P., Nagajyothi, S. Mukherjee, C. J. de Almeida, L. A. Jelicks, W. Schubert, Y. Lin, D. S. Jayabalan, D. Zhao, V. L. Braunstein, S. Landskroner-Eiger, A. Cordero, S. M. Factor, L. M. Weiss, M. P. Lisanti, H. B. Tanowitz, and P. E. Scherer. 2005. The adipocyte as an important target cell for Trypanosoma cruzi infection. *The Journal of biological chemistry* 280:24085-24094.

10. Doege, H., and A. Stahl. 2006. Protein-mediated fatty acid uptake: novel insights from in vivo models. *Physiology (Bethesda)* 21:259-268.

11. Glatz, J. F., J. J. Luiken, and A. Bonen. 2010. Membrane fatty acid transporters as regulators of lipid metabolism: implications for metabolic disease. *Physiol Rev* 90:367-417.

12. Gimeno, R. E. 2007. Fatty acid transport proteins. *Current Opinion in Lipidology* 18:271-276.

13. El-Sayed, N. M., P. J. Myler, D. C. Bartholomeu, D. Nilsson, G. Aggarwal, A. N. Tran, E. Ghedin, E. A. Worthey, A. L. Delcher, G. Blandin, S. J. Westenberger, E. Caler, G. C. Cerqueira, C. Branche, B. Haas, A. Anupama, E. Arner, L. Aslund, P. Attipoe, E. Bontempi, F. Bringaud, P. Burton, E. Cadag, D. A. Campbell, M. Carrington, J. Crabtree, H. Darban, J. F. da Silveira, P. de Jong, K. Edwards, P. T. Englund, G. Fazelina, T. Feldblyum, M. Ferella, A. C. Frasch, K. Gull, D. Horn, L. Hou, Y. Huang, E. Kindlund, M. Klingbeil, S. Kluge, H. Koo, D. Lacerda, M. J. Levin, H. Lorenzi, T. Louie, C. R. Machado, R. McCulloch, A. McKenna, Y. Mizuno, J. C. Mottram, S. Nelson, S. Ochaya, K. Osoegawa, G. Pai, M. Parsons, M. Pentony, U. Pettersson, M. Pop, J. L. Ramirez, J. Rinta, L. Robertson, S. L. Salzberg, D. O. Sanchez, A. Seyler, R. Sharma, J. Shetty, A. J. Simpson, E. Sisk, M. T. Tammi, R. Tarleton, S. Teixeira, S. Van Aken, C. Vogt, P. N. Ward, B. Wickstead, J. Wortman, O. White, C. M. Fraser, K. D. Stuart, and B. Andersson. 2005. The genome sequence of Trypanosoma cruzi, etiologic agent of Chagas disease. *Science* 309:409-415.

14. Minning, T. A., D. B. Weatherly, J. Atwood, 3rd, R. Orlando, and R. L. Tarleton. 2009. The steady-state transcriptome of the four major life-cycle stages of Trypanosoma cruzi. *BMC Genomics* 10:370.

15. Tyler, K. M., and D. M. Engman. 2000. Flagellar elongation induced by glucose limitation is preadaptive for Trypanosoma cruzi differentiation. *Cell Motil Cytoskeleton* 46:269-278.

16. Canavaci, A. M. C., J. M. Bustamante, A. M. Padilla, C. M. P. Brandan, L. J. Simpson, D. Xu, C. L. Boehlke, and R. L. Tarleton. 2010. In Vitro and In Vivo High-Throughput Assays for the Testing of Anti-Trypanosoma cruzi Compounds. *Plos Neglect Trop D* 4:-.

17. Studier, F. W. 2005. Protein production by auto-induction in high density shaking cultures. *Protein Expression and Purification* 41:207-234.

18. Cooley, G., R. D. Etheridge, C. Boehlke, B. Bundy, D. B. Weatherly, T. Minning, M. Haney, M. Postan, S. Laucella, and R. L. Tarleton. 2008. High throughput selection of effective serodiagnostics for Trypanosoma cruzi infection. *PLoS Negl Trop Dis* 2:e316.

19. Bourguignon, S. C., W. de Souza, and T. Souto-Padron. 1998. Localization of lectin-binding sites on the surface of Trypanosoma cruzi grown in chemically defined conditions. *Histochem Cell Biol* 110:527-534.

20. Teixeira, M. M., and N. Yoshida. 1986. Stage-specific surface antigens of metacyclic trypomastigotes of Trypanosoma cruzi identified by monoclonal antibodies. *Mol Biochem Parasitol* 18:271-282.

21. Yan, W., and S. N. Moreno. 1998. A method to assess invasion and intracellular replication of Trypanosoma cruzi based on differential uracil incorporation. *Journal of Immunological Methods* 220:123-128.

22. Bustamante, J. M., L. M. Bixby, and R. L. Tarleton. 2008. Drug-induced cure drives conversion to a stable and protective CD8+ T central memory response in chronic Chagas disease. *Nature Medicine* 14:542-550.

23. Cummings, K. L., and R. L. Tarleton. 2003. Rapid quantitation of Trypanosoma cruzi in host tissue by real-time PCR. *Mol Biochem Parasitol* 129:53-59.

24. Schaffer, J. E., and H. F. Lodish. 1994. Expression Cloning and Characterization of a Novel Adipocyte Long-Chain Fatty-Acid Transport Protein. *Cell* 79:427-436.

25. Faergeman, N. J., C. C. DiRusso, A. Elberger, J. Knudsen, and P. N. Black. 1997. Disruption of the Saccharomyces cerevisiae homologue to the murine fatty acid transport protein impairs uptake and growth on long-chain fatty acids. *The Journal of biological chemistry* 272:8531-8538.

26. Zhang, L., and R. L. Tarleton. 1999. Parasite persistence correlates with disease severity and localization in chronic Chagas' disease. *J Infect Dis* 180:480-486.

27. DaRocha, W. D., K. Otsu, S. M. Teixeira, and J. E. Donelson. 2004. Tests of cytoplasmic RNA interference (RNAi) and construction of a tetracycline-inducible T7 promoter system in Trypanosoma cruzi. *Mol Biochem Parasit* 133:175-186.

28. Banaszynski, L. A., L.-c. Chen, L. A. Maynard-Smith, A. G. L. Ooi, and T. J. Wandless. 2006. A Rapid, Reversible, and Tunable Method to Regulate Protein Function in Living Cells Using Synthetic Small Molecules. *Cell* 126:995-1004.

29. Ma, Y. F., L. M. Weiss, and H. Huang. 2012. A method for rapid regulation of protein expression in Trypanosoma cruzi. *International Journal for Parasitology* 42:33-37.

30. Scahill, M., I. Pastar, and G. Cross. 2008. CRE recombinase-based positive–negative selection systems for genetic manipulation in Trypanosoma brucei. *Mol Biochem Parasit* 157:73-82.

31. Martin, D. L., D. B. Weatherly, S. A. Laucella, M. A. Cabinian, M. T. Crim, S. Sullivan, M. Heiges, S. H. Craven, C. S. Rosenberg, M. H. Collins, A. Sette, M. Postan, and R. L. Tarleton. 2006. CD8+ T-Cell responses to Trypanosoma cruzi are highly focused on strain-variant trans-sialidase epitopes. *PLoS Pathog* 2:e77.

CHAPTER 3

CHEMOKINE RECEPTOR 7 (CCR7)-EXPRESSION AND IFNγ PRODUCTION DEFINE VACCINE-SPECIFIC CANINE T CELL SUBSETS[2]

[2] Hartley, A.N. and R.L. Tarleton. To be submitted to *Veterinary Immunology and Immunopathology.*

3.1 Abstract

Canines suffer from and serve as strong translational animals models for many immunological disorders and diseases. Commercially available reagents and described techniques are limited for identifying and characterizing canine T cell subsets and evaluating T cell-specific effector function. To define reagents for delineating naïve versus activated T cells and identify antigen-specific T cells, we tested anti-human and anti-bovine T-cell specific cell surface marker reagents for cross-reactivity with canine PBMCs. Both $CD4^+$ and $CD8^+$ T cell from healthy canine donors showed reactivity to CCL19-Ig, a CCR7 ligand, and coexpression with CD62L. An *in vitro* stimulation with concavalin A validated downregulation of CCR7 and CD62L expression on stimulated control PBMCs, consistent with an activated T cell phenotype. Anti-IFNγ antibodies identified antigen-specific IFNγ-producing $CD4^+$ and $CD8^+$ T cells upon *in vitro* vaccine antigen PBMC stimulation. PBMC isolation within 24 hours of sample collection allowed for efficient cell recovery and accurate T cell effector function characterization. These data provide a reagent and techniques platform for identifying canine T cell subsets and circulating antigen-specific canine T cells for use in diagnostic and field settings.

3.2 Introduction

Domestication and tractability have allowed dogs to serve as research subjects for canine-specific diseases as well as models for human disorders. In particular, dogs serve as robust translational models in cardiovascular (1), neoplastic (2, 3), immunological (4, 5), neurological (6, 7), and genetic (8) research studies. Canines are also susceptible to and serve as models of zoonotic diseases such as leishmaniasis and American

trypanosomiasis and hence used to evaluate anti-parasitic chemotherapeutic regimens (9). Techniques and commercially available reagents are scarce for studying the canine immune system, especially as compared to those available for humans. As basic research pursues translational applications in animals more physiologically similar to humans, and veterinary medicine strives for more individualized patient therapies, an increasing need exists for identifying, characterizing, and monitoring the canine immune response.

The First International Canine Leukocyte Antigen Workshop (CLAW) was a significant step in identifying canine homologs of human CD antigens that delineated leukocyte populations by monoclonal antibodies (10). Clusters of antibodies collected from several sources identified canine equivalents of CD4, CD8, and Thy1.1 antigens from peripheral blood. Additional antibodies reactive to canine leukocyte antigens including CD45R (11) CD45RA (12), CD11/CD18 (13, 14), and CD62L (15) and to platelet and erythrocyte antigens (16) have been described separately from the CLAW workshop. Testing of monoclonal antibodies specific for cytokines in other species have also identified IL-4-, IL-8-, and IFN-γ-producing canine PBMCs and expanded the repertoire of canine specific reagents (17). However, despite these advances, delineating and characterizing naïve, activated, and memory T cell subsets in canines has remained limited.

The aim of this project was to identify and validate immunological reagents for characterizing canine T cells through phenotypic and effector function evaluation-based assays. Detection of the canine cross-reactive CCL19-hIg, a ligand for CCR7, identified naïve and antigen-experienced but not recently activated canine T cells. CCR7 cell surface expression was consistent with CD62L, a L-selection expressed by naïve and

central memory T cells during homing to secondary lymphoid organs. Decreases in CCR7 and CD62L expresson following antigen stimulation or mitogen activation correlated with upregulation of the activation marker, CTL2.58, and delineated activated T cells. IFNγ-production following PBMC whole vaccine stimulation defined antigen-specific T cell effector function. Extended time between blood collection and PBMC isolation of up to twenty-four hours revealed no significant loss in identifying vaccine-specific IFNγ-producing T cells. These data provide a reagent platform for identifying and characterizing canine T cell populations and assessing antigen-specific effector function.

3.3 Materials and Methods

3.3.1. *Animals and isolation of mononuclear cells*

Approximately 40-50mls of blood from four clinically healthy dogs were drawn into heparinized tubes (Vacutainer, Becton-Dickinson, Franklin Lakes, NJ, USA) by venipuncture. Isolation of peripheral blood mononuclear cells (PBMCs) occurred immediately following collection or as otherwise indicated and as previously described for human subjects (18). Plasma samples were collected and frozen at -20°C. PBMCs were washed in Hank's buffered balance salt solution (Mediatech Inc., Manassas, VA, USA) and resuspended in RPMI-1640 (Mediatech Inc.) completed with 50uM 2-β-mercaptoethanol, 2mM L-glutamine, 25ug/mL gentamicin, 200U/mL penicillin (Mediatech Inc), 2ug/mL streptomycin (Mediatech Inc), 1mM sodium pyruvate, and 10% heat-inactivated (30min, 56°C) and aggregate-removed (800gx30mins) fetal calf serum (HI-FCS) (HyClone Laboratories, ThermoScientific, Logan, UT, USA). Resuspended cells were frozen in media containing 10% dimethyl sulfoxide (Acros Organics, Fair

Lawn, NJ, USA) in liquid nitrogen for long-term storage. Prior to use, PBMCs were recovered, thawed at 37°C, washed and resuspended in complete RPMI-1640 + 10% HI-FCS. These purification, storage, and recovery procedures consistently yielded >95% viability, as determined by microscopic examination of trypan blue dye exclusion. All animal use protocols were approved by the University of Georgia Institutional Animal Care and Use Committee.

3.3.2. *PBMC antibody reactivity*

For testing canine T cells antibody reactivity, a minimum of $2x10^5$ PBMCs, were stained at 1:50 antibody dilution in PBS containing 1% BSA and 0.05% sodium azide (PAB; both from Sigma-Aldrich, St. Louis, MO, USA) at 4°C for 45 minutes. Antibodies tested were those defined in Table 1. Cells were fixed in 2% formaldehyde prior to flow cytometric collection.

3.3.3. *T cell stimulation and proliferation assessment assays*

A total of $4x10^5$ PBMCs were stimulated in a 96-well flat-bottom tissue culture plate (Costar, Corning, NY, USA) at 37°C in the presence of media, 15ug/mL anti-canine CD3 (AbD Serotec, Raleigh, NC, USA), or 0.25ug/mL concanavalin A (Sigma-Aldrich) for the indicated days. For assessment of proliferation, PBMCs were washed twice with PBS, incubated with 5μM CFSE (Molecular Probes, Eugene, OR), quenched with FCS, and plated. Two days post-stimulation, centrifuged and washed cells were incubated with or without CCL19-hIg (ELC; (19)) supernatant at 4°C for 45 minutes. Antibodies used were anti-CD8-Pacific Blue, anti-CD62L-PE (AbD Serotec), anti-human IgG-AF488 (Molecular Probes), and a cocktail containing anti-dog Pan T cell-APC, anti-B cell-PE, and anti-dog T cell Activation marker-FITC (Dog Activated T Lymphocyte Cocktail, BD

Pharmingen, BD Biosciences, San Jose, CA). 7-amino-actinomycin D (7AAD; BD Pharmingen) was included for live/dead cell discrimination. Cells were stained in PAB for 45 minutes at 4°C, washed, and fixed in 2% formaldehyde.

3.3.4 *Intracellular cytokine staining*

For assaying IFNγ levels, $4x10^5$ PBMCs were stimulated for 5hr in the presence of 2ng/mL phorbol 12-myristate 13-acetate (PMA), 4ug/mL Ca^{2+} ionomycin (Sigma-Aldrich), and brefeldin A (BD GolgiPlug; BD Biosciences) (17). For polyclonal activation, PBMCs were plated with 15ug/mL anti-CD3 (AbD Serotec) or diluted whole vaccine antigens, incubated overnight at 37°C and brefeldin A added 5hr prior to end of incubation. Canine vaccines were IMRAB 3TF (Rabies; Merial, Athens, GA, USA), Duramune 5 (Canine distemper-Adenovirus Type 2-Parainfluenza-Parvovirus (DAPP); Fort Dodge Animal Health, Fort Dodge, IA, USA), and Leptovax 4 (Leptospirosis bacterial extract; Fort Dodge Animal Health) vaccines. Cells were stained with anti-CD8-Pacific Blue and anti-CD4-FITC (AbD Serotec) followed by intracellular staining with anti-bovine anti-IFN-γ AF647 (AbD Serotec) according to the BD Cytofix/Cytoperm kit (BD Biosciences).

3.3.5 *Flow Cytometry and Analysis*

A minimum of 250,000 events were collected for each sample on a CyAn ADP using Summit, version 4.3 (Beckman Coulter, Fullerton, CA, USA). FlowJo flow cytometry analysis software, version 9 (Tree Star, Ashland, OR, USA) was used for analyses.

3.4 Results

As $CD4^+$ and $CD8^+$ T cells play critical roles in various infections, our primary efforts focused on identifying T cells and discriminatory surface markers for naïve,

activated, and memory T cells subsets. A reagent panel used for testing of cross-reactivity with canine peripheral blood mononuclear cells (PBMCs) included antibodies purchased commercially or kindly provided by other investigators (Table 3.1). A reagent was judged as positive if reactive with >2% of PBMCs. Utilizing this strategy, fifteen of twenty-six reagents were cross-reactive with canine PBMCs as denoted in Table 3.1, with eleven of twelve (91.7%) previously referenced reactive antibodies confirmed in this study. If a reagent distinguished distinct cell populations individually or following incubation in a T cell stimulation protocol, the reagent was found to be discriminatory, as noted in Table 3.1.

For antibodies recognizing putative cell surface markers on T cells, we repeated staining to validate marker expression on $CD4^+$ and $CD8^+$ T cells. Canine T cell reactivity was found with CCL19-Ig (ELC), a fusion protein serving as a chemokine ligand of CCR7 (19) and previously described to have reactivity with naïve and central memory ovine T cells (20). As circulating T cells traffic from the blood and home to lymph nodes, naïve and central memory T cells express CCR7 and other adhesion molecules, like L-selection (CD62L) and LFA-1, to tether and arrest to endothelium for transmigration across high endothelial venules. To investigate if circulating canine $CD4^+$ and $CD8^+$ T cells express both CCR7 and L-selectin (CD62L), PBMCs were stained with anti-CD4, anti-CD8, CCL19-Ig, and anti-CD62L. In clinically healthy canine donors, $CD4^+$ and $CD8^+$ T cells expressed measureable levels of CCR7 (Figure 3.1A). Unlike CCR7 expression in human $CD8^+$ T cells (21), CCR7 expression by canine $CD8^+$ T cells varied greatly between individual dogs. In comparison to humans and sheep where >85% of $CD4^+$ T cells express CCR7 (20, 21), approximately 40-50% of canine $CD4^+$ T cells

from healthy donors expressed CCR7. The observed difference is likely explained by the decreased ability of CCL19-hIg to delineate distinct peaks associated with $CCR7^+$ and $CCR7^-$ canine $CD4^+$ T cells populations (Figure 3.1A) versus a difference in species or health status of the hosts. Exploration of alternative secondary fluorophore combinations yielded similar $CCR7^+CD4^+$ T cell percentages (not shown). Both canine $CD4^+$ and $CD8^+$ T cells also showed reactivity to the lymph node homing marker CD62L (Figure 3.1B) and this expression agreed with that of CCR7 (Figure 3.1C), as the predominance of $CD4^+CD62L^{hi}$ T cells expressed CCR7, results consistent with that observed in human peripheral blood (21). Taken together, the cell surface markers of CCR7 and CD62L identified canine $CD4^+$ and $CD8^+$ T cell populations consistent with the phenotype of naïve or central memory T cells.

To evaluate if CCR7 and other cross-reactive antibodies identified in Table 3.1 were discriminatory for naïve versus activated T cells, a method and assay for T cell activation was used. For this purpose, CFSE-labeled canine PBMCs were incubated in media alone or with the T cell mitogen concanavalin A (ConA), and stimulation and proliferation was evaluated by changes in cell size and CFSE dilution. A comparison of forward versus side scatter revealed PBMC stimulated with ConA were on average volumetrically larger than unstimulated cells, consistent with cellular activation (Figure 3.2A). CFSE dilution indicated cell division of ConA-stimulated $CD8^+$ T cells as early as three days post stimulation (Figure 3.2B).

As we proposed the CCR7 and CD62L reagents identified naïve and central memory canine T cells, we hypothesized that following T cell activation canine T cells would decrease expression of CCR7 and CD62L. To address this hypothesis, canine

PBMCs were cultured in the presence of anti-CD3, ConA, or media alone. Even before detectable proliferation by CFSE dilution two days post stimulation (Figure 3.3A), $CD8^+$ T cells expressed less CCR7 (Figure 3.3B) and CD62L (Figure 3.3C) when activated. Expression levels of these two markers were consistent with the strength of stimulus, as ConA-stimulated $CD8^+$ T cells expressed less CCR7 and CD62L than cells stimulated with anti-CD3. Co-expression of both CCR7 and CD62L also decreased in stimulated cells, with ConA-stimulated cells showing greater decreases than cells incubated with anti-CD3 (Figure 3.3D). Downregulation of CCR7 and CD62L cell surface expression further correlated with increased expression of the activation marker ($CTL2.58^+$) on stimulated T cells (Figure 3.3E) and $CD8^+$ T cells (Figure 3.3F). These experiments identified markers for defining activated $CTL2.58^+CD8^+$ T cells and naïve or central memory-like $CCR7^+CD62L^{hi}CD8^+$ T cells in dogs. Testing of other canine T cell reactive reagents listed in Table 1, including CD45RA, CD45RO, and CD11a, in media versus stimulatory conditions did not alter antibody T cell reactivity in our stimulation assay or were not detectable using secondary antibody reagents and therefore were not investigated further. These results are noted as "not discriminatory" in Table 3.1.

Cognate antigen recognition through the TCR results in effector cytokine production, and thereby provides a method for evaluating and delineating antigen-specific T cells. To assay the production of the effector cytokine IFNγ by canine T cells in response to previously seen antigens, PBMCs were isolated from three healthy dogs vaccinated three weeks prior with IMRAB 3TF (Rabies), Duramune 5 (Canine distemper-Adenovirus Type 2-Parainfluenza-Parvovirus (DAPP)), and Leptovax 4 (Leptospirosis bacterial extract) vaccines. Following incubation of cells with media or vaccine antigen

overnight, intracellular IFNγ staining was performed to identify vaccine-specific $CD4^+$ and $CD8^+$ T cells. $CD4^+$ T cells from three of three dogs produced IFNγ in response to rabies vaccine, whereas only one of three had IFNγ-producing cells when stimulated with DAPP vaccine antigens (Figure 3.4A). $CD8^+$ T cells from two of three dogs produced IFNγ in response to rabies vaccine, but all appeared to not be significantly different from media controls when stimulated with the DAPP vaccine (Figure 3.4B). Despite differences in vaccine sources and stimulus concentrations, the low levels of detectable of IFNγ-producing T cells following canine distemper vaccine (DAPP) stimulation were consistent with previously published ELISAs of stimulated PBMC culture supernatants (22). Both $CD4^+$ and $CD8^+$ T cell subsets failed to produce robust IFNγ in response to the Leptovax 4 vaccine, suggesting this vaccine failed to elicit a strong T cell-specific immune response three weeks post administration, consistent with the predominant humoral response elicited by the bacterial antigens of the leptospiral vaccine (23). These results provide a flow cytometric method for identifying antigen-specific $CD4^+$ and $CD8^+$ T cells and evaluating IFNγ production for individual canine T cells.

In fieldwork settings, circumstances may arise where PBMC isolation will occur hours following sample collection, as is the case in field sampling. We asked how this timing would affect sample quality and ability to identify antigen-specific and cytokine-producing T cells. To address this question, we determined recovery and effector function of T cells isolated at various times post-blood collection. Incubation of cells with media or PMA/Ca^{2+} ionomycin followed by intracellular cytokine staining revealed no significant loss in quantities or percentages of IFNγ-producing T cells isolated up to 24 hours post collection (Figure 3.5). In PBMCs purified 48 hours following

venipuncture, a five-fold reduction in recovery of both $CD4^+$ and $CD8^+$ T cell as compared to the 24 hours post collection time point was observed. Additionally, unstimulated $CD4^+$ T cells produced significantly higher levels of IFNγ. These data provide an optimal method for PBMC isolation for application to fieldwork settings and for accurate evaluation of T cell effector function.

3.5 Discussion and Conclusion

T cells play a central role in the initiation and regulation of the immune response. T cells modulate cell surface expression of ligands and receptors to execute effector function and communicate with the environment. T-cell receptor complex signaling and CD28 co-stimulation results in naïve T cells downregulating lymph node homing receptors (CD62L and CCR7) while upregulating expression of cell adhesion molecules (CD44), T-cell receptor signaling (CD45RO), and early activation (CD69) antigens. Reliable expression of these cell surface molecules following cognate antigen encounter affords T cell monitoring during disease processes. Diagnosis and progression of human T cell lymphoproliferative disorders have been examine through flow cytometic immunophenotyping. Similar individualized diagnostics are being pursued for veterinary patients, but the paucity of literature describing the detection and characterization of antigen-driven T cell responses limits reaching this goal.

To address the growing need of canine immune system characterization for individualized diagnoses and toward furthering dogs as suitable translational research models, we aimed to identify and validate canine-specific reagents for discriminating naïve versus activated T cells. Novel canine T cell reactivity of CCL19-Ig defined CCR7 expression in $CD4^+$ and $CD8^+$ T cells of healthy donors. CCR7 co-expression with

CD62L and decreased expression following stimulation validated these markers for defining naïve or central memory $CD8^+$ T cells. The activation marker CTL2.58 further delineated activated T cells. Combining these reagents into a single panel would allow for identification of naïve or central memory T cells as $CCR7^+CD62L^{hi}CTL2.58^-$ and activated T cells as $CCR7^-CD62L^{lo}CTL2.58^+$. To our knowledge, these results are the first to describe and validate these markers for identifying naïve and activated canine T cell subsets.

With cognate antigen recognition stimulating cytokine-mediated T cell effector function, identification of IFNγ-producing T cells is critical for evaluating appropriate T cell responses. Monitoring antigen-specific T cell responses induction is a critical component for evaluating efficacy of T cell-mediated vaccines, especially in the era of canine oral malignant melanoma DNA vaccines (24) where cytotoxic T cells would be proposed to mediate protection. Here, we described a method for defining vaccine-specific $CD4^+$ and $CD8^+$ T cells through intracellular cytokine staining following rabies, canine distemper-adenovirus-parainfluenza-parvovirus, and leptospirosis bacterial extract vaccination. Determining induction, kinetics, and effector function of these antigen-specific T cells are ideal for evaluating appropriate and protective vaccine responses and defining goals for future vaccines, where T cells are primary mediators of immune control for the targeted disease.

In instances where immediate PMBC isolation may be unavailable due to geographical location, evaluating appropriate storage conditions, subsequent cell isolation, and cytokine production following extended times post blood sampling is critical. For example, immunophenotyping of lymphoma of a dog living in a rural area or

research studies involving characterization of T cell responses of dogs living in an international locale would likely require significant time between blood collection and PBMC isolation and storage. Data herein illustrates these canine subjects can be examined and immune responses characterized, expanding the translational application of this study beyond laboratory settings. These techniques and reagents are powerful in scenarios where human vaccination efforts would be unethical or inaccessible and dogs serve as models of natural infection and appropriate targets for control efforts, such as American trypanosomiasis (25).

In conclusion, limited resources and techniques for phenotyping and characterizing canine T cells have restricted canine adaptive immune system studies. The tools defined here provide a platform for defining T cell subsets and identifying circulating antigen-specific T cells. The impact of this work for improving canine health and facilitating the translational applications of dogs for human disease modeling is promising. As individualized T cell immunophenotyping becomes more accessible for human patients, application to veterinary medicine and animal patients is encouraging.

Table 3.1. Reagent panel used to study canine peripheral mononuclear cells.

Antigen	Antibody	Host species	Target species	Source (citation)	Reagent specificity	Dog PBMC reactivity	Reactivity in this study	Discriminatory
Leukocyte cell lineages								
CD3	CA17.2A12	mouse	dog	AbD Serotec (26)	T cells	(26)	+	n.d.
CD11a	CA11.4D3	mouse	dog	AbD Serotec (10, 27)	integrin, all leukocytes	(10)	-	no
CD11c	BU15	mouse	human	AbD Serotec	dendritic cells, monocytes, macrophages, neutrophils	(28)	+	n.d.
Lymphocyte subsets								
B cell	LSM11.425	mouse	dog	BD Pharminogen (10, 29, 30)	B cells	(10)	+	yes
Pan T cell	LSM8.358	mouse	dog	BD Pharminogen (10)	T cells	(10)	+	yes
CD4	YKIX302.9	rat	dog	AbD Serotec (10)	$CD4^+$ T cells	(10)	+	yes
CD4	RPA-T4	mouse	human	BioLegend (31)	$CD4^+$ T cells		-	
CD8	YCATE55.9	rat	dog	AbD Serotec (10)	$CD8^+$ T cells	(10)	+	yes
CD8a	RPA-T8	mouse	human	BioLegend (31)	$CD8^+$ T cells		-	
T cell-specific antigens								
T cell activation	CTL2.58	mouse	dog	BD Pharminogen (30)	activated T cells		+	yes
CD25	2A3	mouse	human	BD Biosciences (32)	activated & regulatory T cells, activated B cells		-	
CD27	M-T271	mouse	human	BD Pharminogen (33)	tumor necrosis factor R'; T cell costimulatory molecule		-	
CD28	CD28.2	mouse	human	BD Pharminogen (34)	T cell costimulatory molecule, required for T cell activation		-	
CD44	IM7	rat	mouse	AbD Serotec (35)	activated effector-memory T cells	(10)	+	no
CD45RA	HI100	mouse	human	BioLegend (36)	naïve T cells		-	
CD45RA	CA4.ID3	mouse	dog	Abd Serotec (10, 12)	naïve T cells	(37)	+	no
CD45RO	UCHL1	mouse	human	Beckman Coulter	memory T cells	(38)	+	no
CD62L	FMC46	mouse	human	AbD Serotec (39)	lymphocyte homing, naïve & memory T cells	(16)	+	yes
CD62L	DREG-56	mouse	human	BD Pharminogen (40)	lymphocyte homing, naïve, & memory T cells		-	
CD127	HIL-7R-M2	mouse	human	BD Pharminogen (41)	IL-7 R' subunit		-	
CD197 (CCR7)	3D12	rat	human	BD Pharminogen (42)	secondary lymphoid organ entry R'		-	
CCL19-hIg	ELC		human	(19)	chemokine ligand for CCR7 on T cells for secondary lymphoid organ migration		+	yes
Other antigens, receptors, and cytokines								
CD85j	GHI/75	mouse	human	BD Pharminogen (43)	leukocyte R' providing inhibitory signals to APCs		-	
HLA-ABC	09HHLA01E			Chemicon Australia (44)	human leukocyte antigen MHCI		+	n.d.
CX3CR1		rabbit	human	Torrey Pines Biolab	chemokine R' expressed by activated T cells (T_{H1}), natural killer, epithelial & endothelial cells		+	n.d.
Interferon-γ	CC302	mouse	bovine	AbD Serotec (17, 45)	natural killer & T cell effector cytokine	(17, 45)	+	yes

Abbreviations: MHCI, major histocompatibility complex I; R', receptor; APC, antigen presenting cell.

Figure 3.1. Co-expression of CCR7 and CD62L on canine $CD8^+$ and $CD4^+$ T cells. Canine PBMCs from two clinically healthy dogs (#1 and #2) were incubated for 1 hour at 37°C and stained with or without CCL19-hIg (ELC), a CCR7 ligand. Cells were stained with anti-CD8, anti-CD4, anti-CD62L, anti-human secondary antibody, and 7AAD. Percentages of $CD8^+7AAD^-$ and $CD4^+7AAD^-$ T cells expressing CCR7 (A) and CD62L (B). Shaded lines are fluorescence-minus-one (FMO) controls for the indicated marker. C, Percentages of $CD8^+7AAD^-$ or $CD4^+7AAD^-$ T cells co-expressing CCR7 and CD62L. Gating strategies are determined by FMO controls, especially noting the highest CCR7 peak present in experimental and FMO control samples is due to nonspecific secondary antibody binding.

Figure 3.1

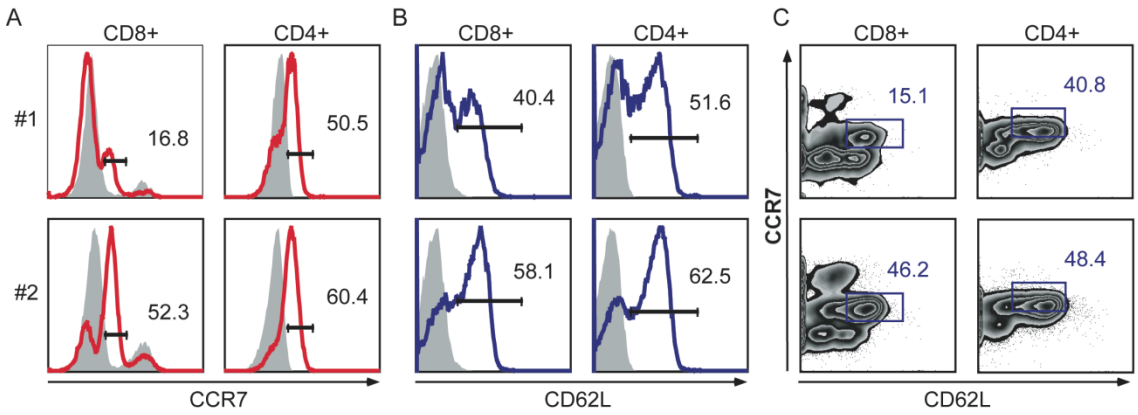
A
CD8+
CD4+
#1
16.8
50.5
#2
52.3
60.4
CCR7
B
CD8+
CD4+
40.4
51.6
58.1
62.5
CD62L
C
CD8+
CD4+
15.1
40.8
46.2
48.4
CCR7
CD62L

Figure 3.2. Measuring stimulation and proliferation using CFSE time-series data. A, Forward scatter (fsc) versus side scatter plots (ssc) of CFSE-labeled PBMCs incubated with media or concavalin A (ConA) for 4 days. Gated cells are displayed in the fsc histogram, comparing ConA-stimulation (blue line) to media alone (grey). B, CFSE-labeled PBMCs were harvested on the indicated days and stained with 7AAD and anti-CD8 antibodies. Histograms represent percentages of $CD8^{+}7AAD^{-}$ T cells with CFSE dilution following incubation with media (grey shaded) versus ConA (green line).

Figure 3.2

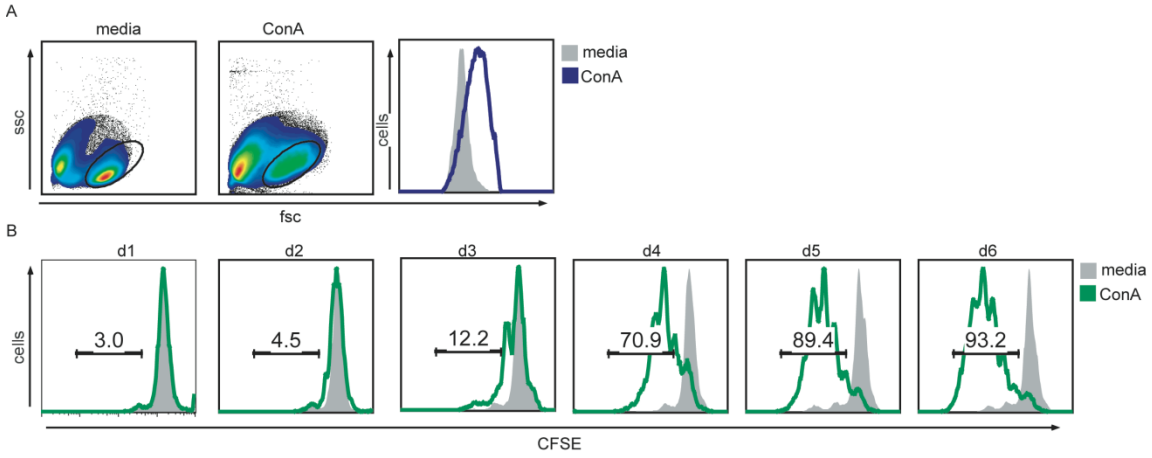
A
media
ConA
ssc
fsc
cells
media
ConA
B
d1
d2
d3
d4
d5
d6
cells
3.0
4.5
12.2
70.9
89.4
93.2
CFSE
media
ConA

Figure 3.3. CCR7, CD62L, and CTL2.58 expression of canine PBMCs in stimulation conditions. Canine PBMCs incubated two days with media, anti-CD3, or ConA, harvested, and stained with various antibody combinations. A, Proliferation of CFSE-labeled $CD8^+$ T cells. B-D, PBMCs incubated with (blue line) and without (grey shaded) CCL19-hIg and stained with anti-human secondary antibody and anti-CD62L. Histograms of CCR7 (B) and CD62L (C) expression of $CD8^+$ T cells. D, Percentages of $CD8^+$ T cells co-expressing CCR7 and CD62L. E-F, PBMCs stained with the dog activated T lymphocyte antibody cocktail, 7AAD, and anti-CD8. Percentages of stimulated $PanT^+$ (E) and $CD8^+$ (F) T cells reactive to the CTL2.58 antibody, an activation marker.

Figure 3.3

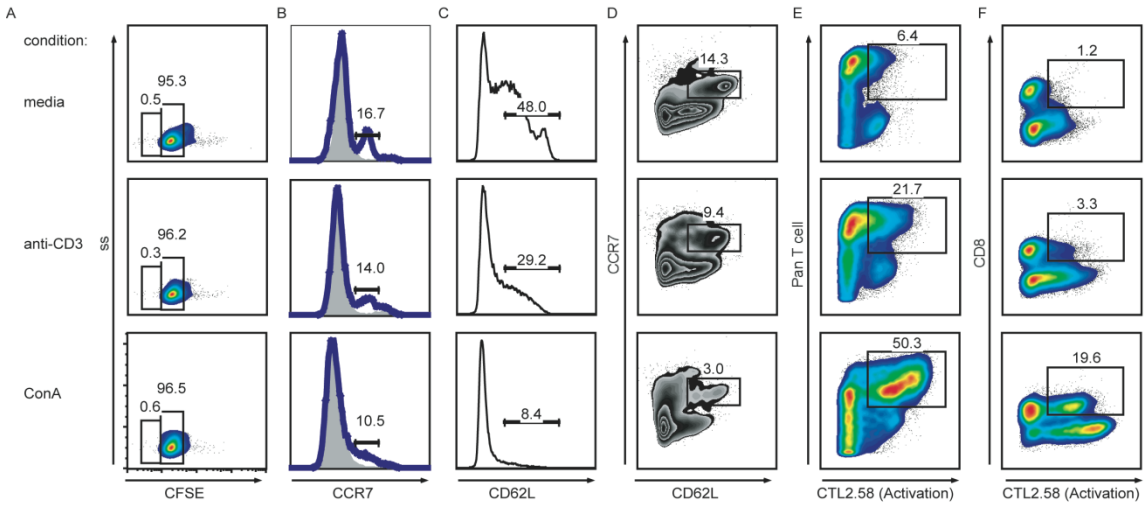
A
B
C
D
E
F
condition:
media
anti-CD3
ConA
95.3
0.5
16.7
48.0
14.3
6.4
1.2
96.2
0.3
14.0
29.2
9.4
21.7
3.3
96.5
0.6
10.5
8.4
3.0
50.3
19.6
SS
CFSE
CCR7
CD62L
CD62L
CCR7
Pan T cell
CTL2.58 (Activation)
CD8
CTL2.58 (Activation)

Figure 3.4. IFNγ production by canine $CD4^+$ and $CD8^+$ T cells upon stimulation with vaccine antigens. PBMCs collected from three dogs three weeks post vaccination with IMRAB 3TF (Rabies), Duramune 5 (DAPP), and Leptovax 4 (Lepto) were incubated with media, PMA/$Ca2^+$ ionomycin, and vaccines. GolgiPlug was added 5hr prior to end of incubation. Cells were stained with anti-CD8, anti-CD4, and anti-bovine IFNγ. A-B, Numbers indicate percentages of $CD4^+$ (A) and $CD8^+$ (B) T cells producing cytokine in each condition.

Figure 3.4

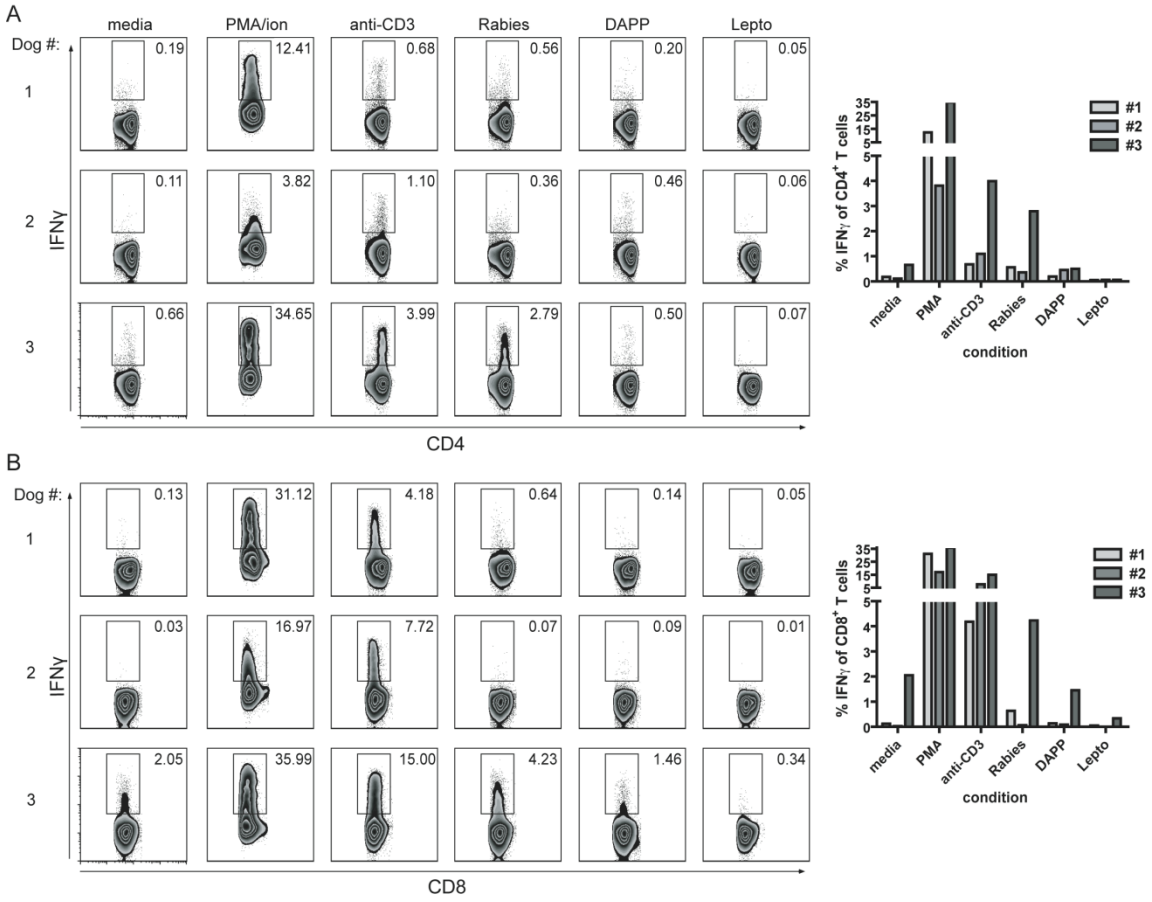
A
media
PMA/ion
anti-CD3
Rabies
DAPP
Lepto
Dog #:
1
2
3
IFNγ
CD4
0.19
12.41
0.68
0.56
0.20
0.05
0.11
3.82
1.10
0.36
0.46
0.06
0.66
34.65
3.99
2.79
0.50
0.07
% IFNγ of CD4+ T cells
#1
#2
#3
media
PMA
anti-CD3
Rabies
DAPP
Lepto
condition
B
Dog #:
1
2
3
IFNγ
CD8
0.13
31.12
4.18
0.64
0.14
0.05
0.03
16.97
7.72
0.07
0.09
0.01
2.05
35.99
15.00
4.23
1.46
0.34
% IFNγ of CD8+ T cells
#1
#2
#3
media
PMA
anti-CD3
Rabies
DAPP
Lepto
condition

Figure 3.5. Viability and effector function of canine $CD4^+$ and $CD8^+$ T cells measured over a 48hr period. Canine blood was collected, incubated on ice, and PBMCs isolated at the indicated time points. PBMCs were incubated at 37°C with PMA/ionomycin or media alone in the presence of GolgiPlug for 5 hours. Cells were stained with anti-CD8 and anti-CD4, permeabilized, and stained for IFNγ. Numbers indicate percentage (gated) and count (bottom right) of $CD8^+$ (A) and $CD4^+$ (B) T cells producing IFNγ at each isolation time point.

Figure 3.5

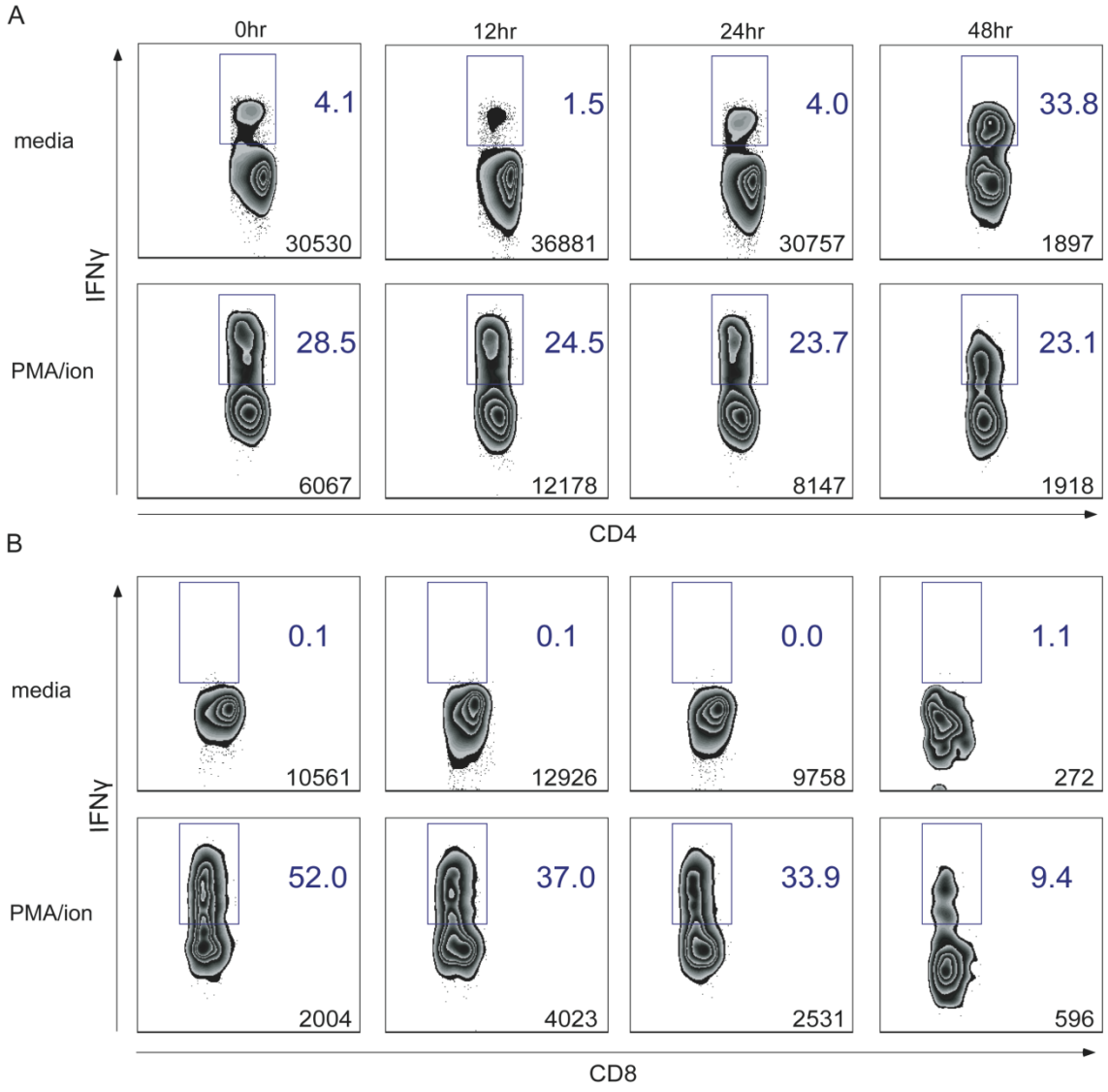
A
0hr
12hr
24hr
48hr
media
PMA/ion
IFNγ
4.1
30530
1.5
36881
4.0
30757
33.8
1897
28.5
6067
24.5
12178
23.7
8147
23.1
1918
CD4
B
media
PMA/ion
IFNγ
0.1
10561
0.1
12926
0.0
9758
1.1
272
52.0
2004
37.0
4023
33.9
2531
9.4
596
CD8

3.6 References

1. Hohnloser, S. H., H. J. Crijns, M. van Eickels, C. Gaudin, R. L. Page, C. Torp-Pedersen, and S. J. Connolly. 2009. Effect of dronedarone on cardiovascular events in atrial fibrillation. *The New England journal of medicine* 360:668-678.

2. Klopfleisch, R., D. Lenze, M. Hummel, and A. D. Gruber. 2010. Metastatic canine mammary carcinomas can be identified by a gene expression profile that partly overlaps with human breast cancer profiles. *Bmc Cancer* 10:-.

3. Khanna, C., K. Lindblad-Toh, D. Vail, C. London, P. Bergman, L. Barber, M. Breen, B. Kitchell, E. McNeil, J. F. Modiano, S. Niemi, K. E. Comstock, E. Ostrander, S. Westmoreland, and S. Withrow. 2006. The dog as a cancer model. *Nature Biotechnology* 24:1065-1066.

4. Creevy, K. E., T. R. Bauer, L. M. Tuschong, L. J. Embree, L. Colenda, K. Cogan, M. F. Starost, M. E. Haskins, and D. D. Hickstein. 2003. Canine leukocyte adhesion deficiency colony for investigation of novel hematopoietic therapies. *Vet Immunol Immunop* 94:11-22.

5. Marsella, R., and G. Girolomoni. 2009. Canine models of atopic dermatitis: a useful tool with untapped potential. *The Journal of investigative dermatology* 129:2351-2357.

6. Selkoe, D. J., D. S. Bell, M. B. Podlisny, D. L. Price, and L. C. Cork. 1987. Conservation of brain amyloid proteins in aged mammals and humans with Alzheimer's disease. *Science* 235:873-877.

7. Awano, T., G. S. Johnson, C. M. Wade, M. L. Katz, G. C. Johnson, J. F. Taylor, M. Perloski, T. Biagi, I. Baranowska, S. Long, P. A. March, N. J. Olby, G. D. Shelton, S. Khan, D. P. O'Brien, K. Lindblad-Toh, and J. R. Coates. 2009. Genome-wide association analysis reveals a SOD1 mutation in canine degenerative myelopathy that resembles amyotrophic lateral sclerosis. *P Natl Acad Sci USA* 106:2794-2799.

8. Wilbe, M., P. Jokinen, K. Truve, E. H. Seppala, E. K. Karlsson, T. Biagi, A. Hughes, D. Bannasch, G. Andersson, H. Hansson-Hamlin, H. Lohi, and K. Lindblad-Toh. 2010. Genome-wide association mapping identifies multiple loci for a canine SLE-related disease complex. *Nat Genet* 42:250-254.

9. Guedes, P. M. D., V. M. Veloso, W. L. Tafuri, L. M. D. Galvao, C. M. Carneiro, M. de Lana, E. Chiari, K. A. Soares, and M. T. Bahia. 2002. The dog as model for chemotherapy of the Chagas' disease. *Acta Trop* 84:9-17.

10. Cobbold, S., and S. Metcalfe. 1994. Monoclonal antibodies that define canine homologues of human CD antigens: summary of the First International Canine Leukocyte Antigen Workshop (CLAW). *Tissue Antigens* 43:137-154.

11. Aguiar, P. H. P., S. M. Barrouin-Melo, C. R. Franke, R. R. B. dos Santos, T. M. C. Silva, J. O. Mengel, W. L. C. dos-Santos, and L. Pontes-de-Carvalho. 2005. A monoclonal antibody against a canine CD45 homologue: Analysis of tissue distribution, biochemical properties and in vitro immunological activity. *Vet J* 173:158-166.

12. Caniatti, M., P. Roccabianca, E. Scanziani, S. Paltrinieri, and P. F. Moore. 1996. Canine Lymphoma: Immunocytochemical Analysis of Fine-needle Aspiration Biopsy. *Vet Pathol* 33:204-212.

13. Danilenko, D. M., P. F. Moore, and P. V. Rossitto. 1992. Canine Leukocyte Cell-Adhesion Molecules (Leucams) - Characterization of the Cd11/Cd18 Family. *Tissue Antigens* 40:13-21.

14. Moore, P. F., P. V. Rossitto, and D. M. Danilenko. 1990. Canine Leukocyte Integrins - Characterization of a Cd18 Homolog. *Tissue Antigens* 36:211-220.

15. Crockett-Torabi, E., and J. C. Fantone. 1997. L-selectin stimulation of canine neutrophil initiates calcium signal secondary to tyrosine kinase activation. *Am J Physiol-Heart C* 272:H1302-H1308.

16. Schuberth, H., G. Kucinskiene, R. Chu, and M. Faldyna. 2007. Reactivity of cross-reacting monoclonal antibodies with canine leukocytes, platelets and erythrocytes. *Vet Immunol Immunop* 119:47-55.

17. Pedersen, L. G., Y. Castelruiz, S. Jacobsen, and B. Aasted. 2002. Identification of monoclonal antibodies that cross-react with cytokines from different animal species. *Vet Immunol Immunop* 88:111-122.

18. Albareda, M. C., G. C. Olivera, S. A. Laucella, M. G. Alvarez, E. R. Fernandez, B. Lococo, R. Viotti, R. L. Tarleton, and M. Postan. 2009. Chronic human infection with Trypanosoma cruzi drives CD4+ T cells to immune senescence. *J Immunol* 183:4103-4108.

19. Hargreaves, D. C., P. L. Hyman, T. T. Lu, V. N. Ngo, A. Bidgol, G. Suzuki, Y. R. Zou, D. R. Littman, and J. G. Cyster. 2001. A coordinated change in chemokine responsiveness guides plasma cell movements. *Journal of Experimental Medicine* 194:45-56.

20. Debes, G. F., C. N. Arnold, A. J. Young, S. Krautwald, M. Lipp, J. B. Hay, and E. C. Butcher. 2005. Chemokine receptor CCR7 required for T lymphocyte exit from peripheral tissues. *Nature Immunology* 6:889-894.

21. Campbell, J. J., K. E. Murphy, E. J. Kunkel, C. E. Brightling, D. Soler, Z. Shen, J. Boisvert, H. B. Greenberg, M. A. Vierra, S. B. Goodman, M. C. Genovese, A. J. Wardlaw, E. C. Butcher, and L. Wu. 2001. CCR7 expression and memory T cell diversity in humans. *Journal of immunology* 166:877-884.

22. Valli, J. L., A. Williamson, S. Sharif, J. Rice, and P. E. Shewen. 2010. In vitro cytokine responses of peripheral blood mononuclear cells from healthy dogs to distemper virus, Malassezia and Toxocara. *Vet Immunol Immunop* 134:218-229.

23. Adler, B., and S. Faine. 1977. Host immunological mechanisms in the resistance of mice to leptospiral infections. *Infection and Immunity* 17:67-72.

24. Grosenbaugh, D. A., A. T. Leard, P. J. Bergman, M. K. Klein, K. Meleo, S. Susaneck, P. R. Hess, M. K. Jankowski, P. D. Jones, N. F. Leibman, M. H. Johnson, I. D. Kurzman, and J. D. Wolchok. 2011. Safety and efficacy of a xenogeneic DNA vaccine encoding for human tyrosinase as adjunctive treatment for oral malignant melanoma in dogs following surgical excision of the primary tumor. *American journal of veterinary research* 72:1631-1638.

25. Padilla, A. M., C. M. P. Brandan, and M. A. Basombrio. 2010. Vaccine Development for Chagas Disease. In *American Trypanosomiasis Chagas Disease*. J. Telleria, and M. Tibayrenc, eds. Elsevier, New York. 827-841.

26. Byrne, K. M., H. W. Kim, B. P. Chew, G. A. Reinhart, and M. G. Hayek. 2000. A standardized gating technique for the generation of flow cytometry data for normal canine and normal feline blood lymphocytes. *Vet Immunol Immunop* 73:167-182.

27. Danilenko, D. M., P. F. Moore, and P. V. Rossitto. 1992. Canine leukocyte cell adhesion molecules (LeuCAMs): characterization of the CD11/CD18 family. *Tissue Antigens* 40:13-21.

28. Trowald-Wigh, G., A. Johannisson, and L. Hakansson. 1993. Canine neutrophil adhesion proteins and Fc-receptors in healthy dogs and dogs with adhesion protein deficiency, as studied by flow cytometry. *Vet Immunol Immunop* 38:297-310.

29. Gebhard, D. H., and P. B. Carter. 1992. Identification of canine T-lymphocyte subsets with monoclonal antibodies. *Vet Immunol Immunop* 33:187-199.

30. Ruslander, D. A., D. H. Gebhard, M. B. Tompkins, C. B. Grindem, and R. L. Page. 1997. Immunophenotypic characterization of canine lymphoproliferative disorders. *In Vivo* 11:169-172.

31. Schlossman, S. F., L. Boumsell, and W. Gilks. 1995. *Leukocyte Typing V: White Cell Differentiation Antigens*. Oxford University Press, New York.

32. Urdal, D. L., C. J. March, S. Gillis, A. Larsen, and S. K. Dower. 1984. Purification and chemical characterization of the receptor for interleukin 2 from activated human T lymphocytes and from a human T-cell lymphoma cell line. *P Natl Acad Sci USA* 81:6481-6485.

33. Bigler, R. D., Y. Bushkin, and N. Chiorazzi. 1988. S152 (CD27). A modulating disulfide-linked T cell activation antigen. *Journal of immunology* 141:21-28.

34. Verwilghen, J., P. Vandenberghe, G. Wallays, M. de Boer, N. Anthony, G. S. Panayi, and J. L. Ceuppens. 1993. Simultaneous ligation of CD5 and CD28 on resting T lymphocytes induces T cell activation in the absence of T cell receptor/CD3 occupancy. *Journal of immunology* 150:835-846.

35. McKallip, R. J., Y. Do, M. T. Fisher, J. L. Robertson, P. S. Nagarkatti, and M. Nagarkatti. 2002. Role of CD44 in activation-induced cell death: CD44-deficient mice exhibit enhanced T cell response to conventional and superantigens. *International immunology* 14:1015-1026.

36. Iannello, A., M. R. Boulassel, S. Samarani, O. Debbeche, C. Tremblay, E. Toma, J. P. Routy, and A. Ahmad. 2010. Dynamics and consequences of IL-21 production in HIV-infected individuals: a longitudinal and cross-sectional study. *Journal of immunology* 184:114-126.

37. Moreno, J., J. Nieto, C. Chamizo, F. Gonzalez, F. Blanco, D. C. Barker, and J. Alva. 1999. The immune response and PBMC subsets in canine visceral leishmaniasis before, and after, chemotherapy. *Vet Immunol Immunop* 71:181-195.

38. Galkowska, H., L. O. Waldemar, and U. Wojewodzka. 1996. Reactivity of antibodies directed against human antigens with surface markers on canine leukocytes. *Vet Immunol Immunop* 53:329-334.

39. Pilarski, L. M., E. A. Turley, A. R. Shaw, W. M. Gallatin, M. P. Laderoute, R. Gillitzer, I. G. Beckman, and H. Zola. 1991. FMC46, a cell protrusion-associated leukocyte adhesion molecule-1 epitope on human lymphocytes and thymocytes. *Journal of immunology* 147:136-143.

40. Kishimoto, T. K., M. A. Jutila, and E. C. Butcher. 1990. Identification of a human peripheral lymph node homing receptor: a rapidly down-regulated adhesion molecule. *P Natl Acad Sci USA* 87:2244-2248.

41. Goodwin, R. G., D. Friend, S. F. Ziegler, R. Jerzy, B. A. Falk, S. Gimpel, D. Cosman, S. K. Dower, C. J. March, A. E. Namen, and et al. 1990. Cloning of the human and murine interleukin-7 receptors: demonstration of a soluble form and homology to a new receptor superfamily. *Cell* 60:941-951.

42. Sallusto, F., D. Lenig, R. Forster, M. Lipp, and A. Lanzavecchia. 1999. Two subsets of memory T lymphocytes with distinct homing potentials and effector functions. *Nature* 401:708-712.

43. Colonna, M., F. Navarro, T. Bellon, M. Llano, P. Garcia, J. Samaridis, L. Angman, M. Cella, and M. Lopez-Botet. 1997. A common inhibitory receptor for

major histocompatibility complex class I molecules on human lymphoid and myelomonocytic cells. *The Journal of experimental medicine* 186:1809-1818.

44. Murakawa, T., J. Nakajima, M. Ono, A. Murakami, Y. Suematsu, and S. Takamoto. 2000. Allogenicity of cryopreserved human fibroblasts: cryopreservation does not downregulate the allogenicity of fibroblasts making up the matrices of allografts. *J Thorac Cardiovasc Surg* 120:712-719.

45. Fellman, C. L., J. V. Stokes, T. M. Archer, L. M. Pinchuk, K. V. Lunsford, and A. J. Mackin. 2011. Cyclosporine A affects the in vitro expression of T cell activation-related molecules and cytokines in dogs. *Vet Immunol Immunop* 140:175-180.

CHAPTER 4

FREQUENCY OF IFNγ-PRODUCING T CELLS CORRELATES WITH SEROREACTIVITY AND ACTIVATED T CELLS DURING CANINE *TRYPANOSOMA CRUZI* INFECTION[3]

[3] Hartley, A.N., G. Cooley, S. Gwen, M.M. Orozco, and R.L. Tarleton. To be submitted to *Veterinary Research.*

4.1 Abstract

Vaccines to prevent *Trypanosoma cruzi* infection in humans or animals are not available, and in many settings, dogs are an important source of domestic infection for the insect vector. Identification of infected canines is crucial for evaluating peridomestic transmission dynamics and parasite control strategies. As immune control of *T. cruzi* infection is dependent on humoral and cell-mediated immune responses, we aimed to define a serodiagnostic assay and T cell phenotypic markers for identifying infected dogs and studying the canine *T. cruzi*-specific immune response. Plasma samples and peripheral blood mononuclear cells (PBMCs) were obtained from forty-two dogs living in a *T. cruzi*-endemic region. Twenty dogs were known to be seropositive and nine seronegative by conventional serologic tests two years prior to our study. To determine canine seroreactivity, we tested sera samples in a multiplex bead array against eleven recombinant *T. cruzi* proteins. Ninety-four percent (17/18) of dogs positive in the multiplex serology were initially positive by conventional serology. The frequency of IFNγ-producing cells in PBMCs responding to *T. cruz*i correlated to serological status, identifying 95% of multiplex seropositive dogs. Intracellular staining identified $CD4^+$ and $CD8^+$ T cell populations as the sources of *T. cruzi* lysate-induced IFNγ. Low expression of CCR7 and CD62L on $CD4^+$ and $CD8^+$ T cells suggested a predominance of effector/effector memory T cells in seropositive canines. These results are the first, to our knowledge, to correlate *T. cruzi*-specific antibody responses with T cell responses in naturally infected dogs and validate these methods for identifying dogs exposed to *T. cruzi*.

4.2 Introduction

Trypanosoma cruzi infects humans, wildlife, and domestic animals throughout the Americas. Worldwide, it is estimated that at least ten million individuals are chronically infected with *T. cruzi*, with twenty-five million more are at risk of infection (1). *T. cruzi* infection predominantly burdens countries of Central and South America but encompasses all of the Americas including the United States, contributing 14,000 deaths annually and 700,000 daily adjusted life years (2). Current methods of parasite control, diagnostics, and treatment are inadequate in completely disrupting transmission as new infections occur annually, and no vaccines are currently available for human or veterinary use.

Dogs play a significant role in *T. cruzi* epidemiology and ecology as reservoirs for infection (3). Preferential (4) and host tolerant (5) vectorial feeding of dogs, higher *T. cruzi* infectivity of *T. infestans* upon feeding on dogs compared to human feeding (6), and the close proximity of dogs to humans in domiciles in *T. cruzi* endemic regions (7) identifies dogs as a critical control point for *T. cruzi* transmission. Strategies for interrupting transmission by targeting the dog have included insecticide-impregnated dog collars (8) and various means of vaccination (9-11). Despite these efforts, peridomestic *T. cruzi* transmission still occurs between humans, dogs, and the insect vector. Identifying infected canines and understanding the immune mechanisms responsible for canine *T. cruzi* recognition and control are critical for designing and evaluating future intervention strategies targeting canines.

Because the results of serological tests for *T. cruzi* infection are not considered to be definitive, positive responses on a minimum of two tests is generally recommended to

identify infected humans (12-14), and dogs (15, 16). For identifying circulating anti-*T. cruzi* antibodies, hemagglutination, complement fixation, indirect immunofluorescence, and direct agglutination tests have been standardized for canine sera (17). These methods, also known broadly as conventional serological assays, predominantly utilize insect stage epimastigote-derived antigens for seroreactivity testing. In an attempt to improve the quality of serological tests for detection of *T. cruzi* infection, we developed a multiplex bead array format utilizing recombinant *T. cruzi* proteins selected for their predicted expression during mammalian infection stages (18), high abundance in trypomastigote and amastigote proteomes (19), and ability to detect the broad array of responses observed in *T. cruzi*-infected humans (20). Investigating serological assays employing mammalian derived proteins could maximize discrimination of seropositive and seronegative canines, thereby reducing the need for multiple tests to identify seroreactive dogs during intervention campaigns.

Studies of human *T. cruzi* infection and experimental animal models have highlighted the role antibodies (21-23), $CD4^+$ and $CD8^+$ T cells (24-26), and effector cytokines (27, 28) serve in immune control of *T. cruzi*, predicting disease development, and determining treatment success. Identification of *T. cruzi*-specific $CD8^+$ T cells by class I MHC tetramers for mice (29) and humans (27) has facilitated monitoring of cell surface marker expression and effector function of *T. cruzi*-specific T cells. In particular, correlation of parasitological cure with increased CD127 and CD62L expression by *T. cruzi*-specific $CD8^+$ T cells in benznidazole-treated mice has identified biomarkers for evaluating parasite burden *in vivo* (30). Characterizing similar canine T cell phenotypes and effector cytokine production is critical for understanding the development of an

appropriate *T. cruzi*-specific immune response in the dog and evaluating modulation of this response following intervention strategies targeting the dog.

The aim of this study was to test the use of a multiplex serodiagnostic assay for *T. cruzi* in dog sera and to further evaluate T cell phenotypes and effector cytokine production associated with canine *T. cruzi* infection. Peripheral blood was collected from dogs previously tested by conventional serology and/or xenodiagnosis and living in a *T. cruzi*-endemic region of northern Argentina. Plasma were submitted to multiplex bead array analysis using eleven recombinant *T. cruzi* proteins, previously described for identifying seroreactive humans and evaluating treatment success (20), and PBMCs were assessed for IFNγ production in response to *T. cruzi* amastigote antigens by ELISpot. Utilizing recently identified T cell reagents identified for the dog (Hartley and Tarleton, unpublished), we assessed expression of canine T cell surface markers associated with naïve or central memory and activated T cells. The results of this study determined dogs living in *T. cruzi*-endemic regions develop robust anti-*T. cruzi* antibody responses which correlate with T cell effector and activation phenotypes. The serological and T cells assays described here provide a platform for monitoring canine immune responses and for developing and evaluating canine-centric *T. cruzi* intervention strategies.

4.3 Materials and Methods

4.3.1 *Animals*

A maximum of 10mls of blood from 42 dogs living in four villages in Pampa del Indio, Chaco, Argentina were drawn into heparinized tubes (BD Vacutainer, BD, Franklin Lakes, NJ, USA) by venipuncture. Approximately 50mls of blood from three clinically healthy dogs from the United States were obtained to serve as controls. Isolation of

peripheral blood mononuclear cells (PBMCs) occurred within 24 hours of collection according to previously described methods (Hartley and Tarleton, unpublished). Briefly, PBMCs were isolated by density gradient centrifugation on Lymphocyte Separation Medium (MP Biomedicals, Solon, OH, USA), resuspended in complete RPMI 1640 supplemented with 10% heat-inactivated FCS (HyClone Laboratories, ThermoScientific, Logan, UT, USA), and stored frozen at -80°C. These purification, storage, and recovery procedures yielded >80% viability for Argentinean and >95% viability for American dogs as determined by microscopic examination of trypan blue exclusion. Plasma samples were collected during PBMC isolation and stored frozen at -20°C. Informed oral consent was requested and obtained from each head of household for samples collected in Argentina. Animal use protocols for samples collected in the United States were approved by the University of Georgia Institutional Animal Care and Use Committee.

4.3.2 *Initial conventional serology and xenodiagnosis*

Indirect hemagluttination assay (IHA) and an in-house enzyme-linked immunosorbent assay (ELISA) modified from a standardized protocol (15) were used to test sera for anti-*T. cruzi* antibodies two years prior to this study and as described (31). Sera were considered discordant if results of IHA and ELISA reactivity mismatched. A subset of animals were also examined by xenodiagnosis, as previously outlined (31) and notated in Table 4.1. Briefly, boxes containing uninfected fourth-instar nymphs of *T. infestans* were exposed to the abdomen of an individual dog. Insect feces were examined microscopically at 30 and 60 days later for *T. cruzi* infection.

4.3.3 T. cruzi *amastigote lysate*

Brazil strain trypomastigotes were cultured overnight in pH 5 RPMI 1640 supplemented with 10% FCS and 10mM phosphate citrate buffer to transform trypomastigotes into amastigotes. After two PBS washes, parasites were frozen at -20C. Frozen aliquots were subjected to five freeze/thaw cycles followed by three 10s sonications in a FS15 sonicator (Fisher Scientific, Pittsburgh, PA, USA). The supernatant of a 12,000 rpm centrifugation was collected, filter sterilized, and protein concentration determined by Bradford assay.

4.3.4 *Serology testing with protein multiplex bioassay*

Canine plasma samples were tested with a recombinant *T. cruzi* protein multiplex assay previously described in detail for testing *T. cruzi* reactivity of human sera samples (20). Briefly, sera are diluted 1:500 and incubated with a pool of 11 recombinant proteins attached to addressable Liquichip Ni-NTA beads (Qiagen Inc, Valencia, CA, USA) and *T. cruzi* amastigote lysate coupled to Carboxy-Ni-NTA beads (Qiagen Inc). Following washing, antibody binding was detected with goat anti-dog IgG conjugated to phycoerythrin (Santa Cruz Biotechnology Inc, Santa Cruz, CA) and quantified on a Bio-Plex Suspension Array System (Bio-Rad, Hercules, CA, USA). Serum samples were assayed in duplicate and weighted mean fluorescence intensity (MFI) was calculated. The ratio of the specific MFI for each antigen versus a negative control (green fluorescent protein) protein was calculated for each antigen and sera in the assay.

4.3.5 *IFNγ ELISpot assays*

Four hundred thousand PBMCs were cultured in media, 2ng/mL phorbol 12-myristate 13-acetate (PMA) and 500ng/mL Ca^{2+} ionomycin (both Sigma-Aldrich, St. Louis, MO, USA), or 10ug/mL *T. cruzi* amastigote lysate for 16 hr at 37°C and 5% CO_2. Cells were

assayed for IFNγ production using the Canine IFN-γ ELISpot kit (cat no. EL781, R&D Systems, Inc, Minneapolis, MN, USA) following standard kit protocol. Enumeration of spot forming cells was completed by an ImmunoSpot analyzer (CTL, Cleveland, OH, USA). Mean numbers of spots from duplicate or triplicate well were obtained for media and *T. cruzi* lysate stimulation conditions. Responses were considered positive if a minimum of 20 spots/10^6 PBMC total were present and this number was at least twice the value of wells assayed with media alone (27).

4.3.6 *Intracellular cytokine staining*

For assaying IFNγ production, $4x10^5$ PBMCs were stimulated for 5hr in the presence of 2ng/mL PMA, 4μg/mL Ca^{2+} ionomycin (Sigma-Aldrich), and brefeldin A (BD GolgiPlug; BD Biosciences, San Jose, CA, USA) adapted from described stimulation conditions (32) or overnight with 40ug/mL *T. cruzi* lysate at 37°C. Brefeldin A was added 5hr prior to end of incubation, and the cells were stained with anti-CD8-Pacific Blue and anti-CD4-FITC (AbD Serotec, Raleigh, NC, USA) followed by intracellular staining with anti-bovine IFN-γ AF647 (AbD Serotec) according to the BD Cytofix/Cytoperm kit (BD Biosciences). Samples were fixed in 2% formaldehyde prior to analysis by flow cytometry.

4.3.7 *CTL2.58 purification and PE-Cy7 labeling*

Culture supernatants containing clone CTL2.58 IgG were a kind gift of Dr. Mary Tompkins, North Carolina State University, Raleigh, NC. Immunoglobulins were purified according to instructions of the Pierce Thiophilic Adsorption Kit (cat no 44916, Thermo Scientific, Rockford, IL, USA). Elutions containing targeted heavy and light chain were confirmed by SDS-PAGE and conjugated to PE-Cy7 using Lightning-Link

PE-Cy7 antibody labeling kit (cat no 762-0015, Novus Biologicals, Littleton, CO, USA) following manufacture instructions. ConA-stimulated canine PBMCs were used for positive reactivity for CTL2.58-Pe-Cy7 staining.

4.3.8 *Cell surface phenotyping*

PBMCs (500,000) were incubated in complete RPMI 1640 supplemented with 10% heat-inactivated FCS for 1 hr at 37°C, centrifuged, and resuspended in 100ul of CCL19-hIg (ELC; (33)) culture supernatant for 45 min at 4°C. After incubation, cells were washed and resuspended for staining in PAB solution containing PBS with 1% BSA and 0.05% sodium azide (both from Sigma-Aldrich). Antibodies used were anti-CD8 PacBlue, anti-CD4 AF647, anti-CD62L PE (AbD Serotec), CTL2.58-PeCy7, and anti-human IgG AF488 (Molecular Probes, Eugene, OR, USA). 7-amino-actinomycin D (7AAD, BD Pharmingen, BD Biosciences, San Jose, CA, USA) was included for live/dead cell discrimination. Following incubation of PBMCs with antibody mixes for 45 mins on ice, cells were washed twice, fixed in 2% formaldehyde, and analyzed by flow cytometry.

4.3.9 *Flow Cytometry and Statistical Analysis*

Fixed PBMC samples were collected on a CyAn ADP using Summit, version 4.3 (Beckman Coulter, Fullerton, CA, USA). FlowJo flow cytometry analysis software, version 8 (Tree Star, Ashland, OR, USA) was used for analyses. Positive gates were determined by relevant fluorescence minus one controls. Statistical analyses were performed using Prism v4.0c (GraphPad Software, La Jolla, CA, USA).

4.4 Results

Our first aim was to test an improved serodiagnostic assay for the ability to detect *T. cruzi* infection in canines. Sera and plasma samples were obtained from eight healthy

dogs from the United States (US) and forty-two dogs living in a *T. cruzi*-endemic region of northern Argentina. Twenty Argentinean dogs were known to be seropositive, nine seronegative, and one discordant by conventional serology two years prior to this study. Ten dogs were new additions to domiciles and had not been previously tested. We employed a multiplex bead array format previously utilized for identifying and discriminating humans reactive to recombinant *T. cruzi* proteins, in which proteins were selected for their predicted expression during mammalian infection stages and high abundance in the trypomastigote and amastigote *T. cruzi* proteome (20). Addressable beads were bound to eleven recombinant *T. cruzi* proteins, incubated with sera, followed with a secondary fluorophore conjugated anti-canine specific IgG, and quantified on a BioPlex Suspension Array System (BioRad) for mean fluorescence intensity (MFI). We first tested a subset of dogs and found that as expected, animals positive by conventional serology had considerably higher MFI values than United States control dogs or seronegative Argentinean dogs (Figure 4.1). All proteins in the multiplex assay showed reactivity with serum from at least one dog with a subset of six recombinant proteins (60S acidic ribosomal subunit protein, microtubule-associated protein homolog, glycosomal phosphoenolpyruvate carboxylase, flagellar calcium binding protein, major paraflagellar rod protein, and a hypothetical protein) identifying all initial conventional serology positive canines. All conventional serology positive dogs showed reactivity above a MFI of 10000 to at least one protein or greater than 6500 MFI for at least four proteins in the multiplex array. One discordant dog, dog 588, failed to have significant responses to the subset of six recombinant proteins identifying all conventional serology positive canines. Dog 588 did have greater than 10000 MFI to calmodulin protein-coated

beads, but this reactivity was not observed in any other dog. These results validate a multiplex serological assay platform for identifying circulating anti-*T. cruzi* antibodies in the dog using mammalian-stage derived *T. cruzi*-recombinant proteins.

We next tested all Argentinean canine plasma samples creating a metric of reactivity by calculating the standard deviation of each individual plasma for each individual protein over reactivity to all conventional serology negative animals. Using a minimum reactivity to two proteins with four standard deviations above that of the seronegative individuals, ninety-four percent (17/18) of the dogs positive by multiplex serology were initially positive with conventional serology (Table 4.1). Two conventional serology positive dogs (dogs 198 and 200) failed to have significant responses to any recombinant proteins in the multiplex assay. All nine initial seronegative dogs were also negative in the multiplex bead serological assay. Analysis of eleven dogs without previous conventional serology revealed two additional seropositive animals, dog O and P.

Measurement of *T. cruzi*-specific T cells has proven useful for confirming and monitoring infection status in humans (23, 27) PBMCs from dogs were evaluated for IFNγ production by ELISpot following stimulation with *T. cruzi* lysate or PMA/ionomycin. Using 20 spot forming units (SFU)/10^6 PBMCs as a cutoff for positive ELISpot responses, 95% (19/20) of dogs seropositive by multiplex were also positive in the ELISpot assay while 96% (24/25) of multiplex seronegative dogs from Argentina or the United States were ELISpot negative (Figure 4.2 and Table 4.1). Significantly higher frequencies of IFNγ-producing T cells in seropositive animals following PBMC incubation with PMA/ionomycin suggested these dogs had a higher overall active T cell

compartment as compared to seronegative dogs (Figure 4.2C). Little to no spontaneous IFNγ production confirms the specificity of the ELISpot assay to identify *T. cruzi*-specific T cells in the dog.

To phenotype the IFNγ producing cells, PBMCs from a subset of ELISpot positive and negative dogs were incubated with *T. cruzi* lysate and assessed for intracellular IFNγ production and co-stained for expression of $CD4^+$ or $CD8^+$ (Figure 4.3A). Of the four ELISpot positive dogs, three possessed $CD4^+$ and $CD8^+$ T cells producing IFNγ in response to lysate stimulation, while one dog, dog 67, had only $CD4^+$ T cells producing IFNγ in response to lysate stimulation (Figure 4.3B-C). Taken together, these data demonstrate that a high percentage of *T. cruzi*-infected dogs have measurable $CD4^+$ and $CD8^+$ T cells responsive to *T. cruzi* lysate.

As T cell surface markers of activation and effector T cell memory correlate with *T. cruzi* infection and disease severity in humans (26, 34), we next aimed to evaluate the impact of *T. cruzi* infection on canine T cell surface antigen expression. Recent validation of T cell surface markers identifying canine T cells with activated ($CTL2.58^+$) and naïve or central memory ($CCR7^+CD62L^{hi}$) phenotypes has provided cell surface markers for delineating canine T cell phenotypes (Hartley and Tarleton, unpublished). Examining the $CD8^+$ (Figure 4.4A) and $CD4^+$ (Figure 4.4B) T cell compartments, both T cell subsets expressed measurable levels of CCR7, CD62L, and CTL2.58. The expression and co-expression of naïve or central memory markers CCR7 and CD62L in T cells from healthy US control dogs were consistently higher or significantly higher as compared to the Argentinean dogs for both $CD8^+$ and $CD4^+$ T cell subsets (Figure 4.4C-E, G-I). These differentiating results most likely reflect the inherent environmental

variation of dogs living in the United States receiving preventative care versus dogs living in a *T. cruzi*-endemic region with limited accessible veterinary care, and thus a higher likelihood of harboring a range of infectious agents. The antibody CTL2.58, a reagent likely recognizing recently activated T cells, did not appear differentially expressed across any of the dog groups (Figure 4.4F and J), but high CTL2.58 expression by $CD8^+$ T cells from a seropositive dog (Figure 4.4A) suggested recent T cell activation had occurred in this dog. Overall, these T cell surface markers correlate a positive *T. cruzi* serological status with a robust activated *T. cruzi*-specific T cell response.

4.5 Discussion

T. cruzi-infected dogs are a major factor in transmission of *T. cruzi* to humans (3) and are present in both rural and urban settings (35). Thus, identification of infected dogs is critical for design and appropriate targeting of *T. cruzi* transmission control and intervention strategies. Towards this goal, we first aimed to test the ability of an improved serological assay utilizing mammalian-stage derived proteins (20) to detect *T. cruzi* infection in dogs. Though the protein panel selected for this multiplex assay was originally defined for discriminating human sera, initial tests with a subset of dog sera revealed high reactivity to the panel (Figure 4.1). In particular, a six-protein subset was highly discriminatory for serological status, with a minimum two-protein reactivity of four standard deviations above seronegative animals identifying 94% (17/18) of multiplex serology positive dogs that were positive by conventional serology (Table 4.1). Selection and screening of additional proteins with canine plasma samples, including a broader set of discordant dogs, would likely improve upon this multiplex bead array assay. A single test format that conclusively determines infection status, as opposed to

the current method of using multiple platforms and the resulting "discordant" samples, would represent an improvement in diagnostics for dogs.

To our knowledge, this was the first study to evaluate and correlate the *T. cruzi*-specific antibody response with T cell phenotype and effector cytokine production in dogs. In humans, decreases in antibody responses and in the frequency of *T. cruzi*-induced IFNγ-production by T cells and following benznidazole treatment have provided methods to evaluate infection and treatment efficacy in people. In the present study, our aim was to determine if antibody responses in dogs naturally infected with *T. cruzi* correlated with *T. cruzi*-specific T cell responses, in efforts for ultimately identifying methods to track canine *T. cruzi* infection. In contrast with human IFNγ-ELISpot assays, where IFNγ-producing PBMCs were detected in 58% of seropositive and 35% of conventional seronegative individuals living in areas of active transmission (36), 95% of seropositive dogs and 4% of seronegative dogs were positive in the canine IFNγ-ELISpot assay. These data suggest dogs not only develop robust T cells response during *T. cruzi* infection but the *T. cruzi*-specific immune responses are much more apparent than those present in humans. Relatively shorter terms of *T. cruzi* infection in dogs, i.e. months to years versus decades in humans, and the resultant decreased potential for T cell exhaustion, as observed in human patients (34), may explain the disparity in seroreactivity and ELISpot results observed between humans and dogs. Intracellular cytokine staining allowed us to identify $CD4^+$ and $CD8^+$ T cells as responsible for IFNγ production (Figure 4.3) at various, but low frequencies. Similar low frequency of IFNγ response to *T. cruzi* lysate has been documented in human Chagasic patients (27). The robust frequency of IFNγ-producing T cells observed in seropositive dogs in the ELISpot

assay provides a diagnostic method to detect, monitor, and track canine *T. cruzi* infection. We would predict that, as in humans, dogs treated with curative anti-*T. cruzi* drugs would exhibit predictable changes in the frequencies of these *T. cruzi*-specific T cell responses (23).

Additionally, the correlation of various T cell surface markers with drug-induced cure has defined T cell biomarkers for assessing antigen encounter and parasite burden during murine *T. cruzi* infection (30). Similar work in humans have correlated T cell surface marker changes with post benznidazole treatment periods (23), although the inability to measure these markers on bona fide *T. cruzi*-specific T cells (27) provides a less dependable marker of treatment efficacy than is possible in the mouse, where these T cells area easily monitored using MHC tetramers. Utilizing T cell-specific surface markers validated for the dog, phenotyping of canine PBMCs provided a method to assess hypothesized differences in global T cell surface marker expression between seropositive and seronegative animals. Though not statistically significant, higher expression of CCR7 and CD62L in seronegative versus seropositive dog T cells are consistent with these cell surface markers identifying naïve or central memory T cells. Seropositve dogs, on the other hand, possessed $CD4^+$ and $CD8^+$ T cells expressing decreased levels of CCR7 and CD62L. Further monitoring of these T cell surface markers during the course of canine *T. cruzi* infection and particularly on IFNγ-producing cells, would greatly enhance our understanding development, maintenance, and persistence of the canine T cell immune responses for evaluating various intervention strategies focused on the dog.

In addition to being important players in the transmission of *T. cruzi* to humans (3, 4, 6, 7), as natural hosts that suffer clinical manifestations of Chagasic disease (37, 38), and as models for testing of anti-trypanosomal drugs (39), canines are strong translational models for studying human *T. cruzi* infection. Understanding and characterizing the canine *T. cruzi*-specific immune response is imperative for identifying infected canines in regions of active transmission, evaluating the efficacy of targeted canine intervention strategies, including potential vaccine strategies, and overall improving our knowledge of antibody and T cells responses during canine disease. The full impact and application of serology and T cell responses for tracking and monitoring canine *T. cruzi* infection and evaluating *T. cruzi* transmission dynamics have yet to be determined.

4.6 Acknowledgements

We greatly acknowledge Dr. Ricardo Gürtler of the University of Buenos Aires, Argentina for acquisition of canine samples from Pampa del Indio, Chaco Province, Argentina. We thank Dr. Susana A. Laucella, Dr. María Cecilia Albareda, and Damián Pérez Mazliah of the Instituto Nacional de Parasitología "Dr. M. Fatala Chaben" of Buenos Aires Argentina for technical assistance with Argentina PBMC purification and ELISpot advisement, Lisa Reynolds of the University of Georgia College of Veterinary Medicine and Julie Nelson of the Center for Tropical and Emerging Global Diseases Flow Cytometry Facility at the University of Georgia, and members of the Tarleton Research Group for helpful discussion. ANH was supported in part by an Ellison Medical Foundation/Center for Tropical and Emerging Global Diseases (EMF/CTEGD) Training in Parasitologic Studies Program (TIPS) fellowship and an NIH training grant

T32 AI-060546 to the CTEGD. This work was supported by NIH Grant POI AI044979 and R01 AI089952 awarded to RLT.

Figure 4.1. Canine plasma samples tested with a multiplex bead array correlate with initial conventional serology results. Seroreactivity to 11 *T. cruzi* recombinant proteins was compared using a selection of initial conventional serology positive (seropositive) and negative (seronegative) results from dogs living in a *T. cruzi*-endemic region of Argentina versus canine sera obtained from dogs in the United States. Vertical bars represent mean fluorescence intensity (MFI) to the recombinant protein on a scale from 0 to 30,000 arbitrary light units. Recombinant GFP and *T. cruzi* lysate-coated beads served as negative and positive controls, respectively.

Figure 4.1

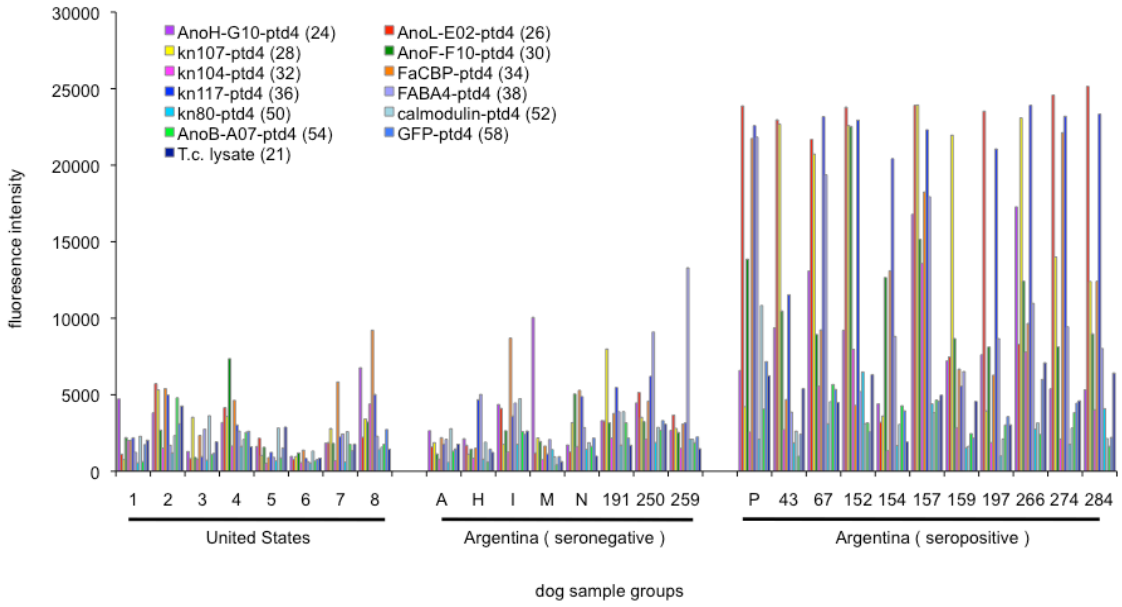
AnoH-G10-ptd4 (24)
AnoL-E02-ptd4 (26)
kn107-ptd4 (28)
AnoF-F10-ptd4 (30)
kn104-ptd4 (32)
FaCBP-ptd4 (34)
kn117-ptd4 (36)
FABA4-ptd4 (38)
kn80-ptd4 (50)
calmodulin-ptd4 (52)
AnoB-A07-ptd4 (54)
GFP-ptd4 (58)
T.c. lysate (21)
fluorescence intensity
30000
25000
20000
15000
10000
5000
0
1 2 3 4 5 6 7 8
A H I M N 191 250 259
P 43 67 152 154 157 159 197 266 274 284
United States
Argentina (seronegative)
Argentina (seropositive)
dog sample groups

Table 4.1. Results of sera and plasma samples with xenodiagnosis, initial conventional serology, multiplex serology, and IFNγ ELISpot assay. Forty-two samples from dogs living in a *T. cruzi*-endemic region are grouped as non-responders and responders based on reactivity to *T. cruzi* lysate in serological and effector function assays. Test reactivity is annotated as positive (+), negative (-), discordant (disc), or not determined (n.d.). Controls are canine samples from dogs living in the United States. Bold data are results presented as # positive individuals/# total individuals of the groups.

Table 4.1

	Results:	Xenodiagnosis	Initial serology	Multiplex serology	IFNγ ELISpot
	Dog ID#	parasites observed	reactivity	# protein >4SD reactivity	SFU per 1x10^6 cells with TcLysate
Non-responders	160	-	-	0	0
	163	-	-	0	0
	280	-	-	0	0
	281	-	-	0	0
	283	-	-	0	3
	187	n.d.	-	0	0
	258	n.d.	-	0	0
	259	n.d.	-	0	0
	267	n.d.	-	0	0
	198	n.d.	+	0	0
	200	n.d.	+	0	0
	588	n.d.	disc	1	0
	260	n.d.	n.d.	0	0
	B	n.d.	n.d.	0	0
	D	n.d.	n.d.	0	0
	F	n.d.	n.d.	0	0
	I	n.d.	n.d.	0	n.d.
	J	n.d.	n.d.	0	0
	K	n.d.	n.d.	0	3
	L	n.d.	n.d.	0	0
	M	n.d.	n.d.	0	0
				0/21	**0/20**
Responders	152	-	+	6	400
	71	+	+	5	55
	154	+	+	3	108
	157	+	+	5	13 (-)
	159	+	+	3	290
	266	+	n.d.	3	55
	272	+	+	2	50
	274	+	+	2	68
	276	+	+	4	363
	284	+	+	3	955
	43	n.d.	+	4	233
	67	n.d.	+	1	80
	69	n.d.	+	5	550
	193	n.d.	+	4	130
	197	n.d.	+	2	63
	434	n.d.	+	5	58
	572	n.d.	+	4	n.d.
	573	n.d.	+	3	398
	589	n.d.	+	4	33
	P	n.d.	n.d.	3	823
	O	n.d.	n.d.	5	520
				20/21	**19/20**
Controls (US)	1	n.d.	n.d.	0	0
	2	n.d.	n.d.	0	3
	3	n.d.	n.d.	0	0
	4	n.d.	n.d.	0	n.d.
	5	n.d.	n.d.	0	n.d.
	6	n.d.	n.d.	0	n.d.
	7	n.d.	n.d.	0	n.d.
	8	n.d.	n.d.	0	n.d.
				0/8	**0/3**

Figure 4.2. Seropositive dogs have significantly higher frequencies of *T. cruzi*-specific PBMCs and reactive T cell compartment. A, Interferon (IFN)-γ enzyme-linked immmunosorbent spot (ELISpot) well images of $4x10^5$ PBMCs cultured with media, PMA/ionomycin (PMA/ion), or *T. cruzi* lysate (TcLysate/Tc) and $1x10^4$ PBMCs stimulated with PMA/ionomycin (PMA/ion (10,000)). Individual dog identification (ID) and results of multiplex serology are denoted above wells. B-C, Numbers of IFNγ-producing PBMCs in the ELISpot assay responding to *T. cruzi* parasite lysate (B) or PMA (C) adjusted to $1x10^6$ or per $1x10^4$ PMBCs, respectively. Each square and dot represents an individual dog, while each diamond represents one of three US dog controls to ensure plate reproducibility. Dogs are grouped by multiplex serology negative (Sero -) or serology positive (Sero +) from Argentina or seronegative dogs from United States. Statistical significance was determined by one-way ANOVA using Prism v4.0c (GraphPad). Horizontal line, threshold for positive/negative response.

Figure 4.2

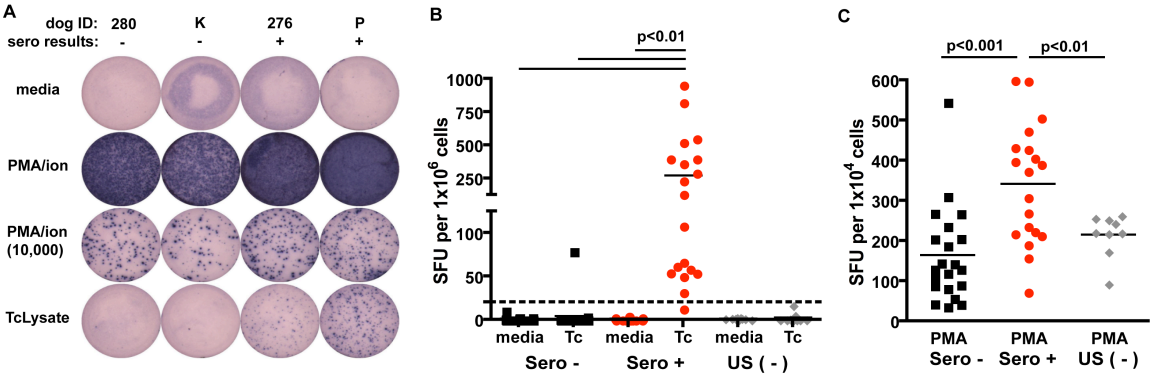
A
dog ID: 280 K 276 P
sero results: - - + +
media
PMA/ion
PMA/ion (10,000)
TcLysate
B
p<0.01
SFU per 1x10^6 cells
1000
750
500
250
100
50
0
media Tc media Tc media Tc
Sero - Sero + US (-)
C
p<0.001
p<0.01
SFU per 1x10^4 cells
600
500
400
300
200
100
0
PMA Sero - PMA Sero + PMA US (-)

Figure 4.3. Intracellular IFNγ staining identifies *T. cruzi*-specific $CD4^+$ and $CD8^+$ T cells. Representative flow plots of intracellular cytokine staining of T cells from ELISpot positive (71, 69, 43, 67) and negative canine (1,2) PBMC cultures incubated with media, PMA/ionomycin, or *T. cruzi* lysate (TcLysate). Numbers indicate percentage of IFNγ-producing $CD4^+$ or $CD8^+$ T cells. B-C, Percentage of IFNγ-producing $CD4^+$ (B) and $CD8^+$ (C) T cells from individual dogs. Each bar represents a dog from Argentina (red) or United States (gray). Results of reactivity in IFNγ ELISpot assay are denoted below each bar.

Figure 4.3

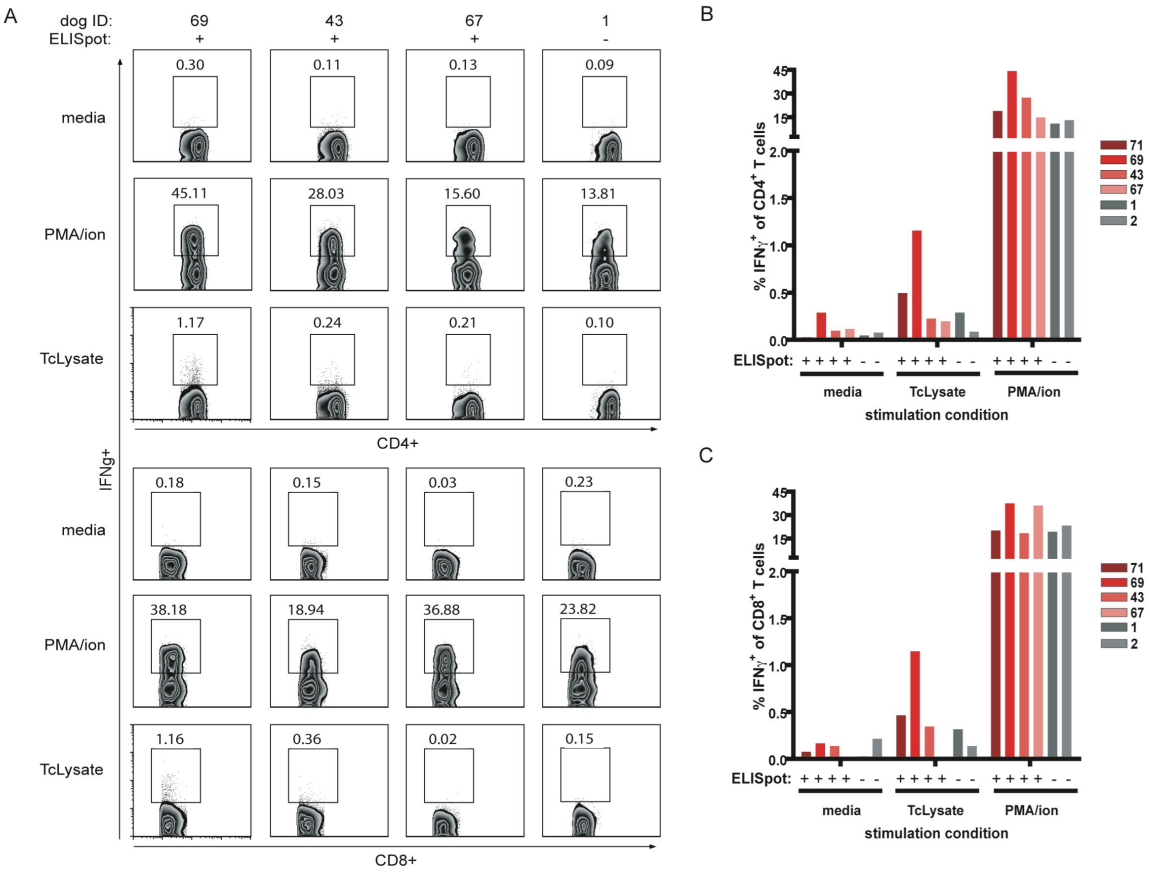
A
dog ID:
ELISpot:
69
+
43
+
67
+
1
-
media
PMA/ion
TcLysate
0.30
0.11
0.13
0.09
45.11
28.03
15.60
13.81
1.17
0.24
0.21
0.10
CD4+
IFNg+
0.18
0.15
0.03
0.23
38.18
18.94
36.88
23.82
1.16
0.36
0.02
0.15
CD8+
B
% IFNγ+ of CD4+ T cells
ELISpot:
media
TcLysate
PMA/ion
stimulation condition
71
69
43
67
1
2
C
% IFNγ+ of CD8+ T cells

Figure 4.4. T cells from seropositive dogs show signs of activation through decreased CCR7 and CD62L expression. T cells from twenty seropositive and twenty seronegative Argentinian dogs were stained with antibodies for CCR7, CD62L, and CTL2.58, an activation marker. A-B. Histograms of CCR7, CD62L, and CTL2.58 expression and dot plots of CCR7 and CD62L co-expression on $CD8^+$ (A) and $CD4^+$ (B) T cells. Numbers indicate percentages of either $CD8^+$ or $CD4^+$ cells expressing CCR7 (C,G), CD62L (D,H), CCR7 and CD62L (E, I), or the activation marker, CTL2.58 (F,J). Statistical significance was determined by one-way ANOVA using Prism v4.0c (GraphPad). ** designates $p<0.001$.

Figure 4.4

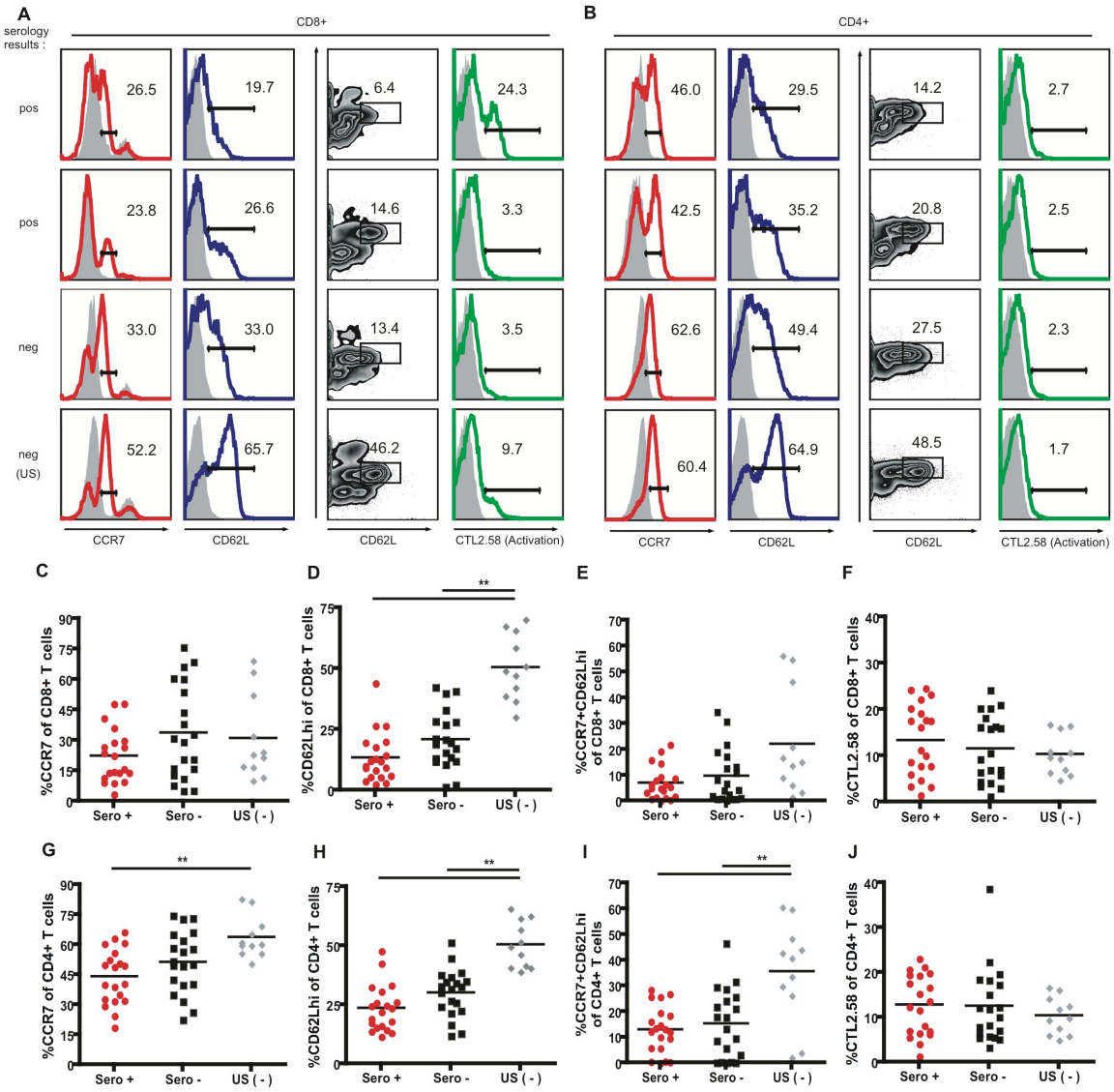
A
serology results :
CD8+
pos
pos
neg
neg (US)
26.5
19.7
6.4
24.3
23.8
26.6
14.6
3.3
33.0
33.0
13.4
3.5
52.2
65.7
46.2
9.7
CCR7
CD62L
CD62L
CTL2.58 (Activation)
B
CD4+
46.0
29.5
14.2
2.7
42.5
35.2
20.8
2.5
62.6
49.4
27.5
2.3
60.4
64.9
48.5
1.7
CCR7
CD62L
CD62L
CTL2.58 (Activation)
C
%CCR7 of CD8+ T cells
D
%CD62Lhi of CD8+ T cells
E
%CCR7+CD62Lhi of CD8+ T cells
F
%CTL2.58 of CD8+ T cells
G
%CCR7 of CD4+ T cells
H
%CD62Lhi of CD4+ T cells
I
%CCR7+CD62Lhi of CD4+ T cells
J
%CTL2.58 of CD4+ T cells
**
Sero +
Sero -
US (-)

4.7 References

1. World Health Organization. 2010. Chagas disease (American trypanosomiasis).

2. Stuart, K., R. Brun, S. Croft, A. Fairlamb, R. E. Gurtler, J. McKerrow, S. Reed, and R. Tarleton. 2008. Kinetoplastids: related protozoan pathogens, different diseases. *J Clin Invest* 118:1301-1310.

3. Gurtler, R. E., M. C. Cecere, M. A. Lauricella, M. V. Cardinal, U. Kitron, and J. E. Cohen. 2007. Domestic dogs and cats as sources of Trypanosoma cruzi infection in rural northwestern Argentina. *Parasitology* 134:69-82.

4. Cohen, J. E., and R. E. Gurtler. 2001. Modeling household transmission of American trypanosomiasis. *Science* 293:694-698.

5. Gurtler, R. E., L. A. Ceballos, P. Ordonez-Krasnowski, L. A. Lanati, R. Stariolo, and U. Kitron. 2009. Strong Host-Feeding Preferences of the Vector Triatoma infestans Modified by Vector Density: Implications for the Epidemiology of Chagas Disease. *Plos Neglect Trop D* 3:-.

6. Gurtler, R. E., M. C. Cecere, M. B. Castanera, D. Canale, M. A. Lauricella, R. Chuit, J. E. Cohen, and E. L. Segura. 1996. Probability of infection with Trypanosoma cruzi of the vector Triatoma infestans fed on infected humans and dogs in northwest Argentina. *Am J Trop Med Hyg* 55:24-31.

7. Lauricella, M. A., A. J. Sinagra, I. Paulone, A. R. Riarte, and E. L. Segura. 1989. Natural Trypanosoma-Cruzi Infection in Dogs of Endemic Areas of the Argentine Republic. *Rev Inst Med Trop Sp* 31:63-70.

8. Reithinger, R., L. Ceballos, R. Stariolo, C. R. Davies, and R. E. Gurtler. 2006. Extinction of experimental Triatoma infestans populations following continuous exposure to dogs wearing deltamethrin-treated collars. *Am J Trop Med Hyg* 74:766-771.

9. Basombrio, M. A., M. A. Segura, M. C. Mora, and L. Gomez. 1993. Field trial of vaccination against American trypanosomiasis (Chagas' disease) in dogs. *Am J Trop Med Hyg* 49:143-151.

10. Aparicio-Burgos, J. E., L. Ochoa-Garcia, J. A. Zepeda-Escobar, S. Gupta, M. Dhiman, J. S. Martinez, R. M. de Oca-Jimenez, M. V. Arreola, A. Barbabosa-Pliego, J. C. Vazquez-Chagoyan, and N. J. Garg. 2011. Testing the Efficacy of a Multi-Component DNA-Prime/DNA-Boost Vaccine against Trypanosoma cruzi Infection in Dogs. *Plos Neglect Trop D* 5.

11. Basso, B., I. Castro, V. Introini, P. Gil, C. Truyens, and E. Moretti. 2007. Vaccination with Trypanosoma rangeli reduces the infectiousness of dogs experimentally infected with Trypanosoma cruzi. *Vaccine* 25:3855-3858.

12. Salomone, O. A., A. L. Basquiera, A. Sembaj, A. M. Aguerri, M. E. Reyes, M. Omelianuk, R. A. Fernandez, J. Enders, A. Palma, J. M. Barral, and R. J. Madoery. 2003. Trypanosoma cruzi in persons without serologic evidence of disease, Argentina. *Emerg Infect Dis* 9:1558-1562.

13. Marcon, G. E., P. D. Andrade, D. M. de Albuquerque, S. Wanderley Jda, E. A. de Almeida, M. E. Guariento, and S. C. Costa. 2002. Use of a nested polymerase chain reaction (N-PCR) to detect Trypanosoma cruzi in blood samples from chronic chagasic patients and patients with doubtful serologies. *Diagn Micr Infec Dis* 43:39-43.

14. Zarate-Blades, C. R., N. Blades, M. S. Nascimento, J. F. da Silveira, and E. S. Umezawa. 2007. Diagnostic performance of tests based on Trypanosoma cruzi excreted-secreted antigens in an endemic area for Chagas' disease in Bolivia. *Diagn Micr Infec Dis* 57:229-232.

15. Lauricella, M. A., M. B. Castanera, R. E. Gurtler, and E. L. Segura. 1998. Immunodiagnosis of Trypanosoma cruzi (Chagas' disease) infection in naturally infected dogs. *Mem I Oswaldo Cruz* 93:501-507.

16. Montenegro, V. M., M. Jimenez, J. C. P. Dias, and R. Zeledon. 2002. Chagas disease in dogs from endemic areas of Costa Rica. *Mem I Oswaldo Cruz* 97:491-494.

17. Lauricella, M. A., C. Wisniveskycolli, R. Gurtler, R. Petersen, M. Bujas, and E. L. Segura. 1993. Standardization of Serological Tests for Detecting Anti-Trypanosoma-Cruzi Antibodies in Dogs. *Mem I Oswaldo Cruz* 88:413-417.

18. Minning, T. A., D. B. Weatherly, J. Atwood, 3rd, R. Orlando, and R. L. Tarleton. 2009. The steady-state transcriptome of the four major life-cycle stages of Trypanosoma cruzi. *BMC Genomics* 10:370.

19. Atwood, J. A., D. B. Weatherly, T. A. Minning, B. Bundy, C. Cavola, F. R. Opperdoes, R. Orlando, and R. L. Tarleton. 2005. The Trypanosoma cruzi proteome. *Science* 309:473-476.

20. Cooley, G., R. D. Etheridge, C. Boehlke, B. Bundy, D. B. Weatherly, T. Minning, M. Haney, M. Postan, S. Laucella, and R. L. Tarleton. 2008. High throughput selection of effective serodiagnostics for Trypanosoma cruzi infection. *PLoS Negl Trop Dis* 2:e316.

21. Tarleton, R. L. 1990. Depletion of CD8+ T cells increases susceptibility and reverses vaccine-induced immunity in mice infected with Trypanosoma cruzi. *J Immunol* 144:717-724.

22. Tarleton, R. L., B. H. Koller, A. Latour, and M. Postan. 1992. Susceptibility of beta 2-microglobulin-deficient mice to Trypanosoma cruzi infection. *Nature* 356:338-340.

23. Laucella, S. A., D. P. Mazliah, G. Bertocchi, M. G. Alvarez, G. Cooley, R. Viotti, M. C. Albareda, B. Lococo, M. Postan, A. Armenti, and R. L. Tarleton. 2009. Changes in Trypanosoma cruzi-specific immune responses after treatment: surrogate markers of treatment efficacy. *Clin Infect Dis* 49:1675-1684.

24. Tarleton, R. L., M. J. Grusby, M. Postan, and L. H. Glimcher. 1996. Trypanosoma cruzi infection in MHC-deficient mice: further evidence for the role of both class I- and class II-restricted T cells in immune resistance and disease. *Int Immunol* 8:13-22.

25. Tarleton, R. L., J. Sun, L. Zhang, and M. Postan. 1994. Depletion of T-cell subpopulations results in exacerbation of myocarditis and parasitism in experimental Chagas' disease. *Infect Immun* 62:1820-1829.

26. Albareda, M. C., S. A. Laucella, M. G. Alvarez, A. H. Armenti, G. Bertochi, R. L. Tarleton, and M. Postan. 2006. Trypanosoma cruzi modulates the profile of memory CD8+ T cells in chronic Chagas' disease patients. *Int Immunol* 18:465-471.

27. Laucella, S. A., M. Postan, D. Martin, B. Hubby Fralish, M. C. Albareda, M. G. Alvarez, B. Lococo, G. Barbieri, R. J. Viotti, and R. L. Tarleton. 2004. Frequency of interferon- gamma -producing T cells specific for Trypanosoma cruzi inversely correlates with disease severity in chronic human Chagas disease. *J Infect Dis* 189:909-918.

28. Michailowsky, V., N. M. Silva, C. D. Rocha, L. Q. Vieira, J. Lannes-Vieira, and R. T. Gazzinelli. 2001. Pivotal role of interleukin-12 and interferon-gamma axis in controlling tissue parasitism and inflammation in the heart and central nervous system during Trypanosoma cruzi infection. *The American journal of pathology* 159:1723-1733.

29. Martin, D. L., D. B. Weatherly, S. A. Laucella, M. A. Cabinian, M. T. Crim, S. Sullivan, M. Heiges, S. H. Craven, C. S. Rosenberg, M. H. Collins, A. Sette, M. Postan, and R. L. Tarleton. 2006. CD8+ T-Cell responses to Trypanosoma cruzi are highly focused on strain-variant trans-sialidase epitopes. *PLoS Pathog* 2:e77.

30. Bustamante, J. M., L. M. Bixby, and R. L. Tarleton. 2008. Drug-induced cure drives conversion to a stable and protective CD8+ T central memory response in chronic Chagas disease. *Nature Medicine* 14:542-550.

31. Enriquez, G. F., M. V. Cardinal, M. M. Orozco, A. G. Schijman, and R. E. Gurtler. 2013. Detection of Trypanosoma cruzi infection in naturally infected dogs and cats using serological, parasitological and molecular methods. *Acta Trop* 126:211-217.

32. Pedersen, L. G., Y. Castelruiz, S. Jacobsen, and B. Aasted. 2002. Identification of monoclonal antibodies that cross-react with cytokines from different animal species. *Vet Immunol Immunop* 88:111-122.

33. Hargreaves, D. C., P. L. Hyman, T. T. Lu, V. N. Ngo, A. Bidgol, G. Suzuki, Y. R. Zou, D. R. Littman, and J. G. Cyster. 2001. A coordinated change in chemokine responsiveness guides plasma cell movements. *Journal of Experimental Medicine* 194:45-56.

34. Albareda, M. C., G. C. Olivera, S. A. Laucella, M. G. Alvarez, E. R. Fernandez, B. Lococo, R. Viotti, R. L. Tarleton, and M. Postan. 2009. Chronic human infection with Trypanosoma cruzi drives CD4+ T cells to immune senescence. *J Immunol* 183:4103-4108.

35. Jimenez-Coello, M., M. Poot-Cob, A. Ortega-Pacheco, E. Guzman-Marin, A. Ramos-Ligonio, C. H. Sauri-Arceo, and K. Y. Acosta-Viana. 2008. American Trypanosomiasis in Dogs from an Urban and Rural Area of Yucatan, Mexico. *Vector-Borne and Zoonotic Diseases* 8:755-762.

36. Olivera, G. C., M. C. Albareda, M. G. Alvarez, A. M. De Rissio, L. E. Fichera, G. Cooley, P. Yachelini, H. A. Hrellac, H. Riboldi, S. A. Laucella, R. L. Tarleton, and M. Postan. 2010. Trypanosoma cruzi-specific immune responses in subjects from endemic areas of Chagas disease of Argentina. *Microbes and Infection* 12:359-363.

37. Barr, S. C. 2009. Canine Chagas' Disease (American Trypanosomiasis) in North America. *Veterinary Clinics of North America: Small Animal Practice* 39:1055-1064.

38. Guedes, P. M. M., V. M. Veloso, L. C. C. Afonso, M. V. Caliari, C. M. Carneiro, L. F. Diniz, E. A. Marques-Da-Silva, I. S. Caldas, M. A. D. Matta, S. M. Souza, M. Lana, E. Chiari, L. M. C. Galvao, and M. T. Bahia. 2009. Development of chronic cardiomyopathy in canine Chagas disease correlates with high IFN-gamma, TNF-alpha, and low IL-10 production during the acute infection phase. *Vet Immunol Immunop* 130:43-52.

39. Guedes, P. M. D., V. M. Veloso, W. L. Tafuri, L. M. D. Galvao, C. M. Carneiro, M. de Lana, E. Chiari, K. A. Soares, and M. T. Bahia. 2002. The dog as model for chemotherapy of the Chagas' disease. *Acta Trop* 84:9-17.

CHAPTER 5

CONCLUSIONS AND FUTURE DIRECTIONS

5.1 Conclusion

Chagas disease, or American trypanosomiasis, has been described as the "most neglected of neglected diseases" (1). Major efforts to prevent *Trypanosoma cruzi* transmission have focused on vector control through residual spraying of insecticides (2). As these multinational vector control initiatives can be expensive, labor intensive, and incomplete in rural areas, implementation of vertical vector control programs coupled with horizontal community surveillance have been described as cost-effective strategies to interrupt parasite transmission in highly endemic, rural areas (3). Despite these efforts, insecticidal resistance remains a possibility (4), warranting investigation into alternative integrated control strategies for identifying *T. cruzi* infection and preventing transmission. Development of alternative *T. cruzi*-specific targeting strategies requires a clear understanding of parasite mechanisms for growth, infection, and persistence and detection by the host's immune system.

Herein, I describe efforts to further understand the metabolic requirements of *T. cruzi*. A dramatic shift in carbohydrate- to lipid-dependent metabolism observed during metacyclic trypomastigote to amastigote transformation (5) focused our initial parasite efforts on understanding parasite dependence on fatty acids. Utilizing *T. cruzi* sequence information (6), life-cycle stage transcript abundance (7), and parasite proteomic analysis (5), we identified a fatty acid transporter protein (*fatp*) gene as a candidate gene for

selective disruption. Efforts to generate null *fatp* parasites failed, suggesting the gene was essential. *Fatp* dKO epimastigotes grew at similar rates to wild-type parasites but exhibited decreased intracellular growth, consistent with what would be expected with a disrupting fatty acid uptake. Despite gene persistence, mutant *fatp* dKO parasites appeared delayed in exogenous fatty acid uptake. *In vivo* infections of severely compromised IFN$\gamma^{-/-}$ mice revealed *fatp* dKO parasites were compromised in replication and persistence as compared to wildtype parasites. Induction of *T. cruzi*-specific T cells with a central memory phenotype in *fatp* dKO-infected C57BL/6 mice with no detectable parasite recrudescence following immunosuppression indicated these parasites were severely compromised in the presence of an appropriate T cell response. These studies demonstrate an underappreciated, essential role for fatty acid uptake in *T. cruzi* amastigotes. Future work to delineate key gene products involved in fatty acid uptake and utilization in *T. cruzi* may identify additional targets for genetic disruption, subsequent attenuation, and application in vaccination strategies.

As sources of infection for feeding insect vectors (8), susceptible to the pathologies of Chagas disease (9), and targets for vaccination strategies (10), dogs play a central role in *T. cruzi* epidemiology. To evaluate the efficacy of a vaccine, determining the generation of an appropriate antigen-specific immune response is required. Such techniques and methods to evaluate and describe the canine immune response, either through serological or cell-mediated mechanism are limitedly described in the veterinary literature. Development and characterization of antigen-specific responses were needed. To address this need, we focused on identifying techniques, methods, and reagents to evaluate the canine immune response in the dog and outlined our progress in Chapter 3.

Validation of CCR7 and CD62L expression in canine PBMCs aids in defining T cell subsets homing to lymph nodes, delineating naïve and central memory-phenotyping cells. We were able to identify activated and naïve T cells and evaluate generation of antigen-specific T cells following common core canine vaccine administration, a scenario that can be applied for evaluating and testing T cell-inducing vaccines aimed at infectious diseases and neoplastic disorders (11).

To test applicability and usefulness in an infectious canine model and towards our ultimate goal of evaluating a genetically altered parasite as an attenuated vaccine candidate in dogs, we explored these reagents and methods with dogs naturally infected with *T. cruzi*. Ninety-four percent of dogs positive in our multiplex bead array against recombinant *T. cruzi* proteins were initially positive by conventional serology. The frequency of PBMCs responding to *T. cruzi* correlated to serological status, and seropositive dogs predominantly bore effector/effector memory T cells. These studies are the first to correlate *T. cruzi*-specific antibody responses with T cells in naturally infected dogs. Validation of these methods provide a mechanism to identify infected canines as well as create a platform for assessing and monitoring the development of protective immune responses in canine-centric vaccination *T. cruzi* transmission control strategies.

5.2 References

1. Anonymous. 2006. Chagas' disease--an epidemic that can no longer be ignored. *Lancet* 368:619.

2. WHO Expert Committee. 2002. Control of Chagas Disease. In *WHO Technical Report Series*. World Health Organization, Geneva.

3. Vazquez-Prokopec, G. M., C. Spillmann, M. Zaidenberg, U. Kitron, and R. E. Gurtler. 2009. Cost-Effectiveness of Chagas Disease Vector Control Strategies in Northwestern Argentina. *Plos Neglect Trop D* 3:-.

4. Lardeux, F., S. Depickere, S. Duchon, and T. Chavez. 2010. Insecticide resistance of Triatoma infestans (Hemiptera, Reduviidae) vector of Chagas disease in Bolivia. *Tropical medicine & international health : TM & IH* 15:1037-1048.

5. Atwood, J. A., D. B. Weatherly, T. A. Minning, B. Bundy, C. Cavola, F. R. Opperdoes, R. Orlando, and R. L. Tarleton. 2005. The Trypanosoma cruzi proteome. *Science* 309:473-476.

6. El-Sayed, N. M., P. J. Myler, D. C. Bartholomeu, D. Nilsson, G. Aggarwal, A. N. Tran, E. Ghedin, E. A. Worthey, A. L. Delcher, G. Blandin, S. J. Westenberger, E. Caler, G. C. Cerqueira, C. Branche, B. Haas, A. Anupama, E. Arner, L. Aslund, P. Attipoe, E. Bontempi, F. Bringaud, P. Burton, E. Cadag, D. A. Campbell, M. Carrington, J. Crabtree, H. Darban, J. F. da Silveira, P. de Jong, K. Edwards, P. T. Englund, G. Fazelina, T. Feldblyum, M. Ferella, A. C. Frasch, K. Gull, D. Horn, L. Hou, Y. Huang, E. Kindlund, M. Klingbeil, S. Kluge, H. Koo, D. Lacerda, M. J. Levin, H. Lorenzi, T. Louie, C. R. Machado, R. McCulloch, A. McKenna, Y. Mizuno, J. C. Mottram, S. Nelson, S. Ochaya, K. Osoegawa, G. Pai, M. Parsons, M. Pentony, U. Pettersson, M. Pop, J. L. Ramirez, J. Rinta, L. Robertson, S. L. Salzberg, D. O. Sanchez, A. Seyler, R. Sharma, J. Shetty, A. J. Simpson, E. Sisk, M. T. Tammi, R. Tarleton, S. Teixeira, S. Van Aken, C. Vogt, P. N. Ward, B. Wickstead, J. Wortman, O. White, C. M. Fraser, K. D. Stuart, and B. Andersson. 2005. The genome sequence of Trypanosoma cruzi, etiologic agent of Chagas disease. *Science* 309:409-415.

7. Minning, T. A., D. B. Weatherly, J. Atwood, 3rd, R. Orlando, and R. L. Tarleton. 2009. The steady-state transcriptome of the four major life-cycle stages of Trypanosoma cruzi. *BMC Genomics* 10:370.

8. Gurtler, R. E., M. C. Cecere, M. A. Lauricella, M. V. Cardinal, U. Kitron, and J. E. Cohen. 2007. Domestic dogs and cats as sources of Trypanosoma cruzi infection in rural northwestern Argentina. *Parasitology* 134:69-82.

9. Barr, S. C. 2009. Canine Chagas' Disease (American Trypanosomiasis) in North America. *Veterinary Clinics of North America: Small Animal Practice* 39:1055-1064.

10. Basso, B., I. Castro, V. Introini, P. Gil, C. Truyens, and E. Moretti. 2007. Vaccination with Trypanosoma rangeli reduces the infectiousness of dogs experimentally infected with Trypanosoma cruzi. *Vaccine* 25:3855-3858.

11. Gilbert, S. C. 2012. T-cell-inducing vaccines - what's the future. *Immunology* 135:19-26.